

**STATIC AND DYNAMIC ANALYSIS OF A LADDER FRAME
TRUCK CHASSIS**

ISMAIL BIN HJ. MUSA

UNIVERSITI TEKNOLOGI MALAYSIA

STATIC AND DYNAMIC ANALYSIS OF A LADDER FRAME TRUCK
CHASSIS

ISMAIL BIN HJ. MUSA

A thesis submitted in fulfilment of the
requirements for the award of the degree of
Master of Engineering (Mechanical)

Faculty of Mechanical Engineering
Universiti Teknologi Malaysia

SEPTEMBER 2009

Specially

To my beloved family members and friends for motivation

To Prof Dr. Roslan Abdul Rahman and Assoc. Prof Mustaffa Yusof for the guidance

To all technicians from vibration and strength laboratory for their support

To whoever provided help and contributions.

ACKNOWLEDGEMENT

Alhamdulillah, I managed to complete the study after gone through many challenges during the periods. All praise and many-many thanks to Allah S.W.T who gave the strength and confident to me to complete the thesis entitle **Static and Dynamic Analysis of a Ladder Frame Truck Chassis**.

Special thanks to my supervisor, Prof. Dr. Roslan and PM. Mustafa for guidance and support through out the course and not to forget to Mr. Affendi for his assistance and commitment during experimental analysis at the laboratory.

Last but not least, special appreciation to my beloved family for their full support, encourage and understanding in order to complete this study successfully.

ABSTRACT

Truck chassis is a major component in a vehicle system. This work involves static and dynamics analysis to determine the key characteristics of a truck chassis. The static characteristics include identifying location of high stress area and determining the torsion stiffness of the chassis. The dynamic characteristics of truck chassis such as the natural frequency and mode shape were determined by using finite element (FE) method. Experimental modal analysis was carried out to validate the FE models. Modal updating of the truck chassis model was done by adjusting the selective properties such as mass density and Poisson's ratio. Predicted natural frequency and mode shape were validated against the experimental results. Finally, the modification of the updated FE truck chassis model was proposed to reduce the vibration, improve the strength and optimize the weight of the truck chassis. The major area of concern in the truck chassis was structural resonance at 52 Hz, experienced during the torsional and bending modes. Modifications to shift natural frequencies were proposed by increasing the thickness of the chassis center section by 2 mm and additional stiffener members located at the center of the base plate with a thickness of 10 mm. The overall modifications resulted in the natural frequency shifted by 13 % higher than the original value, increased the torsion stiffness by 25 % and reduced the total deflection by 16 %. The overall weight of the new truck chassis was increased by 7%.

ABSTRAK

Struktur chasis trak adalah merupakan komponen utama dalam sesebuah sistem kenderaan. Kajian yang dijalankan melibatkan analisis statik and dinamik bertujuan untuk menentukan ciri utama struktur trak tersebut. Untuk kaedah statik, ia bertujuan untuk menentukan kawasan yang mempunyai tegasan yang paling tinggi dan nilai tegaran daya kilasan. Kaedah kedua adalah kaedah korelasi dinamik yang diaplikasikan dengan menggunakan kaedah unsur terhingga bagi menentukan frekuensi tabii dan juga bentuk ragam struktur tersebut. Analisis ujikaji modal telah dijalankan untuk mengesahkan keputusan yang diperolehi dari analisis unsur terhingga. Seterusnya, kemaskini model telah dijalankan dengan menukarkan ciri dan sifat bahan seperti ketumpatan jisim dan Nisbah Poisson. Keputusan frekuensi tabii dan bentuk ragam yang diperolehi melalui model unsur terhingga ditentusahkan dengan model eksperimen. Seterusnya, beberapa cadangan pengubahsuaian dilakukan terhadap model unsur terhingga tersebut untuk mengurangkan tahap getaran, meningkatkan kekuatan struktur kerangka dan mengoptimumkan berat bagi chasis tersebut. Perkara utama yang perlu di beri perhatian pada struktur chasis tersebut adalah resonan pada frekuensi 52 Hz yang berlaku semasa mod daya kilasan dan lenturan. Justeru itu, beberapa langkah telah diambil untuk menganjak frekuensi tabii tersebut seperti menambahkan ketebalan kerangka pada bahagian tengah sebanyak 2 mm dan menambah sokongan tambahan pada bahagian tengah struktur setebal 10 mm. Secara keseluruhannya, pembaikan dan pengubahsuaian yang dilakukan terhadap struktur kerangka tersebut telah berjaya menganjakkkan frekuensi sebanyak 13% lebih tinggi daripada yang asal, tegaran daya kilasan meningkat sebanyak 25% dan mengurangkan terikan sebanyak 16%. Berat keseluruhan meningkat sebanyak 7% daripada nilai asal.

TABLE OF CONTENTS

CHAPTER	TITLE	PAGE
	TITLE PAGE	i
	DECLARATION	ii
	DEDICATION	iii
	ACKNOWLEDGEMENT	iv
	ABSTRACT	v
	ABSTRAK	vi
	CONTENTS	vii
	LIST OF TABLES	xi
	LIST OF FIGURES	xiii
	LIST OF SYMBOLS	xvi
	LIST OF APPENDIXES	xvii
1	INTRODUCTION	
	1.1 Types of truck	1
	1.1.1 Compact truck	2
	1.1.2 Full size truck	2
	1.1.3 Mid size truck	2
	1.2 The cultural significant of the truck	3
	1.2.1 The Australian Truck	3

1.2.2	Truck in Europe	3
1.2.3	Military use	4
1.3	Basic Frames	4
1.4	Problem statement	6
1.5	Objective	8
1.6	Scope of work	8
1.7	Expected result	9
2	LITERATURE REVIEW	
2.1	Truck chassis research	10
2.1.1	Overall discussion on research	18
2.2	Overview type of chassis	19
2.2.1	Definition of chassis	19
2.2.2	Ladder frame	19
2.2.3	Twin Tube	20
2.2.4	Spaceframes	21
3	RESEARCH METHODOLOGY	
3.1	Identification of problem	23
3.2	Research methodology	25
4	TORSIONAL TESTING OF CHASSIS	
4.1	Theory of load cases	28
4.2	Aims of the testing	30
4.3	Chassis overview	31

4.4	List of instrumentation	32
4.5	Calculation of the Global Torsion Stiffness	33
4.6	Test rig operational and mechanism	35
4.7	Preparation of test model and instrumentation set-up	36
4.8	Torsion Test	38
4.9	Torsion stiffness test using Finite Element	40
4.10	Torsion analysis result	43
4.10.1	Experimental result	44
4.10.2	Finite element result of torsion test	45
5	MODAL ANALYSIS ON CHASSIS	
5.1	List of Instrumentation	47
5.2	Experiment Set-up	50
5.2.1	Impact Hammer	50
5.2.2	Shaker Test	51
5.3	Experimental procedure	52
5.4	Analysis of data	55
5.5	Experimental modal analysis result	56
5.5.1	Impact Hammer Test result	56
5.5.2	Shaker Test result	59
5.6	Comparison between result from Impact Hammer & Shaker Test	61
6	FINITE ELEMENT ANALYSIS & BASE LINE MODEL	
6.1	Model Analysis of Finite Element Method	63
6.1.1	Mode Shape	65
6.2	Comparison of results between experimental	

and finite element	69
6.3 Model updating results	70
7 STRUCTURAL MODIFICATION	
7.1 Structural modification and parametric analysis	73
7.2 Static and dynamic test	78
8 OVERALL DISCUSSION	
8.1 Creation of FE baseline model	81
8.2 Design improvement study	83
8.3 Final result	84
9 CONCLUSION & RECOMMENDATION	
9.1 Summary	85
9.2 Conclusion	86
9.3 Recommendation for future research	88
REFERENCES	89
Appendices A - G	91

LIST OF TABLES

TABLE NO.	TITLE	PAGE
2.1	Comparison between natural frequency before and after modal updating	14
3.1	Material specification of truck chassis	25
4.1	List of instrumentation for torsion test	32
4.2	Experimental results of torsion test	44
4.3	Experimental results of torsion test - FEA	45
4.4	Comparison of FEA and experimental torsion analysis	45
5.1	List of instrumentation and function	47
5.2	Modal parameter	57
5.3	Modal parameters base on shaker test	59
5.4	Comparison for natural frequency, damping value and mode shape	62
6.1	Natural frequency from Finite Element Method	64
6.2	Mode pair with difference frequency	70
6.3	Comparison between natural frequency before and after	71
6.4	Overall updated result	71
7.1	Modification made on FE model	75
7.2	Comparison between natural frequency	76
7.3	Comparison on weight	77
7.4	Comparison on deflection	77
7.5	Comparison of Torsion Stiffness before & after modification	77

7.6	Result of static and dynamic simulation test	79
8.1	Final result of improvement study	84

LIST OF FIGURES

FIGURE NO.	TITLE	PAGE
1.1	Cutting process	4
1.2	Welding process	5
1.3	Finishing process	5
1.4	Final assembly	6
1.5	Chevy master rail	6
1.6	Sample of truck chassis	7
1.7	Global module concept	8
2.1	Truck chassis response spectra	12
2.2	Finite element model of # 3 cross member	15
2.3	General truck view	16
2.4	Failure location	17
2.5	Ladder frame	20
2.6	Twin tube chassis	21
2.7	Space frame	22
3.1	Parallel ladder frame type	24
3.2	Research methodology flow chart	27
4.1	Bending load case	29
4.2	Torsion load case	29
4.3	Chassis and suspension as springs	30
4.4	Ladder type structure	32
4.5	Outline of experimental set-up	33
4.6	Force direction	35

4.7	Hydraulic cylinder arrangement	36
4.8	Test rig mechanism	36
4.9	Test rig and chassis	37
4.10	Chassis side view	37
4.11	Chassis rear view	38
4.12	Structural at minimal load	38
4.13	Structural at the maximum load @ 1000 kgf	39
4.14	Rear view during testing	39
4.15	Side view during load test	40
4.16	Rear support	40
4.17	Dimension of the truck chassis	41
4.18	Truck chassis model meshed with tetrahedral-10 elements	42
4.19	Torsion test using ANSYS software.	43
5.1	Experimental set-up for impact hammer test	51
5.2	Experimental set-up for impact hammer test	51
5.3	Shaker test set-up	52
5.4	Calibration of measurement	53
5.5	The 22 section excitation & reference points	55
5.6	Superimposed FRF_impact hammer (Direction-Z)	57
5.7	Superimposed FRF_impact hammer (Direction-X)	57
5.8	Experimental mode shape	58
5.9	Superimposed FRF by Shaker test	60
5.10	Mode shape result by Shaker result	61
6.1	Truck chassis model meshed with tetrahedral-10 elements	64
6.2	FEA 1 st mode shape @ 29.71 Hz	66
6.3	FEA 2 nd mode shape @ 39.03 Hz	66
6.4	FEA 3 rd mode shape @ 47.92 Hz	67
6.5	FEA 4 th mode shape @ 59.40 Hz	67
6.6	FEA 5 th mode shape @ 69.53 Hz	68
6.7	FEA 6 th mode shape @ 74.51 Hz	68
6.8	FEA 7 th mode shape @ 86.43 Hz	69
7.1	Testing structure and modification made on chassis	74
7.2	Dynamic test	78
7.3	Static test	79

8.1	Stress analysis result (Before)	82
8.2	Stress analysis result (After)	83
8.3	Overall chassis improvement	83

LIST OF SYMBOLS

c	–	Damping coefficient
E	–	Young's Modulus
f	–	Natural frequency
F	–	Force
k	–	Spring stiffness
x	–	Displacement
m	–	Mass
t	–	Time
ν	–	Poisson's ratio
ρ	–	Mass density
$\{u\}$	–	Displacement matrix
$\{a\}$	–	Acceleration matrix
$\{f\}$	–	Vector of applied forces
$\{\phi\}$	–	Eigenvector or mode shape
$[M]$	–	Mass matrix to represent inertial properties of a model
$[K]$	–	Stiffness matrix to represent elastic properties of a model
λ	–	Eigen values (the natural or characteristic frequency)

LIST OF APPENDIXES

APPENDIX	TITLE	PAGE
A	Project schedule	91
B	Preparation of Truck Chassis	93
C	Engineering drawing	95
D	Test model, Stress test #5 & Calibration result	98
E	Instrumentation	101
F	ANSYS Report of Test #5	112
G	Theory of Chassis Design	120

CHAPTER 1

INTRODUCTION

The truck industry has experienced a high demand in market especially in Malaysia whereby the economic growths are very significantly changed from time to time. There are many industrial sectors using this truck for their transportations such as the logistics, agricultures, factories and other industries. However, the development and production of truck industries in Malaysia are currently much relying on foreign technology and sometime not fulfill the market demand in term of costs, driving performances and transportations efficiency.

1.1 Types of truck

There are many types of truck in all over the world. Majority of truck's manufacturers receiving order from many industries for transportation purposes in various types and specifications in term of size and truck capacity. Based on that, there are three types or categories which are currently available in the market namely, the compact truck, full size truck and mid size truck.

1.1.1 Compact truck

The compact truck is the most widespread form of pickup truck worldwide. It is built like a mini version of a two-axle heavy truck, with a frame providing structure, a conventional cab, a leaf spring suspension on the rear wheels and a small I4 or V6 engine, generally using gasoline.

The compact truck was introduced to North America in the 1960s by Japanese manufacturers. Datsun (Nissan 1959) and Toyota dominated under their own nameplates through the end of the 1970s.

1.1.2 Full size truck

A full size truck is a large truck suitable for hauling heavy loads and performing other functions. Most full-size trucks can carry at least 450 kg in the rear bed, with some capable of over five times that much.

1.1.3 Mid size truck

In North America, trucks were commonly used as general purpose passenger cars. They were popular not only with construction workers, but also with housewives and office workers. Thus arose the need for a pickup truck that was bigger than a compact and smaller and more fuel-efficient than the full-size pickup.

1.2 The cultural significant of the truck

There are many types of truck that have been developed in the market especially for the cultural needs. The research and development have always found the new technology, which have really contributed to their needs especially for private use as well as organization and country.

1.2.1 The Australian Truck

The Australian utility truck, or more affection ally called “ute”, is the mainstay variety of truck in Australia. Since the modern design of the ute first rolled off the assembly line at the Ford factory in Geelong in 1934, which Henry Ford described as the “kangaroo chaser”. There were two common types exist, which is the American style truck, commonly popular with farmers. It is usually Japanese or Australian built model, such as the Isuzu Rodeo or the Toyota Hilux. These are popular in a variety of forms, two and four wheel drive, single or dual cab integrated tray or flat bed. These kinds of vehicles are also common in New Zealand, where they are also referred to as “utes”. The other type of vehicle commonly referred to as a “ute” is quite different-a two-seater sporty version of typical saloon cars, featuring a “ute”-type integrated tray back.

1.2.2 Truck in Europe

In Europe, pickups truck is considered light commercial vehicles for farmers. Until the 1990s, pickup trucks were preferred mainly as individual vehicles in rural

areas, while vans and large trucks were the preferred method of transportation for cargo.

1.2.3 Military use

Pickup trucks have been used as troop carrier in many parts of the world, especially in countries with few civilian roads of very rough terrain. Pickup trucks have also been used as fighting vehicles, often equipped with a machine-gun mounted on the bed.

1.3 Basic Frames

Below is some basic technique in developing the frame commonly used by truck chassis manufacture in the world since it was introduced in 1977. The frame rails start as 1/8" flat steel. Side rails, boxing plates, top and bottom lips are plasma cut to shape and fully jig welded. (Figure 1.1)

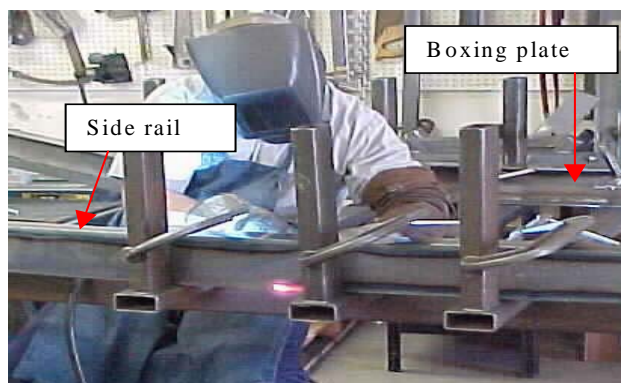


Figure 1.1: Cutting process

The top and bottom lips are then full length welded on the inside as well as the outside as illustrated in Figure 1.2. The reason is to make the rails stronger so that crack will not occur at the weld seams.

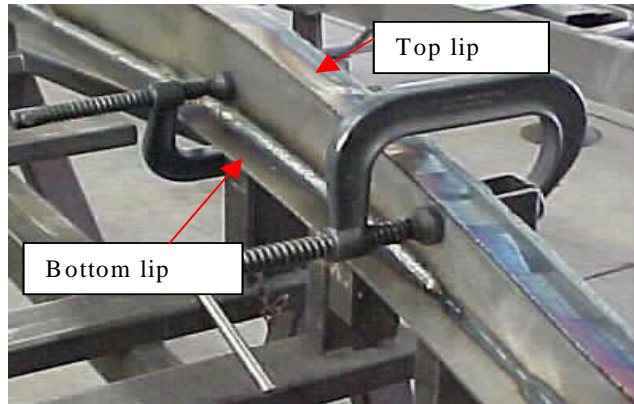


Figure 1.2: Welding process

The rails are fully ground and smoothed as shown in Figure 1.3.



Figure 1.3: Finishing process

Finally, the rails are clamped back into fixture, ready for the cross members to be welded into place. (Figure 1.4)



Figure 1.4: Final assembly

Figure 1.5 is a set of 1933 Chevy Master Rails, completed and ready.



Figure 1.5: Chevy Master Rail [12]

1.4 Problem Statement

The vehicle models that have been developed almost the same appearance since the models developed in 20 or 30 years ago. This indicates that the evolutions of these structures are still behind from other countries and research and development technology is not fully utilized in our country. This is a major challenge to truck

manufacturers to improve and optimize their vehicle designs in order to meet the market demand and at the same time improve the vehicles durability and performance. Since the truck chassis is a major component in the vehicle system, therefore, it is often identified for refinement and improvement for better handling and comfortably.

The frame of the truck chassis is a backbone of the vehicle and integrates the main truck component systems such as the axles, suspension, power train, cab and trailer. The typical chassis is a ladder structure consisting of two C channel rails connected by cross-members as illustrated in Figure 1.6. Almost all the chassis development is varying in design, weight, complexity and cost. However, the effects of changes to the frame and cross-members are not well understood in term of vehicle response during riding especially on bumpy and off road conditions. For example, if the torsion stiffness of a suspension cross-member is lowered, what is the effect on the vehicle's roll stability, handling, ride and durability? Therefore, the main criteria in the analysis are the behavior of truck chassis, how to improve the current design for better riding quality and suitably to customer needs.

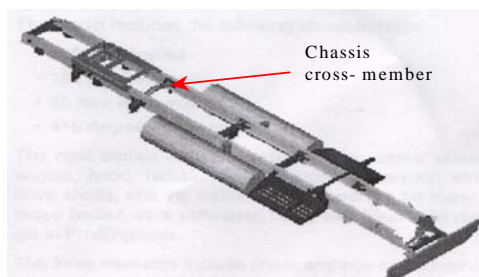


Figure 1.6: Sample of the Truck Chassis [1]

On overall, this research study is really requiring attention to improve the existing condition for betterment of riding quality and comfortably. There are major areas need to be established in the study to come out with proper investigation on truck chassis especially research methodology on experimental and computational analysis. The ultimate result would be improvement of vehicle quality, reliability, flexibility, efficiency and low production cost. Figure 1.7 below shows an example of the global module concept, which has been implemented by most truck's manufacturer in the world.

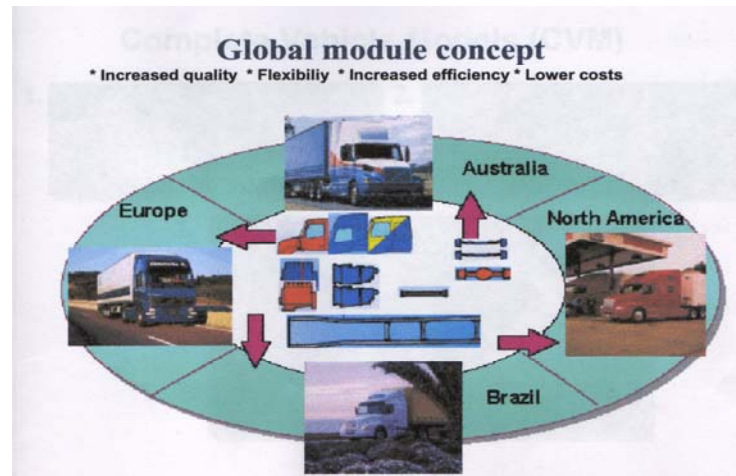


Figure 1.7 Global Module Concepts [2]

1.5 Objective

The objectives of this study are:

- i) To determine the torsion stiffness and static and dynamic mode shape of the truck chassis by using torsion testing, modal analysis and finite element method.
- ii) To improve the static and dynamic behavior of the truck chassis by changing the geometrical dimension and structural properties.
- iii) To develop a new truck chassis.

1.6 Scope of work

The scope of work includes:

- i. Literature review associated with truck chassis development, design and analysis to the commercial truck chassis.
- ii. This study will concentrate on truck chassis of not more than 2 ton
- iii. Simulation and experimental work on the existing truck chassis
- iv. Correlation of simulation and experimental results.
- v. Model updating process, which include parameters adjustment in order to obtain a good model of truck chassis
- vi. Improvement of truck chassis characteristic by changing the geometry, material and structure to the existing model.
- vii. Development of new truck chassis.

1.7 Expected result.

Base on the research and development planning, it is expected to achieve a better performance of truck chassis and the main focuses of the analysis are listed below:

- i. To improve the existing chassis performance such as the torsion stiffness, strength and dynamic behavior due to dynamic load. The result shall be able to present the static and dynamics motion of the truck chassis which include the natural frequency, mode shapes and damping value.
- ii. The experimental data will be used to validate a finite element model and the updated model shall represent the real structure of the chassis.
- iii. The improvement of structures and supports shall be done to the existing chassis in order to fulfill the customer's requirement such as cost, reliability, conformability and better performance.

CHAPTER 2

LITERATURE SURVEY

There are two main objectives, which involves on the development of truck chassis. Firstly, the appropriate static and dynamic characteristics of the existing chassis have to be determined. Secondly, structural development process in order to achieve high quality of the product. There are many factors involve and must take into account, which can affect on the vehicle rolling, handling, ride stability and etc. Today, there are many researches and development program available in the market especially by the international truck manufacturers, which are very much related to this study. Therefore, there are several technical papers from the 'Engineering Society for Advancing Mobility Land Sea Air & Space' (SAE) and some other sources which are reviewed and discussed in this chapter.

2.1 Truck Chassis Research

Dave Anderson and Greg Schade[1] developed a Multi-Body Dynamic Model of the Tractor-Semitrailer for ride quality prediction. The studies involved representing the distributed mass and elasticity of the vehicle structures e.g. frame

ladder, the non-linear behavior of shock absorbers, reproduce the fundamental system dynamics that influence ride and provide output of the acceleration, velocity and displacement measures needed to compute ride quality. There were three main factors contributed in this study. Firstly, the author had come out with the development of an ADAMS multi-body dynamics model for use as a predictive tool in evaluating ride quality design improvement. The model includes frame, cab and model generated from finite element component mode synthesis. Second, the construction and correlation of the model has been developed and followed a multi-step process in which each of the major sub-systems were developed and validated to test results prior to corporation in the full vehicle model. Finally, after a series of refinements to the model, the next steps were implemented to obtain an acceptable degree of correlation. The author had managed to evaluate the model's ability to predict ride quality by using accelerations measured in the component, which were then processed through an algorithm to compute an overall ride comfort rating.

I.M. Ibrahim, et.al. [2] had conducted a study on the effect of frame flexibility on the ride vibration of trucks. The aim of the study was to analyze the vehicle dynamic responses to external factors. The spectral analysis technique was used in the problem study. Other than that, the driver acceleration response has been weighted according to the ISO ride comfort techniques. From the author point of view, the excessive levels of vibration in commercial vehicles were due to excitation from the road irregularities which led to ride discomfort, ride safety problems, road holding problems and to cargo damage or destruction. Also, it has been found that the frame structure vibrations due to flexibility have a similar deleterious effect on the vehicle dynamic behavior. In order to study the frame flexibility, the author had came out with the truck frame modeled using the Finite Element Method (FEM) and its modal properties have been calculated. Numerical results were presented for the truck, including power spectral densities and root mean square values of the vehicle dynamic response variables. The results show that there was good agreement with the experimental analysis and that modeling technique was a very powerful and economical for the analysis of complex vehicle structures. From the comparison of the responses of the rigid and flexible body models it has been found that the frame flexibility strongly affects the accelerations of both driver and truck body. Therefore, the author suggested that the frame flexibility effects were taken into account in the

design of primary, cab and engine suspension systems. As a comparison, Figure 2.1 is shown the response of the rigid and flexible body model of the parameters that has been tested.

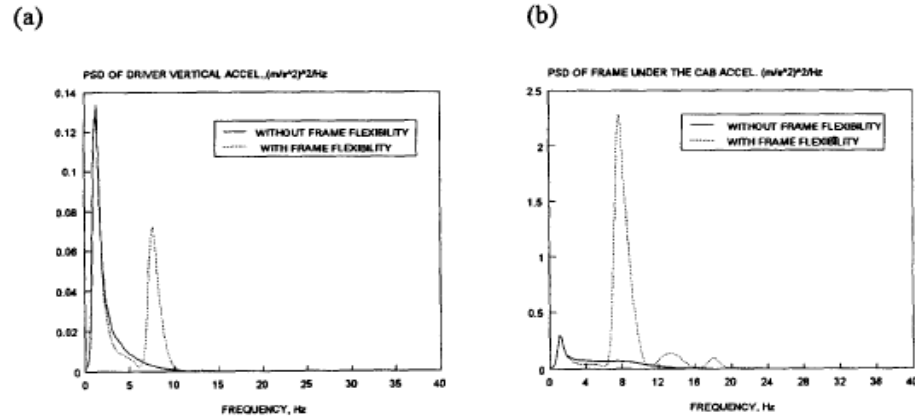


Figure 2.1 – Truck responses spectra [2]

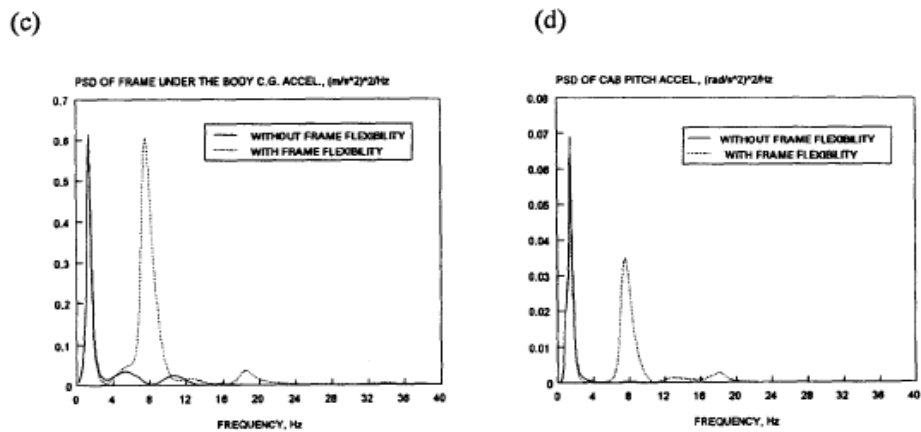


Figure 2.1 – Truck responses spectra – Continued [2]

Another case study was presented by Romulo Rossi Pinto Filho [3], who analyzed on the Automotive Frame Optimization. The objective of his study was basically to obtain an optimized chassis design for an off-road vehicle with the appropriate dynamic and structural behavior. The studies were consisted of three main steps. Firstly, the modeling of the chassis used in a commercial off-road vehicle using commercial software based on the finite elements method (FEM). Secondly, a series of testing were conducted to obtain information for modeling and validation. Finally, the validated model allowed the optimization of the structure seeking for higher torsion stiffness and maintenance of the total structure mass.

In the finite element model, the author has developed the chassis by using steel with closed rectangular profile longitudinal rails and tubular section cross-member. The geometry of the chassis was measured directly in the reference vehicle real structure. Then, a modal analysis procedure was accomplished on the real chassis and finite element model structure in order to establish the real structure to the chassis structures. The natural frequencies were extracted. For the frame optimization, the author tried to use groups of numerical and programming techniques to search for the optimum value of mathematical functions. In other words, the purpose of the optimization is to facilitate in finding results that best fills out the needs. Based on the result, the analysis and experimental procedure applied had significantly improved the overall structural stiffness by 75% by maintaining the center of gravity and the total weight was increased by 6%.

Other than that, Izzudin B. Zaman [4] has conducted a study on the application of dynamic correlation and model updating techniques. These techniques were used to develop a better refinement model of existing truck chassis with approximately 1 tone and also for verification of the FEA models of truck chassis. The dynamic characteristics of truck chassis such as natural frequency and mode shape were determined using finite element method. From the initial result, both analysis show that the truck chassis experienced 1st torsion mode for 1st natural frequency, 1st bending mode for 2nd natural frequency, 2nd torsion mode for 3rd natural frequency and 2nd bending mode for 4th natural frequency.

Based on the results, the modal updating of truck chassis model was done by adjusting the selective properties such as Modulus Young and Poisson ratio in order to get better agreement in the natural frequency between both analyses. The modification of the updated FE truck chassis model was suggested and also to consider by adding the stiffener. The purpose was to reduce the vibration as well as to improve the strength of the truck chassis. Table 2.1 shows the comparison between the natural frequencies from the original Finite Element model, the updated and the experimental results. From the results shown, the overall accuracy of the model results had increased by about $\pm 2\%$.

Table 2.1: Comparison between natural frequencies before and after model updating [4]

Mode	EMA(Hz)	First FE		Updated FE	
		(Hz)	Error (%)	(Hz)	Error (%)
1	35.2	43.7	24.29	35.8	1.64
2	63.4	64.8	2.22	62.4	-1.58
3	86.8	99.1	14.11	87.7	0.99
4	157.0	162.3	3.43	156.5	-0.31

The significant of this study were, the author had managed to determine the structural behavior of truck chassis and high vibration occurred through the overall chassis structure due to resonance effect. Based on modification that was made on the structural by adding the stiffener, the overall vibration and displacement had significantly reduced by 3.28%.

Lonny L. Thomson, et. al., [5] had presented his paper on the twist fixture which can measure directly the torsion stiffness of the truck chassis. The fixture was relatively lightweight and portable with the ability to be transported and set-up by one person. The extensive testing has been carried out to check on the accuracy of the fixture and was found to be within 6% accuracy.

Using the twist fixture design, the author has managed to test on several chassis of different manufacturers. These tests were performed to compare the stiffness values of the different chassis. The results show that the uncertainty and standard error were below 5%. Due to this uncertainty in the measured data, small changes in stiffness such as that contributed by the engine cannot be measured reliably with the fixture.

In addition to measuring the overall stiffness of a chassis, the author also had recommended that the fixture also could be used to measure the deflection distribution along the length of a chassis. Using several additional dial indicators located at key locations, the fixture could determine sections of the chassis that

deflect more than others. Therefore, the chassis could be strengthened in those areas to increase the overall torsion stiffness.

Finally, the used of twist fixture also could be used to validate finite element models. Several models have been developed to predict the torsion stiffness of the chassis as well as the roll stiffness of the combined suspension and chassis system. The use of twist fixture on a chassis that has been measured for a finite element model will be very beneficial in ensuring that the models were accurate.

Murali M.R. Krishna [6] has presented his study on the Chassis Cross-Member Design Using Shape Optimization. The problem with the original chassis was that the fundamental frequency was only marginally higher than the maximum operating frequency of the transmission and drive shaft, which were mounted on these cross-members. The aim of this testing was to raise the cross-member frequency as high as possible (up to 190-200 Hz) so that there was no resonance and resulting fatigue damaged. The Finite Element Model (FEM) of the frame with the #3 cross member was shown in Figure 2.2. The frame was completely fixed at the four corners of the side rails as shown. A modal analysis performed on this model indicated that the first natural frequency was about 179 Hz. Firstly, a sizing optimization was attempted which indicated that the mass was a predominant factor. Four additional holes were added to the sides of the cross-member to reduce its mass. Another tests also have been conducted which the holes on the sides had to be expanded, the bottom holes to be reduced in size, the thickness of the attachment bracket to be increased etc. Based on those testing, the fundamental frequency of the cross-member was raised by about 4 Hz, resulting in a better design.

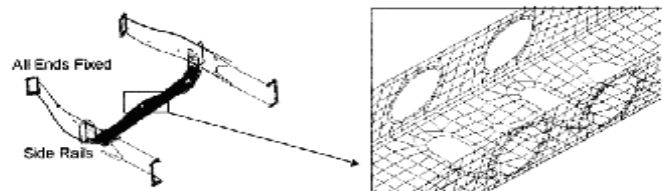


Figure 2.2: Finite Element Model of #3 Cross-members [6]

On the other hands, the author had analyzed the cross-member in order to

obtain the global torsion value of truck chassis. This value was utilized as a reference for future study in order to improve ride ability and conformability during operation. From the literature study, it has been found both theories and practices found that the torsion affect was more severe load case rather than bending load.

One of case study conducted by Wesley Linton [7] from Cranfield University on the chassis supplied by Luego Sports Cars Ltd stated that, the initial torsion value was calculated about 1330 Nm/deg. from a mass of 120.1 kg. There were many types of adjustment and modification made to the chassis to improve the torsion stiffness values such as the additional cross bar structures, improvement of the structure material and many others. As a result, the overall torsion stiffness has been significantly increased to 337% of its initial value. Therefore, a significant changed on modification has resulted the overall chassis structure has tremendously improved and enhanced the chassis performance such as ride quality, vibration and etc.

Another case study was conducted by Marco Antonio Alves [8] on the Avoiding Structural Failure via Fault Tolerance Control. There were two approaches or option used, firstly the structural modification and secondly by some active modification. In this case the author has chosen the second option only. The aims of study were to decrease the vibration on the truck and consequently increase life of the structure. The study used a Finite Element Model of a truck to represent the vibrations phenomena as shown in Figure 2.3.

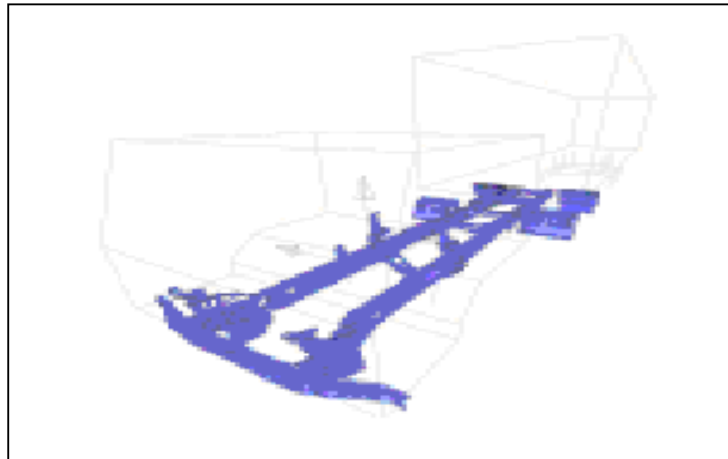


Figure 2.3: General truck view

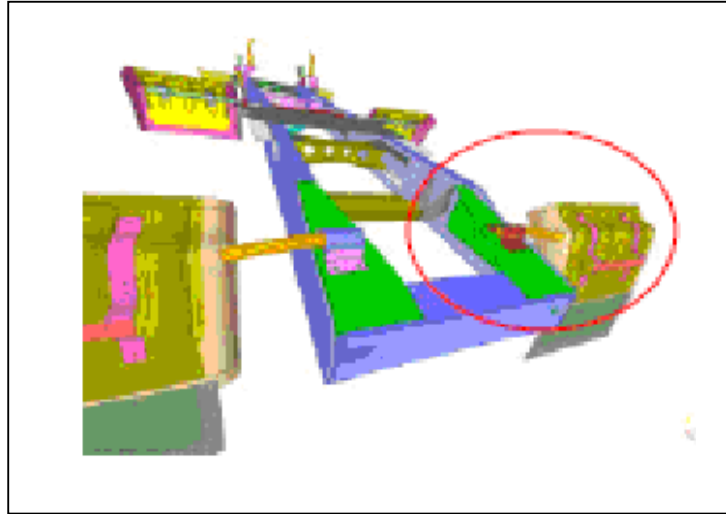


Figure 2.4: Failure Location

Figure 2.4 shows the chassis that has high stress level. The stress levels were the consequences of the truck vibration. This problem decreased the operation life of the truck and consequently the maintenance cost was increased. The author had used finite element model (FEM) to simulate the transient response. With this result a state model was estimated and based on it the process control was implemented. The results show that the first situation was solved with good quality. The amplitude was very high and after the control application the amplitudes became $\pm 2Gs$. The first conclusion was that the high amplitude could be solved by a traditional control. The necessary force to reduce the amplitudes was something possible to implement because the maximum force was $\pm 700 N$.

The second problem investigated was the amplitude variation when a failure happens during the control process. The results showed a significant variation proving the lost of quality. In order to solve this bad situation a second controller was implemented and applied. It seems that the result would have the result improved by a better variation of controller.

The author from Clemson University, Lonny L. Thompson [12] had conducted a study on the effects of chassis flexibility on roll stiffness of a racecar. The primary objectives of his study were to determine the effects of overall chassis flexibility on roll stiffness and wheel chamber response to the racecar chassis and

suspension. The methodology that he had applied was the Finite Element Model (FEM). The model was built based on an assembly of beam and shell elements using geometry measured from a typical of a racecar. In order to validate the model, the author had managed to test the chassis with the wheel loads changed when the jacking force was applied to rolls the chassis. Then, he found that, the result from FEM and measured data were agreed between each other.

Further analysis on the effects of the chassis flexibility on roll, the torsional stiffness was increased by 130% by adding strategic members to the chassis structure. The results from FEM had indicated that, the effective roll stiffness on the front suspension interacting with the chassis increased by 7.3% over a baseline chassis. Based on those results, it can be concluded that as the chassis stiffness was increased, the front roll stiffness had changed very little. Therefore, it can be concluded that, the minimum torsional stiffness was required so that the effective roll stiffness of the front suspension was within 3%.

2.1.1 Overall Discussion on Truck Chassis Research

It can be concluded that, many of the truck structures found in the research are subjected to internal and external loads, which affected the ride quality of vehicle. These loads and behavior can be determined through a series of processes namely, Modal Analysis, Finite Element and Torsional Analysis. Besides that, the correlation and modal updating technique also important in order to create a good model for further analysis. From the global torsion analysis, it has been found that the torsion load is more severe than bending load. In order to overcome this problem, a cross bar and material selection are very important to consider during design stage. Furthermore, the overall achievement is mainly to reduce the vibration level, so that the life of the structure and performance can be maximized.

2.2 Overview of chassis types

2.2.1 Definition of a Chassis

The chassis is the framework that is everything attached to it in a vehicle. In a modern vehicle, it is expected to fulfill the following functions:

- i. Provide mounting points for the suspensions, the steering mechanism, the engine and gearbox, the final drive, the fuel tank and the seating for the occupants;
- ii. Provide rigidity for accurate handling;
- iii. Protect the occupants against external impact.

While fulfilling these functions, the chassis should be light enough to reduce inertia and offer satisfactory performance. It should also be tough enough to resist fatigue loads that are produced due to interaction between the driver, engine, power transmission and road conditions.

2.2.2 Ladder frame

The history of the ladder frame chassis dates back to the times of the horse drawn carriage. It was used for the construction of 'body on chassis' vehicles, which meant a separately constructed body was mounted on a rolling chassis. The chassis consisted of two parallel beams mounted down each side of the car where the front and rear axles were leaf sprung beam axles. The beams were mainly channeled sections with lateral cross members, hence the name. The main factor influencing the design was resistance to bending but there was no consideration of torsion stiffness.

A ladder frame acts as a grillage structure with the beams resisting the shear forces and bending loads. To increase the torsion stiffness of the ladder chassis cruciform bracing was added in the 1930's. The torque in the chassis was restrained by placing the cruciform members in bending, although the connections between the beams and the cruciform must be rigid. Ladder frames were used in car construction until the 1950's but in racing only until the mid 1930's. A typical ladder frame shown as below in Figure 2.5.

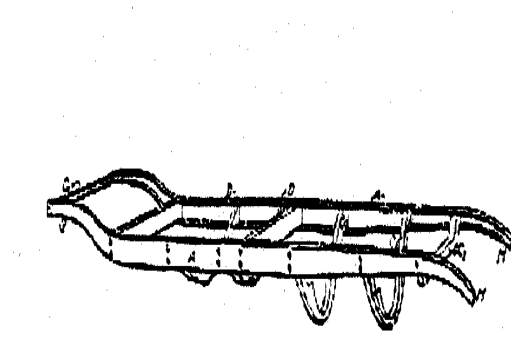


Figure 2.5: Ladder frame chassis

2.2.3 Twin tube

The ladder frame chassis became obsolete in the mid 1930's with the advent of all-round independent suspension, pioneered by Mercedes Benz and Auto Union. The suspension was unable to operate effectively due to the lack of torsion stiffness. The ladder frame was modified to overcome these failings by making the side rails deeper and boxing them. A closed section has approximately one thousand times the torsion stiffness of an open section. Mercedes initially chose rectangular section, later switching to oval section, which has high torsion stiffness and high bending stiffness due to increased section depth, while Auto Union used tubular section. The original Mercedes design was further improved by mounting the cross members through the side rails and welding on both sides. The efficiency of twin tube chassis' is usually low due to the weight of the large tubes. They were still in use into the 1950's, the

1958 Lister-Jaguar being an example of this type. A typical twin-tube chassis is shown in Figure 2.6.

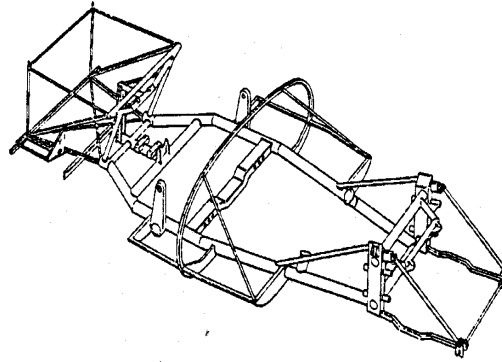


Figure 2.6: Twin-tube chassis

2.2.4 Space frame

Although the space frame (Figure 2.7) demonstrated a logical development of the four-tube chassis, the space frame differs in several key areas and offers enormous advantages over its predecessors. A space frame is one in which many straight tubes are arranged so that the loads experienced all act in either tension or compression. This is a major advantage, since none of the tubes are subject to a bending load. Since space frames are inherently stiff in torsion, very little material is needed so they can be lightweight. The growing realization of the need for increased chassis torsion stiffness in the years following World War II led to the space frame, or a variation of it, becoming universal among European road race cars following its appearance on both the Lotus Mk IV and the Mercedes 300 SL in 1952. While these cars were not strictly the first to use space frames, they were widely successful, and the attention they received popularized the idea.

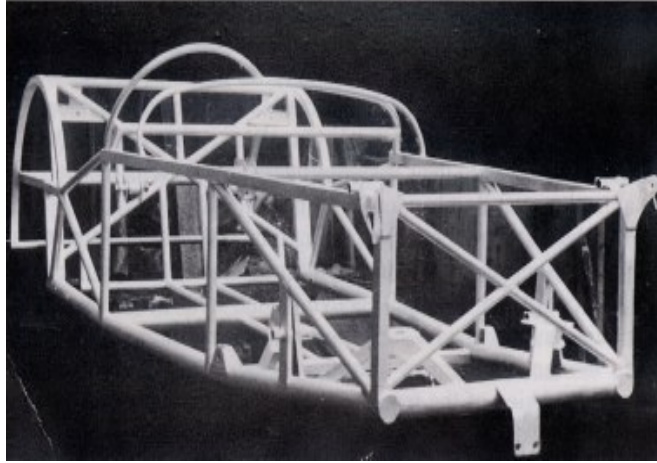


Figure 2.7: 1952 Lotus Mk.IV spaceframe

CHAPTER 3

RESEARCH METHODOLOGY

3.1 Identification of Problem

The chassis frame forms the backbone of the truck and its chief function is to safely carry the maximum load wherever the operation demands. Basically, it must absorb engine and axle torque and absorb shock loads over twisting, pounding and uneven roadbeds when the vehicle moving along the road.

For this project, the truck chassis is categorized under the ladder frame type chassis. Figure 3.1 shows a typical ladder frame chassis for commercial vehicle. A ladder frame can be considered structurally as grillages. It consists of two side members bridged and held apart by a series of cross members. The side members function as a resistance to the shear forces and bending loads while the cross members give torsion rigidity to the frame. Most of the light commercial vehicle chassis have sturdy and box section steel frames, which provide this vertical and lateral strength and resistance to torsion stress.

There are some advantages and disadvantages when using ladder frame chassis. One of the advantages is the ease of mounting and dismounting the body structure. Various body types ranging from flat platform, box vans and tankers to detachable containers can be adapted easily to a standard ladder frame chassis. Besides that, the noise generated by drive train components is isolated from the passenger compartment through the use of rubber chassis design which yields a relatively inexpensive and easy manufacturing process compare to other type of chassis.

While the main disadvantages of the ladder frame is its torsion rigidity. Since it is a two-dimensional structure, its torsion rigidity is very much lower than other chassis, especially when dealing with vertical load or bumps. The weight of the ladder chassis is also high compare to other types of chassis. Besides that, the overall chassis structure is currently not so good for the actual analysis due to the chassis being old and several portions are badly corroded and therefore, the strength of the structure especially at the welding area may affect the analysis results. The chassis specifications specifically for this study are listed in Table 3.1 below.



Figure3.1: Parallel ladder type frame

Table 3.1: Material specification of truck chassis

Model	Material	Dimension (m)	Young Modulus,GPa	Density (kg/m ³)	Poisson's ratio
Suzuki	Mild Steel	3.1x1.08x0.1	200	7850	0.30

3.2 Research Methodology

In this project, Modal Analysis, Torsion Test, Finite Element and other analysis were used to determine the characteristics of the truck chassis. All methodology principles and theories discussed in Chapter 2 were utilized to achieve the project's objectives. The combination of all the analysis results were used to develop virtual model created using FEM tools and the model was updated based on the correlation process. Further analysis and modification were then executed to the existing truck chassis design and finally proposed a new truck chassis.

For the purpose of this study, the truck chassis was modeled using Solid works software according to the original size of structures. The model was then imported into Finite Element software (ANSYS). The purpose was to determine the natural frequencies and mode shapes. For the meshing analysis, 10 node-tetrahedral elements were chosen to model the solid chassis. Study by previous researches [2] found that 10 node-tetrahedral elements gave a closer dynamic behavior to the experimental results.

The next step was to undertake Experimental Modal Analysis. This was to determine the natural frequencies, mode shapes and damping ratio from the real structure of the truck chassis. In order to maintain the quality of results, impact hammer and shaker force methods were used and both results were compared to get better agreement in term of data precision, quality and reliability. Then, the result from finite element

analysis and experimental modal analyses were then compared in order to find the correlation between both methods.

The purpose of carrying out the correlation analysis was to determine how far the finite element analysis agrees with the model testing. If there were discrepancies between both analyses, thus the model updating analysis was performed. The experimental data were made as a reference in model updating analysis. Based on overall result, proper modifications on the verified model of truck chassis were carried out to improve the chassis's strength. All the steps required in each of the method used to have a valid FE model representative were described in the following section.

The research methodology flowchart for this project was shown in Figure 3.2. The literature review of the truck chassis was carried out to obtain basic understanding of the project. Information like typical natural frequency values of truck chassis, excitation sources and mode shape of truck chassis were searched and reviewed. Then the dimension of an existing truck chassis was measured. The chassis chosen was a Suzuki Jeep model of mass approximately 75kg. The type of chassis was known as parallel ladder type frame with box section as shown in Figure 3.1. The next step was the chassis structural preparation and set up for measurement purposes. The measurement of Frequency Response Function (FRF) data was performed and there were 22 measurement points through out the chassis structure. The FRF data were then transformed into ME's Scope software for further analysis on Modal Analysis.

The Computed Aided Design (CAD) modelling was performed on the existing chassis by using Solids Work Modelling Software. Then, the chassis modelled was completely transformed into the finite element software for further analysis of finite element analysis. Then, the result from both analysis were then compared and the virtual structural model was developed using FEM tools. In this stage, the finite element and experimental torsional analysis were also performed. The objective of these tests were to find the torsion stiffness of the structure and the response of the applied load at different loading condition.

The next step were the correlation and model updating process to obtain the virtual structure of the chassis. Then, the final stage was the modification of the virtual model to find the optimum chassis condition and suited with current market demand. The final result of the modification of finite element analysis was then proposed for future actual modification.

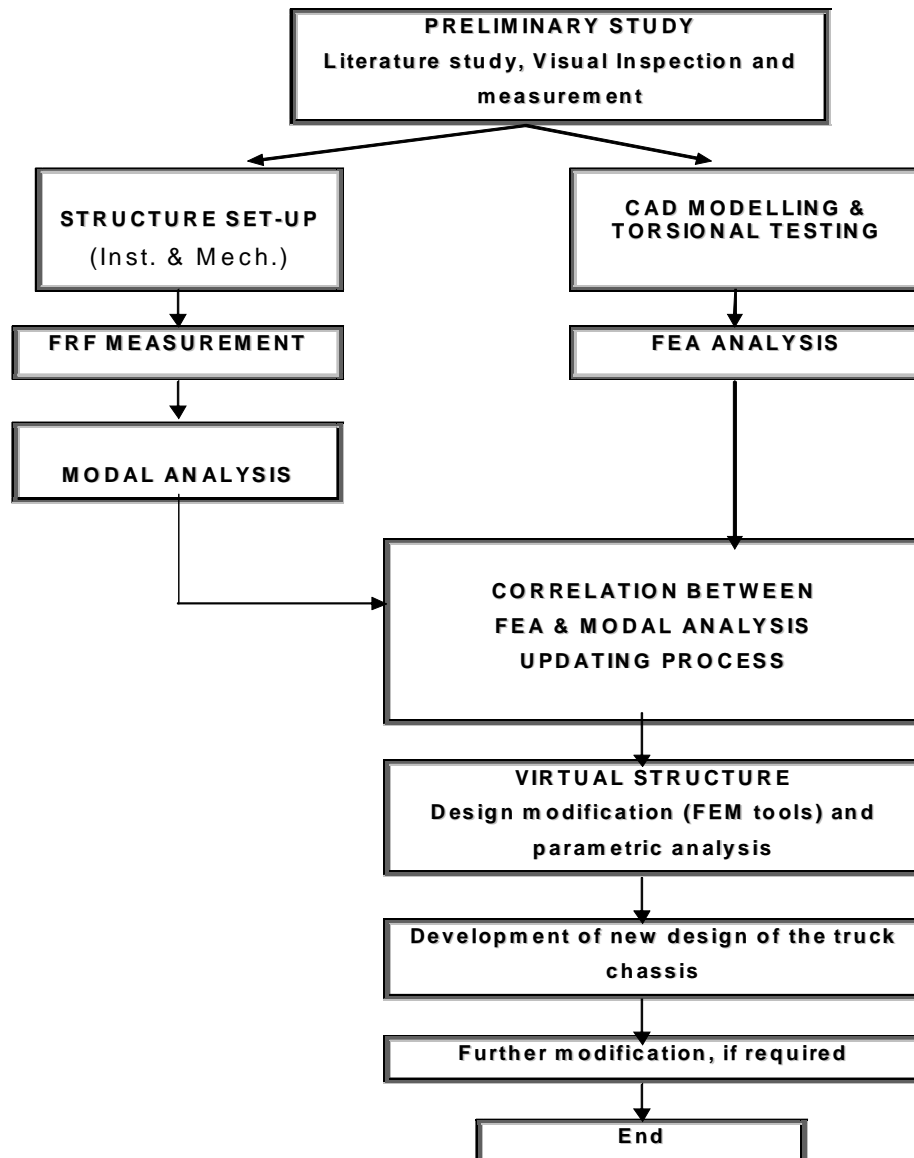


Figure 3.2: Research Methodology Flow Chart

CHAPTER 4

TORSION TESTING OF CHASSIS

This chapter discusses on experimental and finite element analysis of the torsion test. The experimental torsion test was conducted in laboratory by using the test rig that specially designed for twisting load applications and the ANSYS simulation system for finite element analysis (FEA). Both of the result were compared and recorded for further analysis.

4.1 Theory of Load Cases

A chassis is subjected to three load cases: bending, torsion and dynamic loads. The bending (vertical symmetrical) load case occurs when both wheels on one axle of the vehicle encounter a symmetrical bump simultaneously. The suspension on this axle is displaced, and the compression of the springs causes an upward force on the suspension mounting points. This applies a bending moment to the chassis about a lateral axis. (Refer to Figure 4.1)

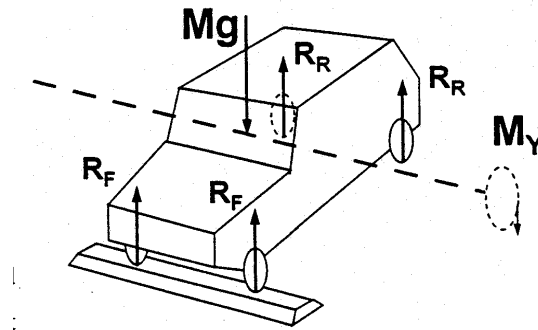


Figure 4.1: Bending Load case [8]

The torsion (vertical asymmetric) load case occurs when one wheel on an axle strikes a bump. This load is causing the chassis in torsion as well as bending. (Figure4.2). It has been found both in theory and in practice that torsion is a more severe load case than bending.

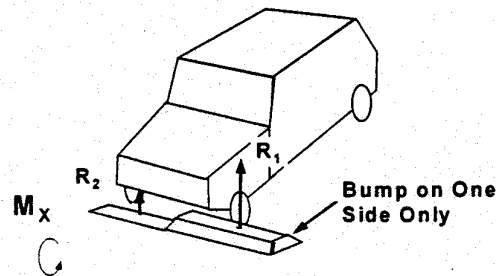


Fig. 4.2: Torsion Load case [8]

The dynamic load case comprises longitudinal and lateral loads during acceleration, braking and cornering. These loads are usually ignored when analyzing structural performance and this analysis will followed the free boundary condition procedures. A torsion stiffness chassis offers a number of advantages:

1. According to vehicle dynamics principles, for predictable and safe handling, the geometry of the suspension and steering must remain as designed. For

instance the camber, castor and toe angles could change with torsion twist causing “bump steer.”

2. Once again according to vehicle dynamics principles, a suspension should be stiff and well damped to obtain good handling. To this end the front suspension, chassis and the rear suspension can be seen as three springs in series as shown in Figure 4.3. If the chassis is not sufficiently stiff in torsion then any advantages gained by stiff suspension will be lost. Furthermore, a chassis without adequate stiffness can make the suspension and handling unpredictable, as it acts as an un-damped spring.

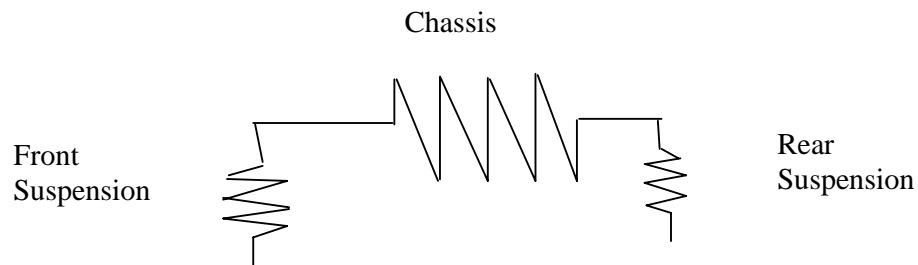


Figure 4.3: Chassis and suspension as springs [8]

3. Movement of the chassis can also cause squeaks and rattles, which are unacceptable in modern vehicles.

4.2 Aims of the testing

The main objectives of the testing were listed below:

- a. To determine the chassis torsion stiffness.

- b. To incorporate a design improvement study and note the effects on the global torsion stiffness of the chassis;

The following limitations were given for this project:

- i. Complex assemblies were avoided.
- ii. The load distribution and adjustment during testing might be altered from zero to 1000 kgf. since there was no load control system from the test rig. The maximum 1000kgf load was applied since there were limitations on the test rig instrumentation, LVDT and due to safety reasons such as high deflection of the chassis could cause failure to the material and support.

4.3 Overview of Chassis Type

The chassis used for this analysis was Suzuki Truck Chassis as shown in Fig.4.4 and it was described as a space frame chassis with ladder type structure. It was constructed from mild steel Rectangular Hollow Section (RHS) and its cross section was supported by mild steel sheet. The majority of the RHS have dimension of 100 x 50 mm with a 2.0mm wall thickness. The detail specifications are as follows:

- Test Sample: Suzuki Truck Chassis
- Material: Mild Steel
- Dimension (LxBxH), mm: 3100x1080x100
- Young Modulus (GPa): 200
- Density (kg/m^3): 7850
- Poisson's Ratio: 0.30



Figure 4.4: Ladder type structure

4.4 List of Instrumentations

Table 4.1 shows the list of tools required for the torsion test.

Table 4.1: List of instrumentations for torsion test

No	Instrumentation	Function
1	Data logger	Data display and set-up measurement controller
2	Linear Variable Displacement Transducer, 50&100mm	To measure the displacement value from truck chassis.
3	Load Cell (5000kgf)	To measure load during testing
4	Testing rig with hydraulic operated machine	Use as a input force during torsion test

4.5 Calculation of the Global Torsion Stiffness

The torsion stiffness was determined from the twist angle between the front and rear axles under a torsion load, either static or dynamic. The static load occurs when the chassis was stationary and one corner elevated, for example under jacking conditions. The forces on the other corners impose a twist torque on the chassis.

The dynamic load occurs when the chassis was moving, for example, when a wheel travels over a bump. The force applied by the bump travels through the wheel and tire into the coil-over and was applied to the coil-over mounting points. This also causes the chassis to twist.

The static load has been chosen for this project as it can be easily replicated for the testing and modeling of the chassis. A load was applied to the mounting points and the torsion stiffness of the chassis can be determined. The torque applied to the chassis was a function of the force acting on the mounting points and the distance between the two fronts or rear mounting points is shown in Figure 4.5 below.

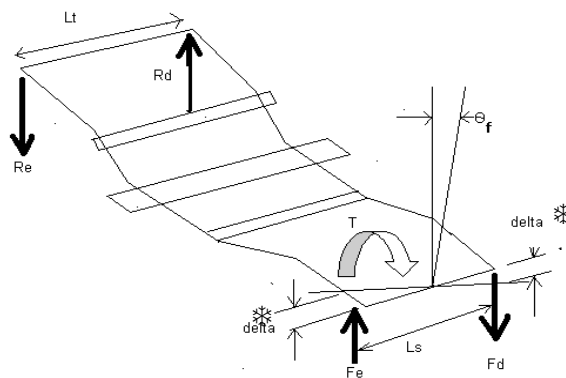


Figure 4.5: Outline of experimental set-up

The global twist angle of the chassis is a function of the vertical displacement between the two involved coil-over mounting points and their distance.

$$\theta_f = 2\delta/L_f \text{ (radians),}$$

where;

L_f : traverse distance to the chassis between the front dial indicators

δ : total deflection of truck chassis ($\delta_d + \delta_e$)

Torque can be derived as:

$$T = [(F_d)/2 + (F_e)/2] \times L_s$$

where,

F_d : force in the right front end of the structure

F_e : force in the left front end of the structure

L_s : traverse distance between the force application points

The torsion angle in the rear part of the structure, θ_t , is determined from the measured displacements in the extremities of the longitudinal rails,

$$\theta_t = [(\delta_d) + (\delta_e)] / L_t$$

where;

δ_d and δ_e are the measured vertical displacements in the dial indicators, separated laterally by a distance L_t .

The global torsion stiffness was measured between the extremities of the chassis. For this load case torsion stiffness could be calculated by:

$$K = T/\theta \text{ (Nm/rad) and , } \theta = \theta_f - \theta_t$$

Where,

K: global torsion stiffness

T: Torque

θ_f : front torsion angle of the structure

θ_r : rear torsion angle of the structure

4.6 Test Rig Operational and Mechanism

For the torsion load testing, the test rig was already available in laboratory testing facilities fabricated specially for this project. It has been designed to cater the torsion and bending load on the chassis. The test rig could be moveable at the front and fixed at the backside. The hydraulic force was controlled by the control valve by pressing the control lever to the required force. (Refer to Figure 4.6 below)

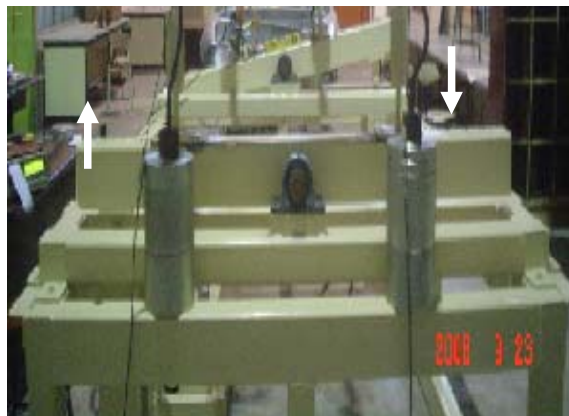


Figure 4.6: Force Direction

The piston cylinder type used for this testing is a double acting type and supplied by Douco Hydro. The traveling speed from bottom to top takes about 8 m/min. The operating temperature was limited to 80 degree Celsius. The maximum operating pressure and design pressure are 160 bars and 200 bars. (Refer to Figure 4.7)

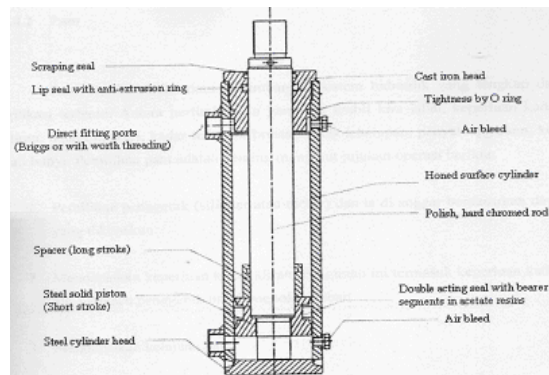


Figure 4.7: Hydraulic Cylinder Arrangement

There are four total cylinders installed at both side of the chassis and it can be adjusted according to the required load. (Refer to Figure 4.8)

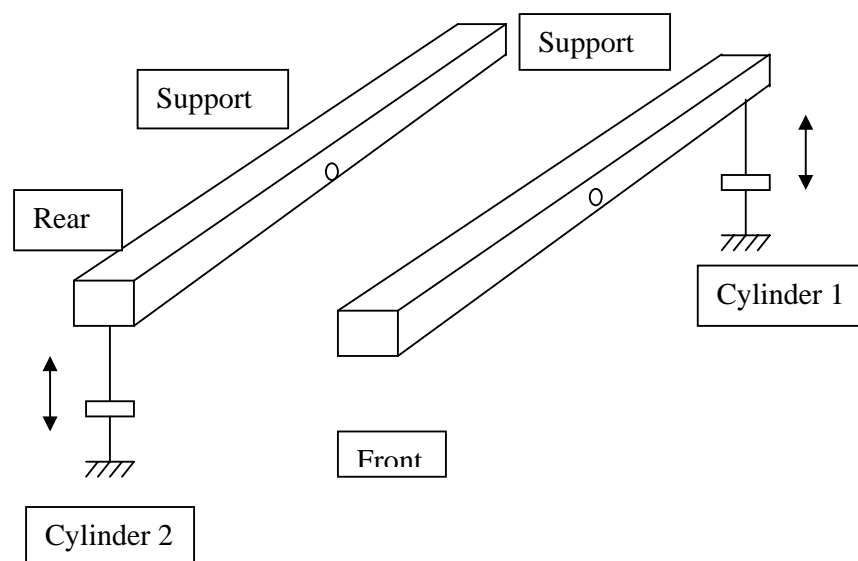


Figure 4.8: Test rig mechanism

4.7 Preparation of test model and Instrumentation Set-Up

The truck chassis was placed onto the test rig and tightened to the position adjustable joint. There were four numbers of adjustable joints attached to the

structure as shown in Figure 4.9 and 4.10. The function of the adjustable joint basically to accommodate variable position of chassis support.

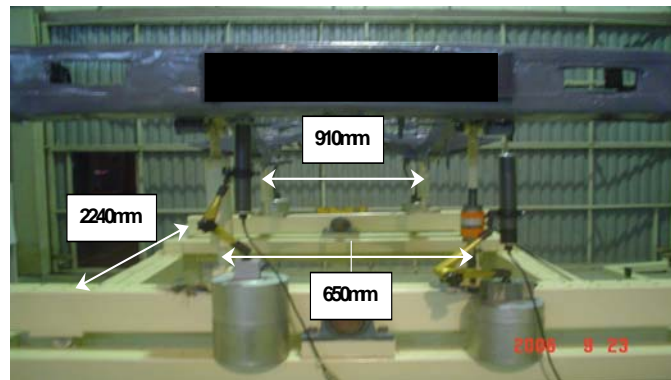


Figure 4.9: Test rig and chassis

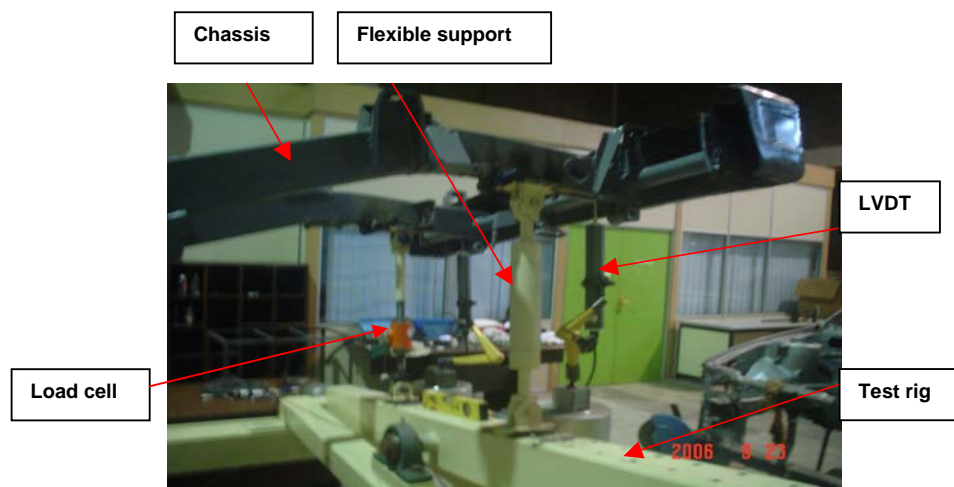


Figure 4.10: Side View

The load cell of 5000 kgf was installed at both sides of the front-end support as shown in Figure 4.10 and monitored closely during the testing. The applied load was recorded by the data logger and captured for each additional load until 1000kgf (9807N). There were two LVDTs installed at the front end as well as at the back of the truck chassis. The range of the LVDT was 0-100mm just to cater the high movement during the testing especially at the front-end structure. (Refer to Figure 4.11)



Figure 4.11: Rear View

4.8 Torsion Test

The truck chassis shown in Figure 4.12 was subjected to minimal load of 200 kgf applied at the front-end side. The front cylinder moved upward while the rear cylinder moved slightly downward. The deflection of the chassis at front and rear support was recorded by the LVDT.



Figure 4.12: Structure at the minimal load

Figure 4.13 shows the truck chassis structure at the maximum load applied. The test requirement was up to 1000kgf (9807N). The chassis structure was at maximum deflection at this moment and recorded through the LVDTs.

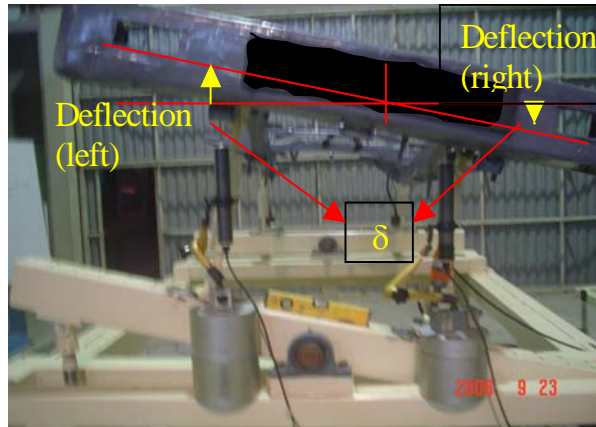


Figure 4.13: Structure at the maximum load@1000kgf

The truck chassis shown in Figure 4.14 was the chassis condition viewed from rear side. The LVDTs were placed at both ends of the truck chassis to measure any deflection during the test. In actual case, the rear end side should be fixed and no more deflection should be occurred.



Figure 4.14: Rear view of testing structure

The chassis shown in Figure 4.15 is the side view of the structure during test. All the connections attached to the chassis were tightened correctly in order to avoid any mistake during the testing. All the LVDTs were installed to the required position. (Refer to Figure 4.16)



Figure 4.15: Side view of testing structure



Figure 4.16: Rear support

4.9 Torsion Stiffness Test using Finite Element

The theoretical analysis has been carried out using the finite element analysis to obtain the torsion value of the truck chassis. The objectives of this analysis are to evaluate and perform the comparison analysis between theoretical and experimental results. The specification of the truck chassis as shown in Figure 4.17 and the step of the full test procedures are highlighted below.

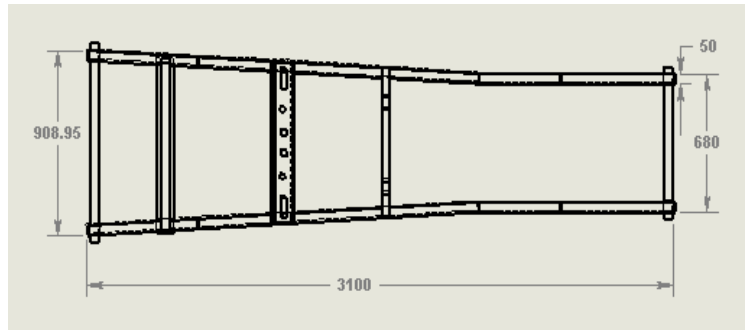


Figure 4.17(a): Dimension of the truck chassis (All dimensions in mm)

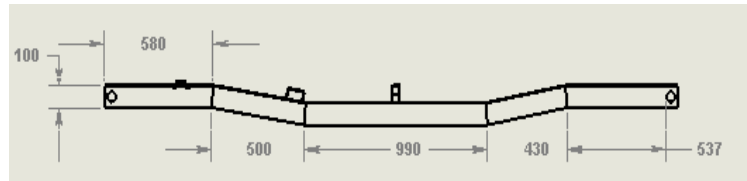


Figure 4.17(b): Dimension of the truck chassis (All dimensions in mm)

- i. Figure 4.17 shows the geometrical dimensions of the truck chassis
- ii. The truck chassis structure was modeled using SOLIDWORK software to create the model as shown in figure 4.18. The chassis structure are closed rectangular profile longitudinal rails and tubular section cross members.
- iii. The drawing was then exported into the finite element software, which the ANSYS software simulation system.
- iv. The material and element properties of the chassis structure were then defined. The chassis properties were listed as below:
 - a. Modulus of Elasticity, E = 200Gpa
 - b. Coefficient of Poisson, ν = 0.30
 - c. Mass density, ρ = 7850 kg/m cubes
- v. The tetrahedral-10 element was used in the meshing procedure because of 3D and solid modeling of truck chassis and was meshed on auto meshing. Figure 4.18 shows the FE model and general overview finite element mesh of the truck chassis with 31,489 elements and 62788 nodes. These results were based on the element set-up on the testing parameter.

- vi. The free-free boundary condition was adopted in order to obtain the natural frequencies and mode shapes. Therefore, neither constraints nor loads were assigned in attempt to stimulate the free-free boundary condition which means all the brackets and support such as absorbers, spring leaves and engine were removed from the chassis as shown in Figure 4.19.
- vii. The normal mode analysis was executed in order to find the natural frequencies and mode shapes of the chassis. The frequency range of interest was set between 20 to 140Hz because the maximum normal frequency for the truck was tuned from 70-80 Hz while in running and the normal engine idling frequency was below 19 Hz.



Figure 4.18: Truck chassis model meshed with tetrahedral -10 elements

Meanwhile, the following considerations were taken into account during the model construction in order to simplify the analysis:

- i. All brackets were excluded from the model.
- ii. The connections between longitudinal rail and cross member were considered perfect. This consideration represents practically a perfect welded joint. However where the weld was not perfect, these consideration could make the model stiffer than the real system.
- iii. The material was considered isotropic in its elastic phase.

The truck chassis was fixed at the rear-end structure. The load was applied at the front-end structure and the applied load was 9807 N on both directions. (Refer to Figure 4.19)

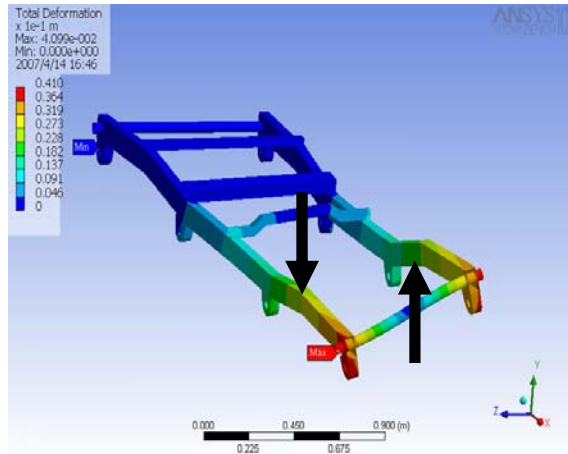


Figure 4.19: Torsion Test using ANSYS software system

From the test result, it shows that the total deformation was 41 mm from the original position, which occurred at front-end and low reading was recorded at the back of the truck chassis that was fixed during the testing.

4.10 Torsion Analysis results

The Torsion test was conducted to the chassis, which comprises of two main testing that include the experimental and finite element analysis. The results were then compared to gauge the improvement result and from there, the torsion stiffness value was utilized for better quality vehicle.

4.10.1 Experimental result

The experimental test was conducted to the truck chassis as shown in Figure 4.5 and the maximum torsion load at 1000kgf was applied and the total deflection was recorded as listed in Table 4.2.

Table 4.2: Experimental results of torsion test

L_f (m)	L_s (m)	L_t (m)	δ (m)	δ_d (m)	δ_e (m)	$(F_d \& F_e, N)$
0.65	0.65	0.91	0.07	0.02	0.02	9806.65

Note:

- ✓ δ is the actual deflection value from front side (front)
- ✓ δ_d & δ_e are the actual deflection from left & right (back)

Based on the results, the analysis of the structure was continued with the calculation of the global torsion stiffness to see how the value and the chassis stiffness can withstand with the existing operational load. As a sample, the calculation was calculated at the maximum load condition:

The twist angle, $\theta_{\text{twist}} = \theta_f = 2\delta/L_f$ (radians)

$$\theta_{\text{twist}} = \theta_f = 2(0.07)/0.65 = 0.2056 \text{ radian.}$$

Torque is calculated from: $T = [(F_d)/2 + (F_e)/2] \times L_s$

$$T = [(9807)/2 + (9807)/2] \times 0.65 = 6374.32 \text{ Nm}$$

The torsion angle in the rear part of the structure, θ_t , was calculated from the measured displacements in the extremities of the longitudinal rails.

$$\theta_t = [(\delta_d) + (\delta_e)] / L_t = [(0.02) + (0.02)] / 0.91 = 0.04 \text{ radian}$$

As a result, the global torsion stiffness can be calculated from,

$$q = T/\theta = 6374.32 / (0.2056 - 0.04) = 38987 \text{ Nm/radian.}$$

4.10.2 Finite Element Result of Torsion Test

The calculation of torsion values were based on the value of deflection recorded by the FEA analysis and therefore,

Table 4.3: Experimental results of torsion test

L_f (m)	L_s (m)	L_t (m)	δ (m)	δ_d (m)	δ_e (m)	(F_d & F_e ,N)
0.65	0.65	0.91	0.05	0	0	9807

The twist angle, $\theta_{\text{twist}} = \theta_f = 2\delta/L_f$ (radians)

$$\theta_{\text{twist}} = \theta_f = 2(0.0509)/0.65=0.1566 \text{ radian.}$$

Torque was calculated from, $T=[(F_d)/2 + (F_e)/2] \times L_s$

$$T=[(9807)/2 + (9807)/2] \times 0.65=6374.32 \text{ Nm}$$

The torsion angle in the rear part of the structure, θ_t , was calculated from the measured displacements in the extremities of the longitudinal rails.

$$\theta_t = [(\delta_d) + (\delta_e)] / L_t = 0 \text{ (Totally fixed)}$$

The global torsion stiffness can be calculated from,

$$q=T/\theta=6374.32/(0.1566)=40700.47 \text{ Nm/radian}$$

Table 4.4: Comparison between FEA & Experimental Torsion analysis at maximum load (1000kgf)

Analysis	Torsion stiff. (kNm/rad.)	Max. Def. (mm)	Torsion stiff. %	(Def., %)
Experimental Analysis	38987	50	4%	0%
FEA Analysis	40700	50		

Result from experimental and finite element analysis of torsion test are shown in Table 4.4. Originally, the purpose of the testing was aimed on increasing the torsion stiffness of existing chassis. Due to that reason, several steps were identified to improve and enhance the quality of truck chassis with additional modification on chassis sub-structures and the thickness of the structure was also increased to certain value with acceptable limit. The initial result from experimental analysis was 4% lower than FEA analysis. The major factor that could relate to this result was the stiffness of the FEA model was greater than the stiffness of the real structure because parts of the real structure were badly corroded thus reducing the stiffness. Also there were probably some errors during testing such as the structure deflection at the back of the structure. After the modification, which the thin wall thickness from the central support had slightly been increased by 2mm (test 1), the torsion stiffness values realized was reduced by 23% from the original value and this result shows that the truck chassis had dominated by the mass instead of thickness.

CHAPTER 5

MODAL ANALYSIS ON CHASSIS

Modal Testing was carried out experimentally to determine the dynamic characteristics of the chassis. These characteristics are the natural frequencies, damping and mode shapes. This chapter presents two methods of testing conducted on the chassis structure, namely Impact Hammer and Shaker tests. The results of both tests were used to justify and update the numerical model.

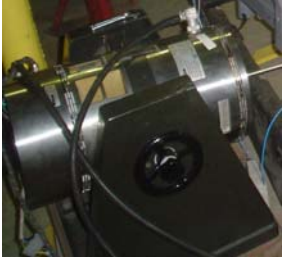
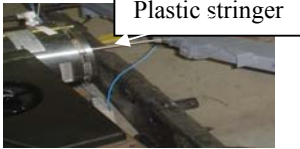
5.1 List of Instrumentation

The instrumentation used during the experimental modal analysis was listed in Table 5.1.

Table 5.1: List of Instrumentation and Function

No	Instrumentation	Function
1	Data analyzer, Model: PAK-MULLER-MK II	Used to analyze or process the output data from hammer force, shaker and accelerometer voltage before it is processed or analyzed by the

		software. The analyzer simultaneously measures the force and response, converts them into digital signals and computes their Discrete Fourier Transform (DFT).
2	Laptop with software PAK Version 5.2 and ME Scope Version 5.0 	Used for data acquisition, display and storage. It displays the frequency response function in different formats of graphical representation such as magnitude frequency, phase frequency & etc.
3	Accelerometer, Model: Kistler 	Measures the dynamic behavior such as the response time of the test input. It generates an electrical output when subjected to mechanical shock or vibration. It is a voltage type with a frequency range of 0-22KHz
4	Impact hammer 	Its function is to create a variety input force waveforms to excite the structural modes. The stainless steel head of impact hammer is equipped with quartz, low impedance force sensor that accepts impact tips varying in hardness.
5	Voltage cable (white)	Connects the accelerometer to a channel of the data analyzer
6	Charge cable (black)	Connects the force transducer to a channel of the data analyzer
7	Plastic Hammer Tips	Produce a signal of the force pulse by doing the impact hammering onto the test sample.
8	Strings/Belt	Acts as a support in hanging the test sample to realize a free-free condition in the experiment.
9	Charge Amplifier type 2525	Charge amplifier is comprehensive equipment, intended for general vibration measurement

		with a piezoelectric accelerometer input. Its output will be routed to frequency analyzer. Input of the charge amplifier is connected to force transducer.
10	Shaker Body Type 4801 with Exciter Head 4812 	Type 4801 with exciter head 4812 is well suited as the motive force generator in mechanical impedance measurements where only smaller forces are required. It can be used in the calibration of vibrations transducers, both to determine their sensitivity accelerometer and to determine their frequency response up to 7200Hz.
11	Plastic Stringer 	It is used to place the force transducer and connect the chassis and shaker. A plastic stringer is also used to avoid moment force.
12	Force Transducer Type 9712B250	It is designed to measure dynamic, short duration static and impact, tensile and compressive forces in machinery and other constructions. It is mounted so that the force to be measured is transmitted through the transducer. Used with vibration exciters, it can be used for the measurement of frequency response function in conjunction with an accelerometer.
13	Power amplifier type 2706	It is designed to drive small vibration exciters, particularly the shaker body type 4801 with exciter head 4812 to full rating. For this application, the maximum output current should be limited to 1.8A.
14	2-Channel Analyzer type 2034	Generate signal for shaker used.

5.2 Experimental Set-up

There were two test methods used to determine the dynamic behavior of the chassis. There were the Impact Hammer and Shaker Test methods. Experimental procedures for both analysis were describes below:

5.2.1 Impact Hammer Test

- (i) The truck chassis was hanged by using soft rubber cable so that it forms a free-free boundary condition as shown in Figure 5.1 (Chassis suspension area). The stiffness of the cable was far smaller than the chassis, thus ensuring free-free condition.
- (ii) The accelerometer was mounted on the chassis by using the magnetic steels adaptor so that accelerometer would have the same vibration as the structure. The accelerometer output was connected to channel 2 of PAK Data analyzer by using charge cable.
- (iii) A plastic tip was attached to the head of impact hammer in order to obtain a good excitation force, which covers the required frequency range and constantly gave good data collection compared to steel metal tip. The impact hammer output was connected to channel 1 of PAK Data analyzer using a voltage cable.
- (iv) The PAK Data analyzer was then connected to the Laptop using a LAN-cable.
- (v) Figure 5.1 and 5.2 shows the experimental setup for impact hammer test.

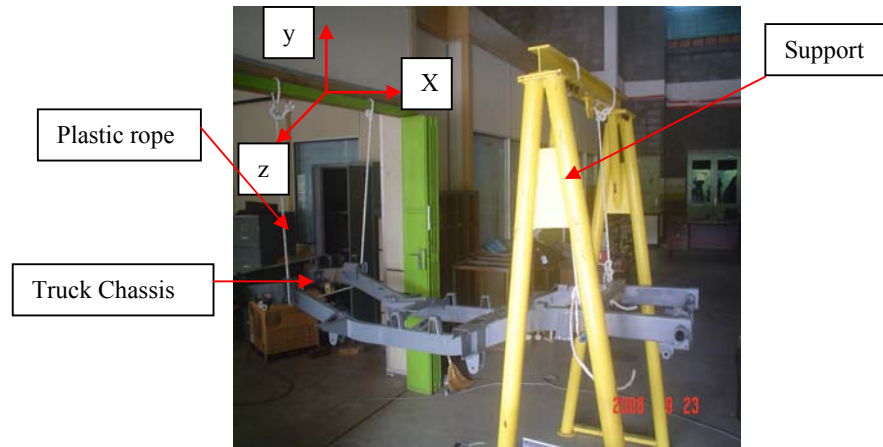


Figure 5.1: Experimental setup for impact hammer test.



Figure 5.2: Experimental setup for impact hammer test.

5.2.2 Shaker Test

- a) A shaker test set-up was shown in Figure 5.3.
- b) Same as in the previous testing, the boundary condition was simulated by hanging the chassis to the testing rig by using very soft plastic rope.

- c) For the shaker excitation, the force transducer was mounted at point 20 in Z direction as shown as in Figure 5.3 between the stringer and truck chassis. The force transducer was then connected to input of the charge amplifier with a cable.
- d) The output of charge amplifier was connected to the channel 1 of PAK Data analyzer using a cable.
- e) The exciter used to perform the analysis is a Shaker Body Type Model 4801 with Exciter Head 4812 where it connects to the output of power amplifier.
- f) An accelerometer was still fixed at one point of the chassis in x-z plane by using wax and then connected to the channel 2 of PAK Data Analyzer.
- g) Finally the PAK Data analyzer was connected to the Laptop using a LAN-cable.



Figure 5.3: Shaker Test Set-up

5.3 Experimental Procedure

Overall experimental procedures were developed into two types of test, which included the experimental impact hammer and shaker test. The arrangements of experimental set-up are shown in Figure 5.1 and 5.2.

5.3.1 Impact Hammer Test

- (i) Firstly, the PAK Data Analyzer and the laptop were switched on.
 - (ii) The PAK program was opened by clicking the icon drive on the PAK data analyzer.
 - (iii) Then, auto-range of the excitation signals was done by knocking the hammer (with plastic tip) at point 1 in y-direction on the chassis three times in order to get the reference excitation signal. This step is to ensure the data collection during testing are reliable and with minimum error.
 - (iv) Upon getting the calibrated signal as reference (as shown in Figure 5.4), the experiment was continued by knocking at the same point as step number (iii) at least 4 times to get 4 valid data of excitation signals.
- Note:** A consistent knocking is necessary to get an accurate data
- (v) From the user interface, the Frequency Response Function (FRF) of the point was obtained.
 - (vi) This process was repeated for the next point until twenty-two points of the truck chassis.
 - (vii) After all the points were taped, the Frequency Response Functions (FRFs) of all the points were saved in UFF format.

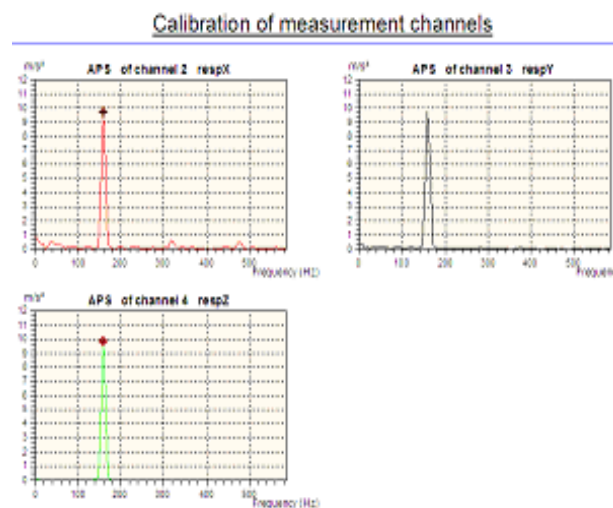


Figure 5.4: Calibration result for experimental Modal Analysis

5.3.2 Shaker Test

- (i) Firstly, the PAK Data Analyzer, Laptop, power amplifier and 2-channel analyzer were switched on.
- (ii) The PAK program was opened by clicking the icon to drive the PAK data analyzer.
- (iii) There are 22 points marked on the chassis. Initially, the accelerometer was mounted at the first point of chassis using wax.
- (iv) Then the noise signal function was set to random type with the built-in generator in 2-channel analyzer to excite the chassis. The reason of using random type signal were basically due to ease on implementation and to prevent leakage of excitation signal that can caused distortion of measured frequency response function.
- (v) The amplifier gain was tuned to level 2 or 3 in order to start the shaker. (Minimum level to excite forces)
- (vi) The start icon on the screen in the PAK interface was clicked to start the test. It was allowed to run until it reaches an averaging of 100 or until the system stabilized using minimum changes in data, then it can be stopped.
- (vii) From the user interface, the Frequency Response Function (FRF) of the point was obtained. This FRF was calculated by PAK-Muller-MKII data analyzer and the frequency range of interest was set to 800 Hz. (Based on initial test, it was identified that the lower natural frequency were below 800Hz)
- (viii) After that, the start button was clicked again and the process was repeated for the second point until last points on the chassis.
- (ix) After all the Frequency Response Function (FRFs) were saved and exported to ME Scope software in UFF format.

5.4 Analysis of Data

The data of experimental result were imported into ME Scope software to carry out the Modal Analysis:

- (i) Open the ME Scope program by clicking the icon on the desktop.
 - (ii) In the ME Scope program, the model of truck chassis with 22 points as shown in Figure 5.5 to represent the testing structure.
 - (iii) The data blocks consisting of Frequency Response Functions (FRFs) of all the points were imported from PAK program.
 - (iv) All the spectrums of each measurement points were then overlaid and the results from the 22 points of the truck chassis were superimposed into one plot.
 - (v) The plot was then curve fitted to extract the modal parameters of the truck chassis. In this case, the modal parameters were calculated using the Multi-Degree of Freedom Global Polynomial Modal Identification Method.
- Note:** Most common method used Multi-Degree of Freedom because the band over which data was attracted, the number of modes contained in the data and the inclusion of residual compensation terms for the estimation of algorithm.
- (vi) The natural frequencies and damping values were then obtained and saved.
 - (vii) After that, the simulation of the mode shape was performed. The figures for the first seven mode shapes were recorded.

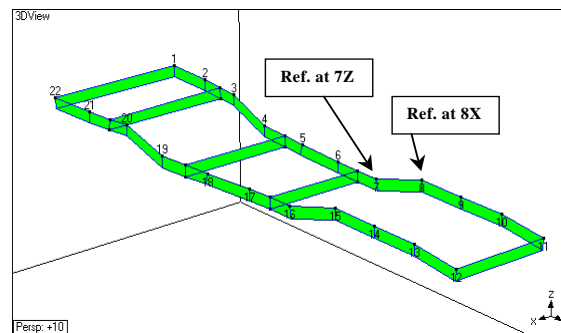


Figure 5.5: The 22 excitation and the reference points

5.5 Experimental Modal Analysis Results

This modal testing was carried out to determine the vibration parameters, which include natural frequency, modal damping and mode shape of the truck chassis. The mode shape was determined in X and Z directions, thus requiring two impact tests. Figure 5.5 shows the orientation of chassis axis. From the mode shape, the deflection patterns of the truck chassis at the first seven natural frequencies were revealed.

5.5.1 Impact Hammer Testing Result

Basically there were 22 points marked on the truck chassis in X and Z directions where at these points frequency response functions, (FRF) were measured. Figure 5.6 and 5.7 show the superimposed frequency response function obtained from point 1 to point 22 during the impact hammer test. Two testing were carried out. The reference was the response where accelerometer placed at point 7 in Z-direction and in another test was placed at point 8 in X-direction. Curve fitting was done by the ME Scope software to all measured FRFs in the range of frequency interest as shown in figure 5.6 and 5.7. From the graph also, it was different between the overlay result in both z-direction and x-direction. These phenomena could be from the stiffness and damping value of truck chassis. The chassis has had higher stiffness and damping characteristic in the X-direction (horizontal lateral) compared to Z-direction (vertical lateral). The fundamental natural frequency obtained from Z-direction was lower than X-direction. These phenomena had resulted from the higher damping and stiffness characteristic in X-direction. Basically, natural frequency was defined as $f = \frac{1}{2\pi} \sqrt{k/m}$. For same chassis and constant mass, the frequency was corresponding directly to stiffness. Then the natural frequency in X-direction start at much higher frequency as the stiffness in X-direction was high, as depicted in Figure 5.7.

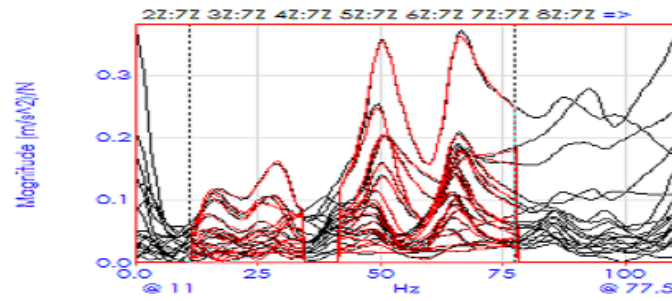


Figure 5.6: Superimposed FRF in Z-direction by impact hammer

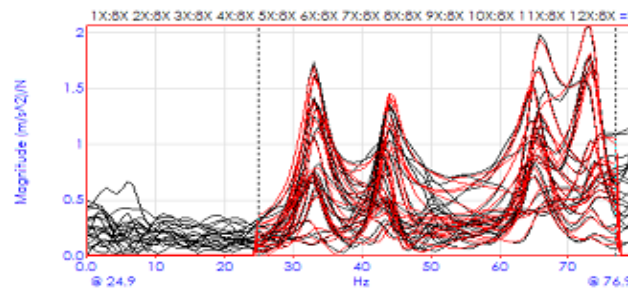


Figure 5.7: Superimposed FRF in X-direction by impact hammer

All the peaks occurred at same frequency. The only difference was the magnitude, which is controlled by the damping at the point of measurement. Then the plot indicates wide differences in damping at all the points of measurement compared to point measured in X-direction as shown in Figure 5.7. All the modal parameters results were tabulated in Table 5.2 while the first 7-mode shape of truck chassis obtained by impact hammer test as shown in Figure 5.8.

Table 5.2: Modal parameters based on impact hammer method (X & Z axis)

Mode	Impact Hammer Test		Mode Shape
	Modal Frequency (Hz)	Damping (%)	
1	23.2	12.40	Torsion
2	30.1	10.20	Torsion
3	32.8	4.97	Bending
4	43.9	3.21	Bending
5	48.3	8.40	Torsion
6	63.8	4.60	Torsion
7	73.7	2.09	Bending

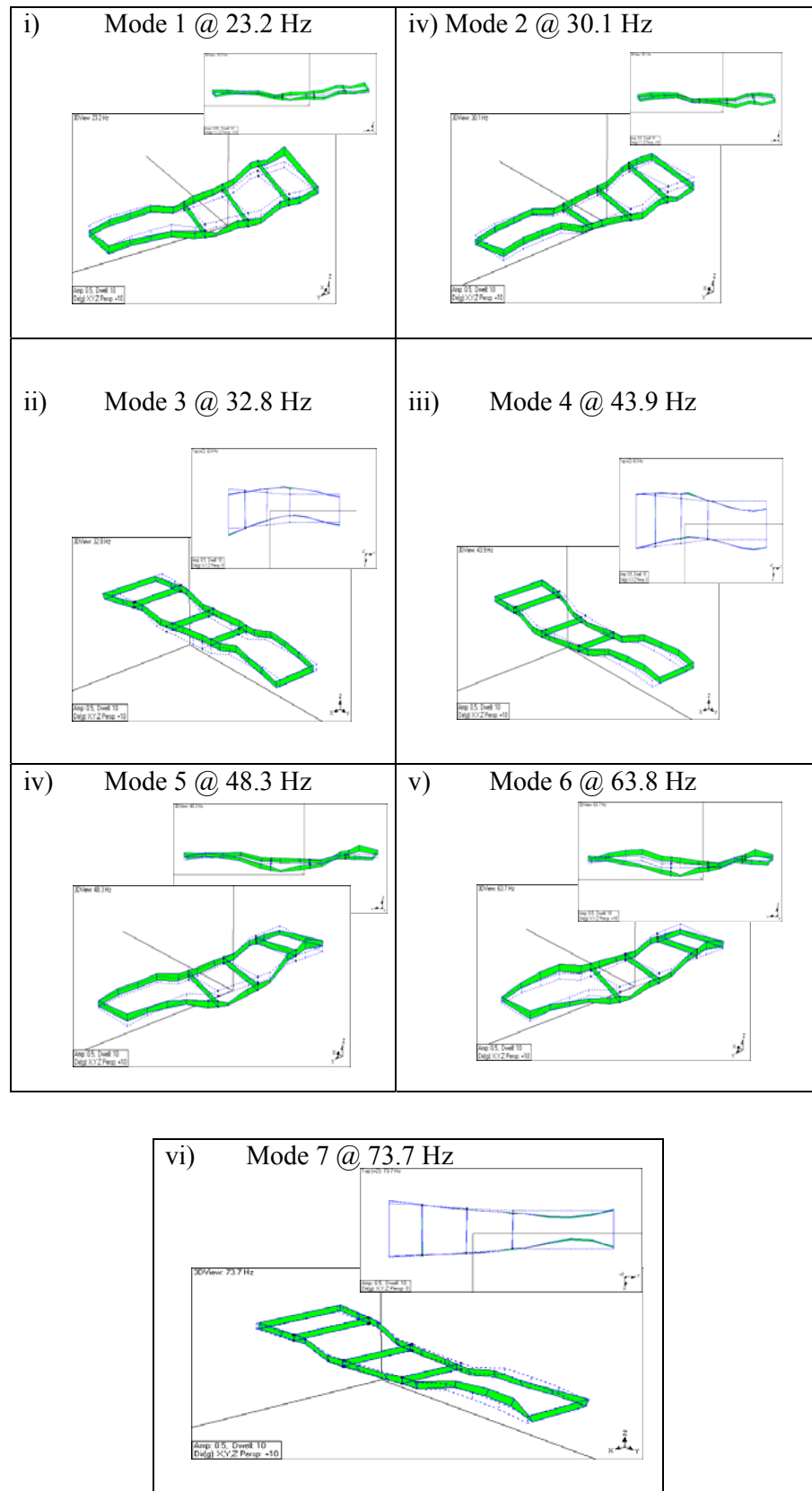


Figure 5.8: Experimental Mode shape by impact hammer

5.5.2 Shaker Testing Result

Figure 5.9 below shows the superimpose FRFs in Z-direction from point 1 to point 22 obtained using random excitation signal in the 0-140 Hz frequency range. In this test, the excitation and response were measured only in Z-direction. The natural frequencies were the frequency of each peak, which occurred within the frequency range. In this test, the coherence check was conducted to ensure that high quality and consistency of data (coherence >0.7) being collected during the FRF measurements. As a result of these checks, it was determined that only 18 points produced satisfactory coherence. Poor coherences (below 0.7) for the remaining test points were due to poor signal-to-noise ratios. This was probably due to inability of the shaker to excite the chassis properly close to supporting belt, particularly around the center location of chassis and near the cross member area. Beside that, the mode shape at 48 Hz was very closed to engine frequency ranges at 51-53 Hz (normal running rpm). This phenomenon had to be eliminated in order to move away the resonance effect on truck chassis. From the frequency range of 110-140 Hz, the result showed was very critical area for chassis to withstand but it was excluded from the analysis due to high frequency range as well as outside the investigation range. The modal properties and the typical mode shapes for the first seven modes of vibration of truck chassis were given in Table 5.3 and Figure 5.10.

Table 5.3: Modal parameters based on shaker test method (Z axis)

Mode	Shaker Test		Mode Shape
	Modal Frequency (Hz)	Damping (%)	
1	21.40	0.488	Torsion
2	27.20	0.173	Torsion
3	38.50	0.338	Bending
4	41.40	0.552	Torsion
5	48.00	0.376	Torsion
6	63.60	0.327	Bending
7	84.20	0.503	Torsion

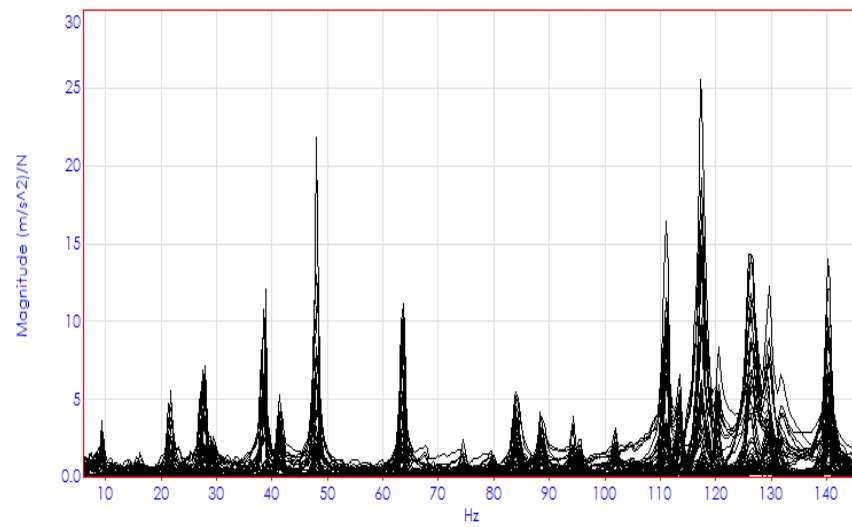
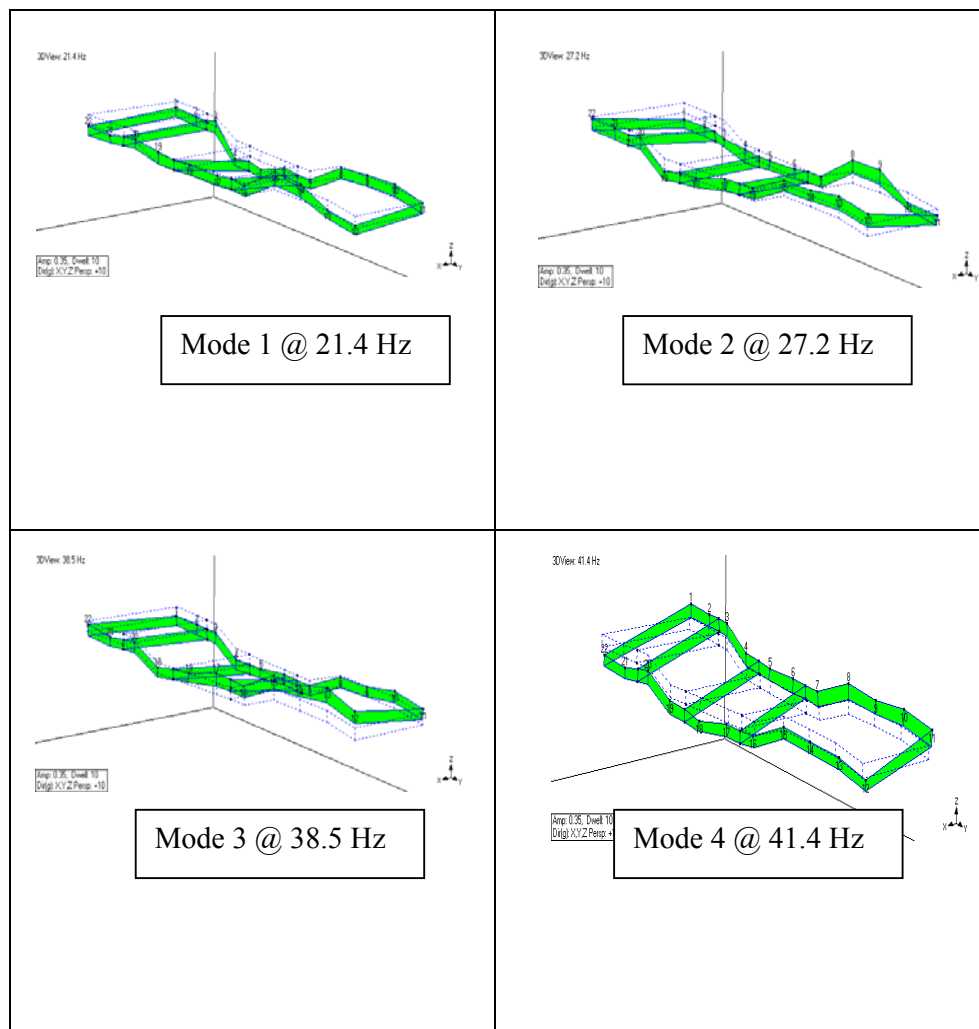


Figure 5.9: Superimposed FRF of truck chassis by shaker test



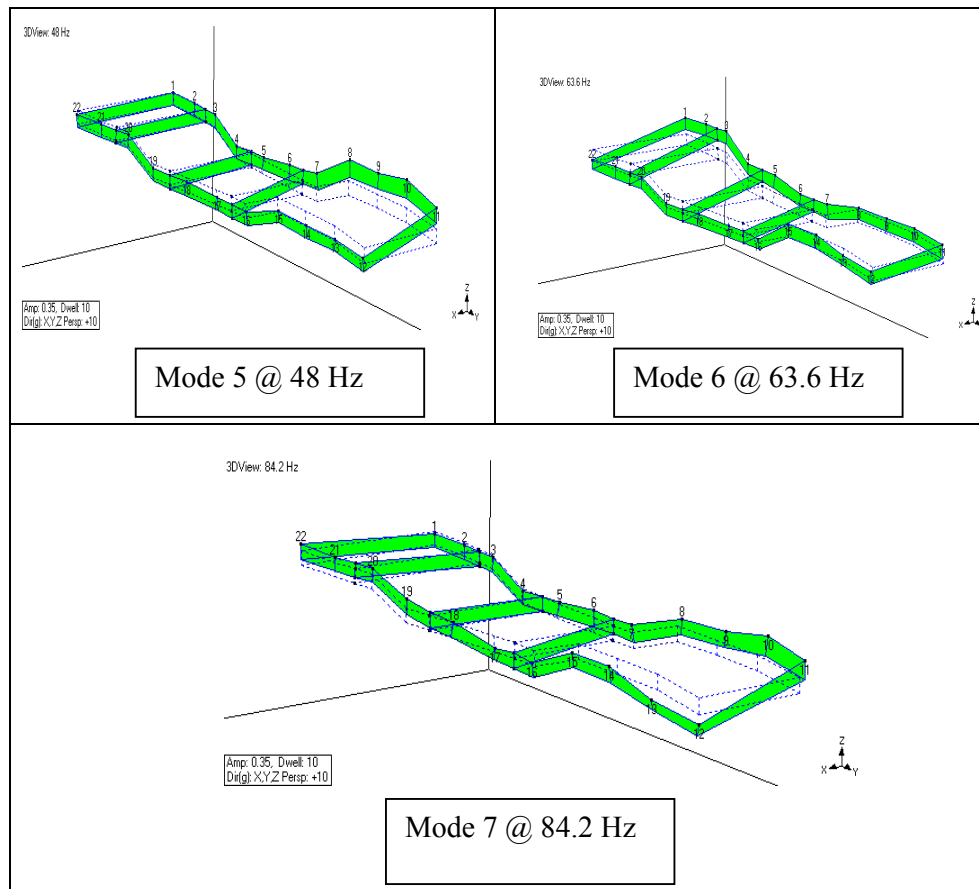


Figure 5.10: Mode shape result by shaker test - continued

5.6 Comparison between result from Impact Hammer and Shaker Excitation

Table 5.4 describes the natural frequency and modal damping value found from both of the experimental analysis. The rigid body frequencies were found below 20 Hz. From the result, the natural frequencies obtained from both analyses were closed to each other except at mode shape number 3 and 7 which slightly lower compared to the shaker test. These minor discrepancies could be from the error during data measurement, such as the excitation from impact hammer was not constantly performed and the accelerometer was not properly fixed to the chassis. Observation from the impact test, each mode showed a very high damping factor especially at the lower modes compared to shaker test. These phenomena could be

from the lower excitation force from the impact hammer, the reference point was far away from the excitation point and human error of instrumentation set-up. Other than that, there were several factors could be related to the errors such as:

- Non-coherent noise – caused by electrical noise on the transducer signals, unmeasured excitation sources and etc.
- Signal processing noise – generated by the signal processing itself, for example the “aliasing” or “leakage” errors.
- Nonlinear noise – if system was nonlinear then measurements may be distorted causing problems when estimating modal parameters.

The 2nd, 3rd and 7th mode shapes had slightly difference compared to others. These phenomena were resulted from the overlaid result and created double or more peak values those very closed from one to another mode shape. The maximum peak values had chosen for further analysis.

Table 5.4: Comparison for natural frequency, damping value and mode shape

Mode	Natural Frequency (Hz)			Damping (%)		Mode Shape	
	Shaker	Impact	%	Shaker	Impact	Shaker	Impact
1	21.40	23.2	8.4	0.488	12.40	Torsion	Torsion
2	27.20	30.1	10.7	0.173	10.20	Torsion	Torsion
3	38.50	32.8	14.8	0.338	4.97	Bending	Bending
4	41.40	43.9	6.0	0.552	3.21	Torsion	Bending
5	48.00	48.3	0.6	0.376	8.40	Torsion	Torsion
6	63.60	63.8	0.3	0.327	4.60	Bending	Torsion
7	84.20	73.7	12.5	0.503	2.09	Torsion	Bending

As a result from these two experimental analysis, the result from the shaker test was chosen for the next analysis due to excitation force from the shaker test was more stabled and reliable as well as the ability to excite to the whole chassis compared with the impact hammer test result. Percentage of dampening effects from the impact test also revealed that the levels of energy from the point of excitation were significantly decreased especially at the lower frequencies but the dampening effect from the shaker test were significantly maintained through out the entire frequencies.

CHAPTER 6

FINITE ELEMENT ANALYSIS AND BASE MODEL

Modal Testing was carried out numerically to determine the dynamic properties of the chassis. These results such as natural frequencies, damping and mode shapes were utilized to compare with the experimental modal analysis result in order to obtain the base modeled for further analysis. Details numerical analysis and model updating result are presented below.

6.1 Modal Analysis of Finite Element (FE) Method

The development of Finite Element (FE) model was conducted using the ANSYS software simulation system. The truck chassis was modeled by SOLIDWORK modeling software and it was exported into the ANSYS simulation system. The tetrahedral-10 element was used in the meshing process because some of the critical point or area in the geometry needs to have a small meshing size in order to give an accurate model for the 3D-elements. Figure 6.1 shows the finite element mesh with 31,489 elements and 62788 nodes. The free-free boundary condition was adopted in order to obtain the natural frequencies and mode shapes. The reason for

using this method was to observe the natural behavior and response of the chassis without external loads or any forces applied to the chassis.



Figure 6.1: Truck chassis model meshed with tetrahedral -10 elements

There were seven natural frequencies calculated for the normal mode analysis and are tabulated in Table 6.1 below. It is observed that all the natural frequencies were below 100 Hz, varying from 20 Hz to 90 Hz. Almost all of the truck chassis designs were based on these frequency ranges to avoid the resonance during the operating condition [4]. Normally, the operating frequency is always related to dynamic forces induced by road roughness, bumps, engine, transmission and many more. Each of these forces has its own excitation frequency.

Table 6.1: Natural frequency from Finite Element Method

Mode	Natural Frequency (Hz)	Description
1	29.71	Global Torsion (Longitudinal)
2	39.03	Global Torsion (Longitudinal)
3	47.92	Global Bending (Longitudinal)
4	59.40	Global Torsion (Longitudinal)
5	69.53	Global Torsion + Bending
6	74.51	Global Bending (localized)
7	86.43	Global Bending (Longitudinal)

It has been reported that the operating frequency varies from 10-80 Hz for the engine, excitation from the transmission system, road excitation and many others [9]. For the long distance traveling, the excitation frequencies were approximately 51-53 Hz. Thus, by comparing these excitation frequencies to the test result, the chassis was actually closed to the resonance phenomena especially at 4th and 5th modes, which could affected the ride quality. It should be noted that these natural frequencies were for free-free boundary condition. In real situation, the chassis were pin supported at some points. However, such different only shifted the natural frequency at very small percentage. [10]

6.1.1 Mode Shape

There are two types of vibration, which are global and local vibrations. The global vibration means that the whole chassis structure is vibrating while local vibration means the vibration is localized and only part of the truck chassis is vibrating.

Figure 6.2 shows the first mode shape of the truck chassis at 29.71 Hz. The chassis experienced first twisting mode about x-axis (longitudinal) and fall under global vibration as the whole chassis follow to vibrate. The maximum translation was at the front end of the truck chassis.

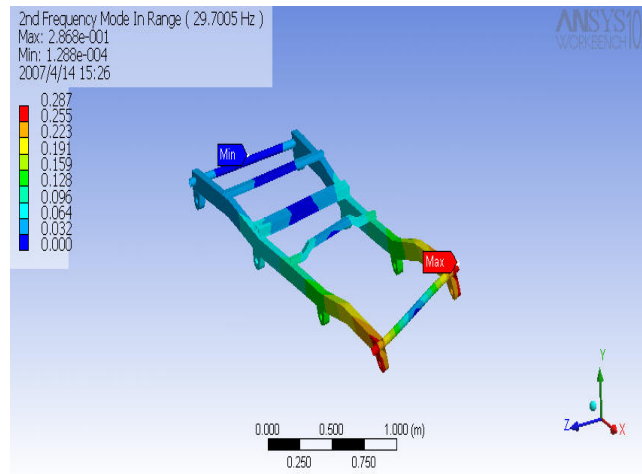


Figure 6.2: FEA first mode shape @ 29.71 Hz

The second mode shape was 2nd twisting about axis-x at 39.03 Hz as shown in Figure 6.3. The maximum translation was again at the front end of the truck chassis.

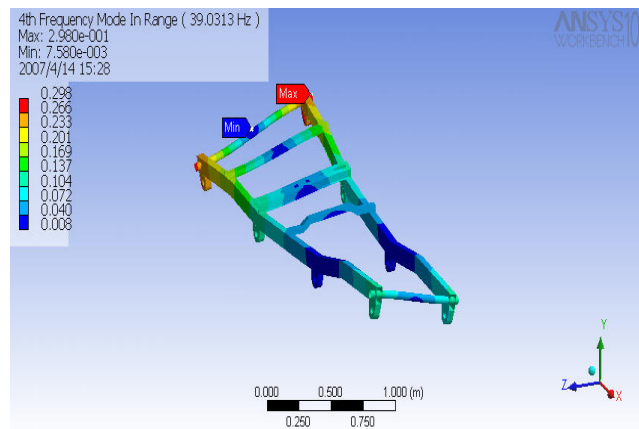


Figure 6.3: FEA second mode shape @ 39.03 Hz

The third mode shape was at 47.92 Hz that experienced first bending about axis-Z. The maximum translation was at the rear end of the chassis as shown in Figure 6.4.

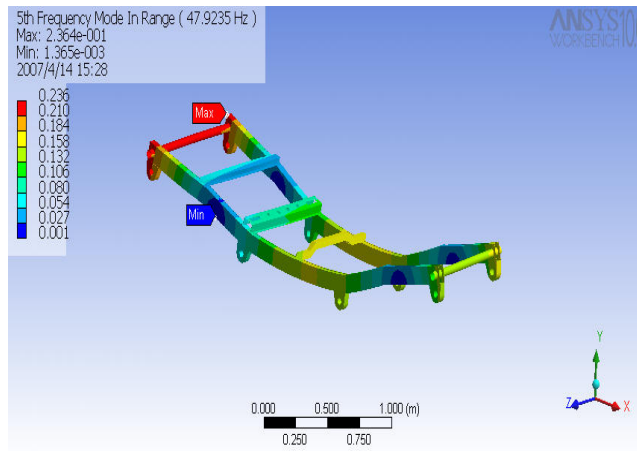


Figure 6.4: FEA third mode shape @ 47.92 Hz

Figure 6.5 shows the fourth mode shape at 59.40 Hz. It experienced second twisting mode about axis-X and maximum translation occurred at front end of the chassis.

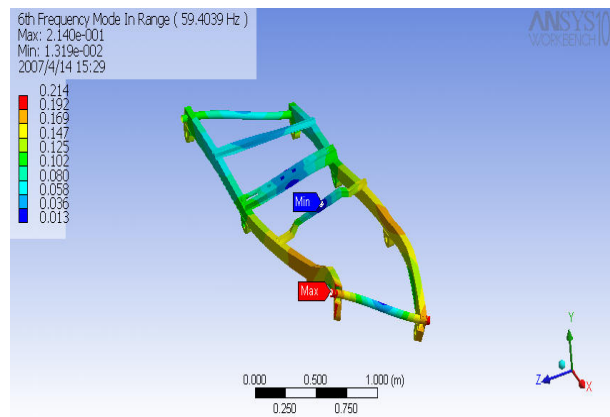


Figure 6.5: FEA fourth mode shape @ 59.40 Hz

The fifth mode shape was 69.53 Hz that experienced combined torsion and twisting mode as illustrated in Figure 6.6. The maximum translation was at the front end of the chassis.

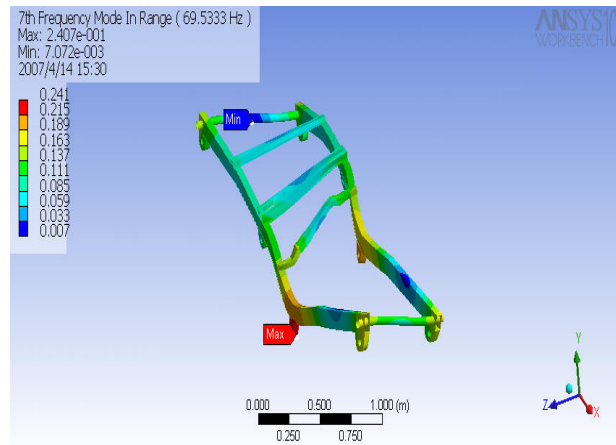


Figure 6.6: FEA fifth mode shape @ 69.53 Hz

The sixth mode shape is shown in figure 6.7. It was found at 74.51 Hz where the chassis experienced the second bending mode. The maximum translation occurs at front end of the chassis.

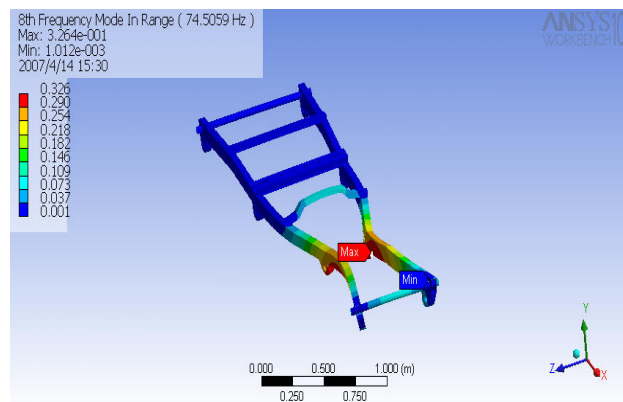


Figure 6.7: FEA sixth mode shape @ 74.51 Hz

The final mode shape occurred at 86.43 Hz, as shown in Figure 6.8. It was found at 86.43 Hz experienced global bending mode about axis-Y. The maximum translation occurs at front rear of the chassis.

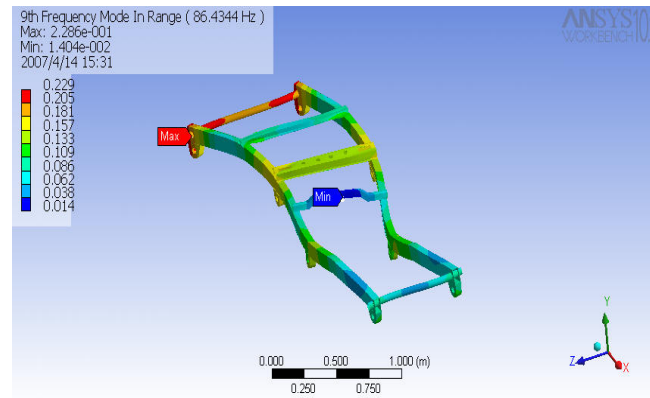


Figure 6.8: FEA seventh mode shape @ 86.43 Hz

Thus based on these mode shapes, most maximum translation occurred at the front end of the chassis, which location of the engine compartment and the driver seats.

6.2 Comparison of results between Experimental and Finite Element Method

Theoretically, each natural frequency from experimental analysis should match with one of the finite element with same boundary condition. In this case, there were several frequencies obtained from the test which were counterpart with each but some others were not. Table 6.2 shows a comparison between natural frequencies from the FE model and the experimental results. Notice that, natural frequencies obtained from FE were slightly higher than its matching test frequency, indicating that the stiffness of the FE model was greater than the stiffness of the real structure. This was probably due to the condition of actual structure where there were lots of rust and corroded members. The 7th mode shape for both analyses was slightly different even though the natural frequencies were closed to each others.

Table 6.2: Mode pairs with frequency difference

Mode	FEA modes Frequency (Hz)	EMA modes Frequency-Shaker Test (Hz)	Error (%)
1	29.71	21.40	38.83
2	39.03	27.20	43.49
3	47.92	38.50	24.47
4	59.40	41.40	43.06
5	69.53	48.00	44.85
6	74.51	63.60	17.15
7	86.43	84.20	2.64

6.3 Model Updating Results

Although the finite element model and modal testing results have demonstrated the existence of closely modes, there were significant discrepancies in the natural frequencies, as can be seen in Table 6.2. Tuning the finite element model was done to match the experimental data in order to create a reliable finite element model suitable for the further analysis. Several time of analysis with different types of parameter changed was performed using FEM tools software to determine parameters having significant changed of the chassis modal properties. As a result, the following parameters were selected for model updating, as examples the Poisson's ratio (ν) and mass density (ρ) of the chassis structure.

Parameters ρ and ν were selected as global updating variables. Table 6.3 shows a comparison between the natural frequencies from the original FE model, updated FE model and the experimental results. It can be seen that the updated model shows better results where the error between FE model and experimental was reduced within $\pm 11\%$.

Table 6.3: Comparison between natural frequencies before and after analysis

Mode	EMA (Hz)	Original FE		Updated FE	
		(Hz)	Error (%)	(Hz)	Error (%)
1	21.40	29.71	38.83	22.76	+6.36
2	27.20	39.03	36.47	29.85	+9.74
3	38.50	47.92	24.47	36.44	-5.35
4	41.40	59.40	43.48	45.25	+9.30
5	48.00	69.53	44.85	52.87	+10.15
6	63.60	74.51	17.15	56.55	-11.08
7	84.20	86.43	2.65	85.86	+1.97

The overall updating process can be concluded as listed in Table 6.4. As for the modification for improvement, the chassis structure was fully updated with ρ and ν of the whole structures during the finite element analysis. Basically, density (ρ) had increased about 23% and ν reduced about 15% compared to EMA (original chassis condition). The higher rate of mass density value was probably due to the condition of the existing chassis, which were old and rusty in some areas, which could possibly reduced the stiffness and weight of the chassis. This factor should be considered in the earlier stage so that any measurement and analysis would be considered the actual condition of the material or specimen that being analyzed and definitely, it should be recommended for any future improvement. Furthermore, the Poisson's ratio also had a small different but very much closed to the original condition.

Table 6.4: Before and after updating process

Parameter	Original Condition	Original FEA	Updated FEA	Overall, %
ρ (kg/m ³)	7715-8030	7850	9900	23
ν	0.27-0.30	0.30	0.23	15

In overall condition, the old, rusty condition and welding defects in some areas were the major reason of such differences between modal (EMA) and finite element analysis (FEA). These conditions had been supported by the APPENDIX B (original chassis) during the chassis preparation and painting work. There were so much metal losses during the cleaning work as well as the welding area of the chassis cross bars and at the main structures. Consideration of all chassis conditions and structural strength would be beneficial to the researchers and would be the best solution to the optimum result.

Finally, by considering the actual chassis conditions and old chassis structures were used for this research, the final updated mode shapes were considered within the acceptable ranges which from mode 1 until mode 7. The differences between the actual and updated parameters were considered small and not really affected the overall chassis performance. Therefore, these updated mode shapes would be fully utilized and used for further modification and testing.

CHAPTER 7

Structural Modification

This chapter discusses on the chassis modification and the improvement made to the existing chassis. The fully updated chassis model from the previous chapter was utilized and several series of testing were performed in order to obtain the optimum structural modification results. Structural modification on the chassis cross members were made and involved both static and dynamic testing. Based on those testing, the procedures and results of the analysis are presented below.

7.1 Structural Modifications and Parametric Analysis

Basically, the natural frequency and corresponding mode shape are very importance parameters in this chassis design. Damages can occur if the truck chassis is excited at the natural frequency during operation. Therefore, the modification on the chassis from FE model was analyzed in order to improve strength as well as reducing in vibration. For the modifications and analysis, the existing truck chassis were added with stiffener and some material properties were slightly changed as described from table 7.1. The results from the analytical model approximations

proved to have moderate correlation with experimental results. The first seven paired mode shapes show a good correlation by superimposed view between FEA model and EMA model. The first seven natural frequencies of the truck chassis were noticed at below 100 Hz and vary from 20 to 80 Hz.

After model updating process, the error (natural frequency and damping) between the FEA model and EMA model were reduced until $\pm 10\%$. Finally, the FE model can now represent the real structure. From the experimental analysis, it can be concluded that the best method to reduce the vibration from a vibrating structure was by identifying the dominant natural frequency and mode shape for effective stiffening. Figure 7.1 shows the overall modifications and testing procedures of the chassis starting with Test no.1 until Test no. 7, as listed in Table 7.1.

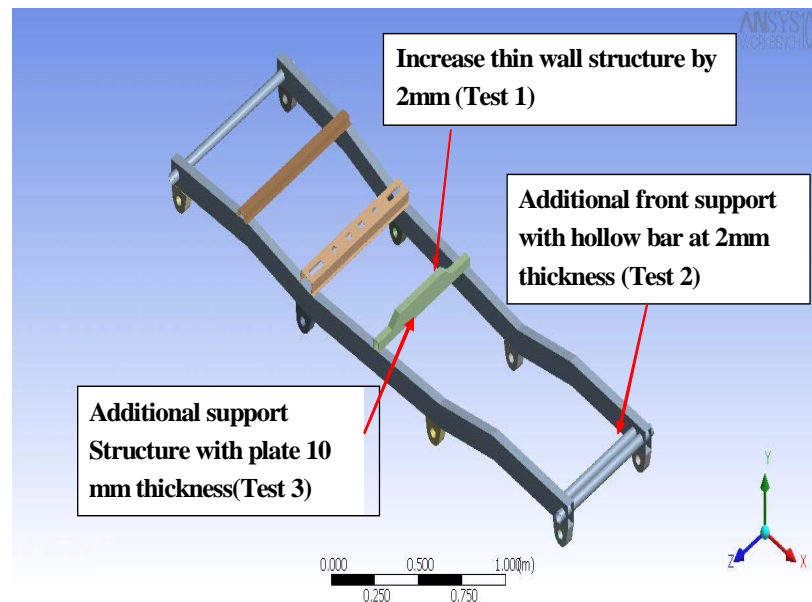


Figure 7.1: Testing structure and modification made on chassis

Table7.1: Modification made on the FE Model

Test No.	Modification Made
1	Increased thin wall thickness by 2 mm
2	Additional hollow bar at front chassis @ thickness 2mm
3	Additional plate on the center cross member @ thickness 10 mm
4	Combination of Test No.1 & 2
5	Combination of Test No.2 & 3
6	Combination of Test No.1 & 3
7	Combination of Test No.1, 2 &3

In this case, the fifth mode shape of truck chassis that experiences torsion load was analyzed because the mode shape at 52 Hz was a predominant natural frequency and present closed to the operating frequency (Normal road excitation frequency at 50-53 Hz). Thus, structural modification was essential to shift the natural frequency away from the operating frequency range and at the same time minimize the torsion impact on the chassis. Table 7.2 shows the comparison results of natural frequency before and after modification. As observed from the table, most of the modification had shifted the natural frequency away from the running frequency. From Test 1, the initial value was shifted from 52 Hz to 56.58 Hz by having the additional thickness about 2 mm at the center. Test 2 was conducted by adding the stiffener (round bar) at the front support and the result shown was unacceptable since the mode # 5 has shifted to 49.04 Hz (closer to running frequency) while the mode # 6 has significantly changed to 57.14 Hz. For the Test 3, the steel plate was added to cross member 'A'. A 4 mm x 20 mm steel plate was added in order to stiffen the truck chassis. The result shown was not good enough to eliminate the resonance effect to the chassis because the mode #5 was shifted too closed to the resonances area. The test results from test 4 also was not very convincing since the mode #4 had shifted closed to running condition even though the mode #5 has significantly increased to 59.64 Hz. The result for test 5 also was not accepted because the mode#5 (51.7Hz) had shifted closed to resonance area. For Test 6, it had improved the truck chassis performance because the modes # 5&6 had shifted away from resonance area. Beside that, the result from the test 7 was

unaccepted due to natural frequency of the mode #4 had shifted closed to running frequency even though mode #5 had shifted away from resonance. Thus, test 1 and test 6 configurations were chosen for further analysis.

Table 7.2: Comparison between natural frequency before and after modification

Test	1	2	3	4	5	6	7	m,kg	δ ,(m)	kNm/rad
Ref.	22.76	29.85	36.44	45.25	52.87	56.55	85.86	67.18	0.05	38.81
T 1	25.92	28.94	35.17	48.58	56.58	58.91	65.87	70.35	0.07	29.86 }
T 2	25.95	30.46	30.55	35.37	49.04	57.14	68.42	70.31	0.07	28.12
T 3	25.64	27.05	31.36	35.65	51.24	59.70	62.36	69.87	0.07	28.23
T 4	28.85	30.32	34.41	50.27	59.64	65.58	68.58	72.37	0.13	15.94
T 5	28.21	30.49	31.43	34.97	51.74	61.35	68.82	71.89	0.04	54.97
T 6	25.66	29.01	34.69	48.79	59.98	60.81	66.02	71.93	0.07	30.21 }
T 7	28.45	29.45	33.34	49.70	59.79	67.62	69.79	73.94	0.06	34.54

Based on these analyses, most of the areas were affected at the front-end side, which are the location of the engine compartment and the driver's seat. Therefore, the deflection of the truck chassis was very significant to control for better ride quality and comfortability. Table 7.4 below shows the deflection values for each test. The deflection at Test 1 and 6 were slightly increased to 30% and 28% respectively. For the Test 6, the deflection value was slightly lower compared to the Test 1 and this discrepancy could be from the additional material added to the chassis structures (combination of modification from Test no. 1 and 6) that contribute to higher

stiffness. Table 7.3 below shows the different weight recorded for each of data during testing. From the data below, the total weight had increased 4.7 % from the original value.

Table 7.3: Comparison of weight before and after modification

Experimental	Mode # 5		%
	Before Modification, Hz	After Modification, Hz	Mass, kg
Test 1	67.18	70.35	+4.72
Test 6	67.18	71.93	+7.07

Based on the result from Test 1 and 6, the overall modification was selected from the Test 1 because the overall weight had significantly reduced from the original values. However, the torsion stiffness of Test 1 configuration had reduced to 29.86 kNm/rad. compared to original value of 38.81 kNm/rad (reduced by 23 %). This is the probable reason why the chassis deflection had increased to 30 %.

Table 7.4: Comparison of displacement before and after modification

Test	Before Modification,(m)	After Modification,(m)	Deflection (%)
Test 1	0.0533	0.0694	+30 }
Test 6	0.0533	0.0686	+28

Table 7.5 shows the result of torsion analysis before and after modification. From the result, it was observed that the torsion stiffness after modifications was slightly reduced by 23 % and 22 % for each of test 1 and 6. These results had shown that the truck chassis was dominated by the mass instead of thickness.

Table 7.5: Comparison of Torsion Stiffness before and after modification

Test	Before Modification KNm/rad	After Modification KNm/rad	Percentage, %
1	38.81	29.86	-23
6	38.81	30.21	-22

7.2 Static and Dynamic Test

In order to get better refinement of the developed chassis, two analyses had been performed, namely static and dynamic test. The objectives of these two tests are to ensure that the mode shape, natural frequency and damping value of the improved chassis are still in acceptable ranges when subjected to static and dynamic load especially during accelerations. The testing methodology was as same as between static and dynamic analyses except the applied load were set up to static and dynamic analysis respectively. The external forces ware applied at the engine compartment area and leaf spring area as shown in Figure 7.2. Then, both of rear side of chassis were pinned and zero movement. The arrangement of the simulation test was shown in Figure 7.2 and 7.3.

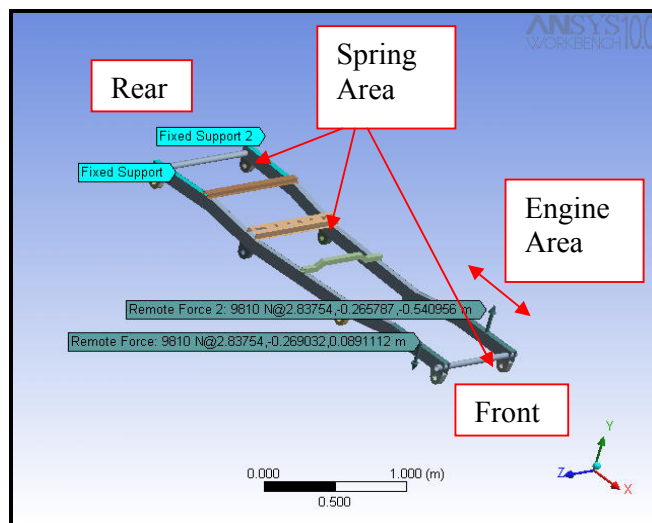


Figure 7.2: Dynamic test of truck chassis

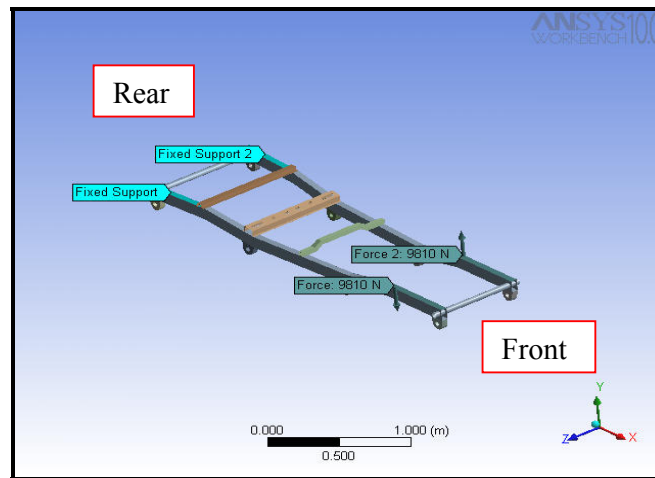


Figure 7.3: Static test of truck chassis

The results of these two analyses are shown in Table 7.6. The dynamic test was performed with three different excitation frequencies, which were at 58.91 Hz, 90 Hz and 180 Hz (road excitation). The aims of these three different categories were to see the different characteristics especially on the chassis displacement and torsion stiffness. For the static test, the excitation frequency was set-up at 58.91 Hz, which normally the idling time for the vehicle during static condition. The displacement value and torsion stiffness were 0.0694 m and 29.87 kNm/rad respectively. Based on the result obtained against the excitation frequency (dynamic test), the displacement value had decreased while the torsion stiffness had increased with increment of the frequency. Therefore, from the overall result it can be concluded that, the chassis wear much stiffer and stable at higher frequencies compared to low frequency especially during dynamic condition. Majorities of the excitation frequencies came from the engine itself and it became more stable during ramp-up and constant RPM especially when it passes through the natural frequency of the vehicle system.

Table 7.6: Result of static and dynamic simulation tests

Test	Frequency (Hz)	Displacement (m)	Torsion Stiffness (kNm/rad)	Mass (kg)
Dynamic Test	58.91	0.01338	154.89	+4.72 %
	90.00	0.00562	368.75	+4.72 %
	180.00	0.00115	1801.27	+4.72 %
Static Test	58.91	0.06937	29.87	+4.72 %

On overall result, the chassis had shown a significant changed in natural frequencies, mode shapes and damping values in different situation due to the static and dynamic loads. The overall chassis performance had significantly increased for Test 6 compared to the Test 1. The natural frequency had been shifted away by 13% from excitation frequency (50-53 Hz), hence the resonance area of existing chassis was successfully eliminated.

CHAPTER 8

OVERALL DISCUSSION

The physical testing supplied empirical expression ($y=mx + c$) of global torsion stiffness, and recorded the mode shape and natural frequency for the truck chassis. These gave a basis with which to validate the results of the Finite Element baseline model. The initial torsion value obtained from the analysis was 38987 Nm/rad. The initial result from the Modal analysis had shown a closed agreement on the mode shape between the impact hammer and shaker test. On the overall damping value between both analyses, a 2-13 % big different was obtained as calculated from Table 5.2 and 5.3. These problems were mainly due to low excitation forces transmitted from the impact hammer and some of the experimental errors during the test. The overall result from shaker test was utilized and had been used as references for further actions.

8.1 Creation of FE baseline model

Finite Element (FE) baseline model was created and represented the chassis as accurately as possible within the constraints necessary for complete modeling by

using the ANSYS simulation system. Once all modeling corrections were completed, the baseline model of the chassis were created and transformed into the finite element software. From the torsion test, the experimental result of the torsion test was significantly importance for the baseline model and for future improvement. The result of the numerical torsion stiffness was slightly higher than that resulting from physical testing (4% higher). These phenomena were expected due to the infinite joint stiffness and small geometrical differences inherent in the model especially due to corrosion. The torsion stiffness value of 40700 Nm/degree (as listed in Table 4.4) was accepted as substantial base from which to incorporate design improvements.

Similarly, the modal analysis result obtained from finite element analysis was slightly higher than the modal testing result by about 17-40 %. After the updating process, the percentage of discrepancies between both finite element and modal analysis had reduced by 10%. The base line study of stress analysis was also conducted to the existing chassis as shown in Figure 8.1. The front chassis's compartments were applied with two twisting forces between the spring mounting points. The rear chassis were fixed at both end structures in order to represent the actual response of acting force during operation. The stress result shown in Figure 8.2 had increased from 1.08 Gpa to 2.99 GPa after the modification. Therefore, the overall performance of the chassis had significantly improved especially after the modification process.

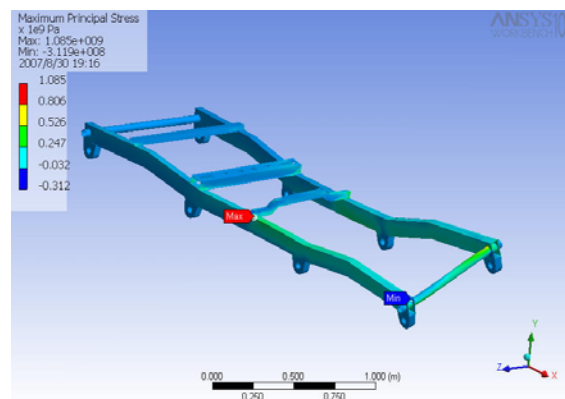


Figure 8.1: Stress Analysis before modification

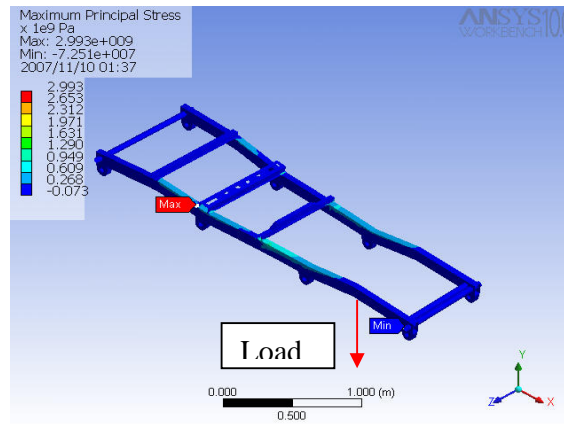


Figure 8.2: Stress Analysis after modification

8.2 Design Improvement Study

On the overall torsion test results from Table 4.4, it was found the overall torsion stiffness had significantly improved by 25% over the base line model. The total deflection also reduced by 16%. A mass of 74 Kg for the additional stiffness was achieved with an increased of 4.7% over the baseline model (Refer to Table 7.3). Figure 8.3 below shows the full modifications that were made to the existing chassis.

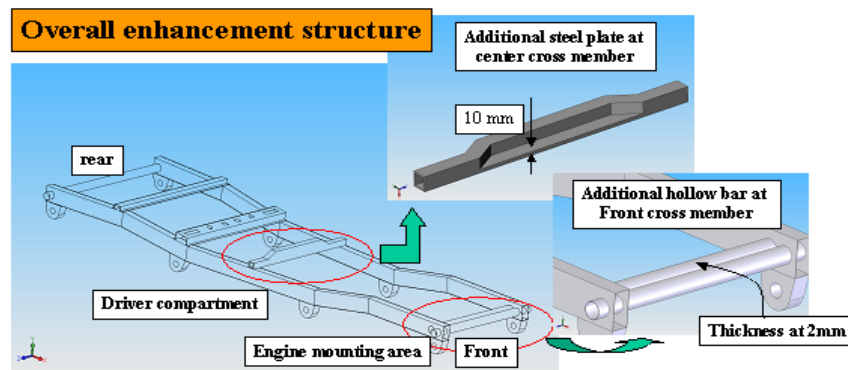


Figure 8.3: Overall chassis improvement

8.3 Final Result

In overall, the objectives of research had successfully achieved in most of the areas especially on the improvement of torsion stiffness, static and dynamic behavior especially on the mode shape, natural frequency and modal damping. The natural frequency of the chassis had increased by 13%, Torsion Stiffness by 25%, weight by 4.7% and the chassis deflection had decreased by 16%. The summary of the results were presented in Table 8.1 below.

Table 8.1: Final Result of improvement study

Test	Natural Frequency	Torsion Stiffness	Weight	Deflection
Chassis	+13% away from operating frequency which at mode 5	+25%	+4.7%	-16%

CHAPTER 9

CONCLUSION AND RECOMMENDATION

This chapter discusses on the overall results presented in the earlier chapters. Base on the overall results, it can be improved further and include several recommendations for future research especially in structural dynamic behavior to any system.

9.1 Summary

The study of static and dynamic behavior of truck chassis had been executed successfully. The application of dynamic correlation technique together with Finite Element Tools had been utilized in order to verify the simulation and experimental analysis of the chassis. Experimental results were used in conjunction with the finite element to predict the dynamic characteristic of truck chassis such as the natural frequency and corresponding mode shape. Basically, the natural frequencies and mode shapes are importance parameters in chassis design. Damage can occur if the truck chassis is excited at resonance during operation. Therefore, based on the result gained from the finite element analysis, further enhancement of the current chassis

had been done through the chassis FE model in order to improve its torsional stiffness as well as reduce the vibration level. Series of modifications and tests were conducted by adding the stiffener in order to strengthen and improved the chassis stiffness as well as the overall chassis performances.

In Finite Element Analysis, the model of truck chassis was created using 10 nodes tetrahedral elements. Normal mode analysis was performed and free-free boundary condition was applied in the analysis to determine the first seven natural frequencies and mode shapes. In the Experiment Modal Analysis, the modal parameter of truck chassis was obtained by using two different methods of excitation test, which were involved the shaker and impact hammer Test 3. Both of these tests were acceptable result and the Shaker test result had been chosen for further analysis were due to acceptable excitation forces during the test and more closer to the finite element result. Moreover, the results from the analytical model approximations proved to have good correlation with experimental results. The first seven paired mode shapes good correlation by superimpose view between FEA and EMA model. However for second, third, fourth and seventh mode shapes were slightly far away between each other. It was noticed that the first seven natural frequencies of the truck chassis were below 100 Hz and vary from 20 to 80 Hz. This problem was resolved by carrying out the Finite Element Model updating, by tuning the material properties. The model updating result show error reduction until 10% the FEA model and EMA models were reduced until $\pm 10\%$. Then, the virtual model from this correlation process was utilized for further refinement. The modification was conducted to the FE model after updating in order to stiffen the chassis as well as to reduce the existing vibration level.

9.2 Conclusion

As conclusion, this study has achieved its core objectives. The dynamic characteristic such as the natural frequencies and corresponding mode shapes of the

truck chassis were determined numerically and experimentally. The experiment data were used to validate a finite element model representing the real structure. The results indicate that the FE model shows a little bit different with the experimental model for both mode shapes and natural frequencies especially for modes 1 to 7. The FE model presented an average of 20-40% higher frequencies than the real chassis. These facts were due to the imperfection of the model and real structure.

The initial result from the Modal analysis showed a closed agreement on the mode shape between the impact hammer and shaker test. But the overall damping value between both analysis should a big different between 2-13 % mainly due to low excitation force transmitted from the impact hammer. Also found that, the chassis was in resonance because the overall vehicle operating frequency (52-53Hz) was very closed to the natural frequency of existing chassis (Mode 5 at 52.87 Hz).

The overall torsion stiffness was significantly improved by 25% over the base line model. The total deflection also reduced by 16%. There were seven total number of test variables conducted to the existing chassis and it was shown that the combination of increasing the wall thickness by 2 mm and adding plate on the center cross member (Test 6) gave optimum results in terms of resonance, natural frequency, deflection and stiffness. The rest were eliminated due to:

- *Test 2: mode 5 closed to natural frequency*
- *Test 3: mode 5 closed to natural frequency*
- *Test 4 & 7: mode 4 very closed to natural frequency*
- *Test 5: mode 5 closed to natural frequency*

It was found that, with the structural modification, the chassis natural frequency was shifted away by 13% higher than the original value, increased the torsion stiffness by 25 % and reduced the total deflection by 16 %. Overall weight was slightly increased by about 7 %.

9.3 Recommendations for Future Research

This chassis structure should be further analyzed and improved on the overall performance especially on structural dynamic behavior and quality auditing for better refinement. Based on these factors, the overall recommendation should include:

1. The study of structural analysis should be covered on the overall truck system and after that focus on the specific area such as this chassis. This analysis will help to make full body refinement and improvement because it can be related to actual running condition.
2. Other tests should be included in the structural analysis such as fatigue analysis and bending test. This because with the recent technology, the computer added engineering codes for fatigue life estimation have improved severely and it is now possible to estimate the fatigue damage to a structure using the full-time history loads from a multi-body simulation as well as bending analysis. This technology has greatly proven and enhances durability of the structure.
3. Further enhancement can be made on the torsion hydraulic test rig by adding load controller for better controlling system during testing and improve the safety features to the test rig. This issue will interface during execution time whereby the structure requires high impact load and failure could happen during that time.

REFERENCES

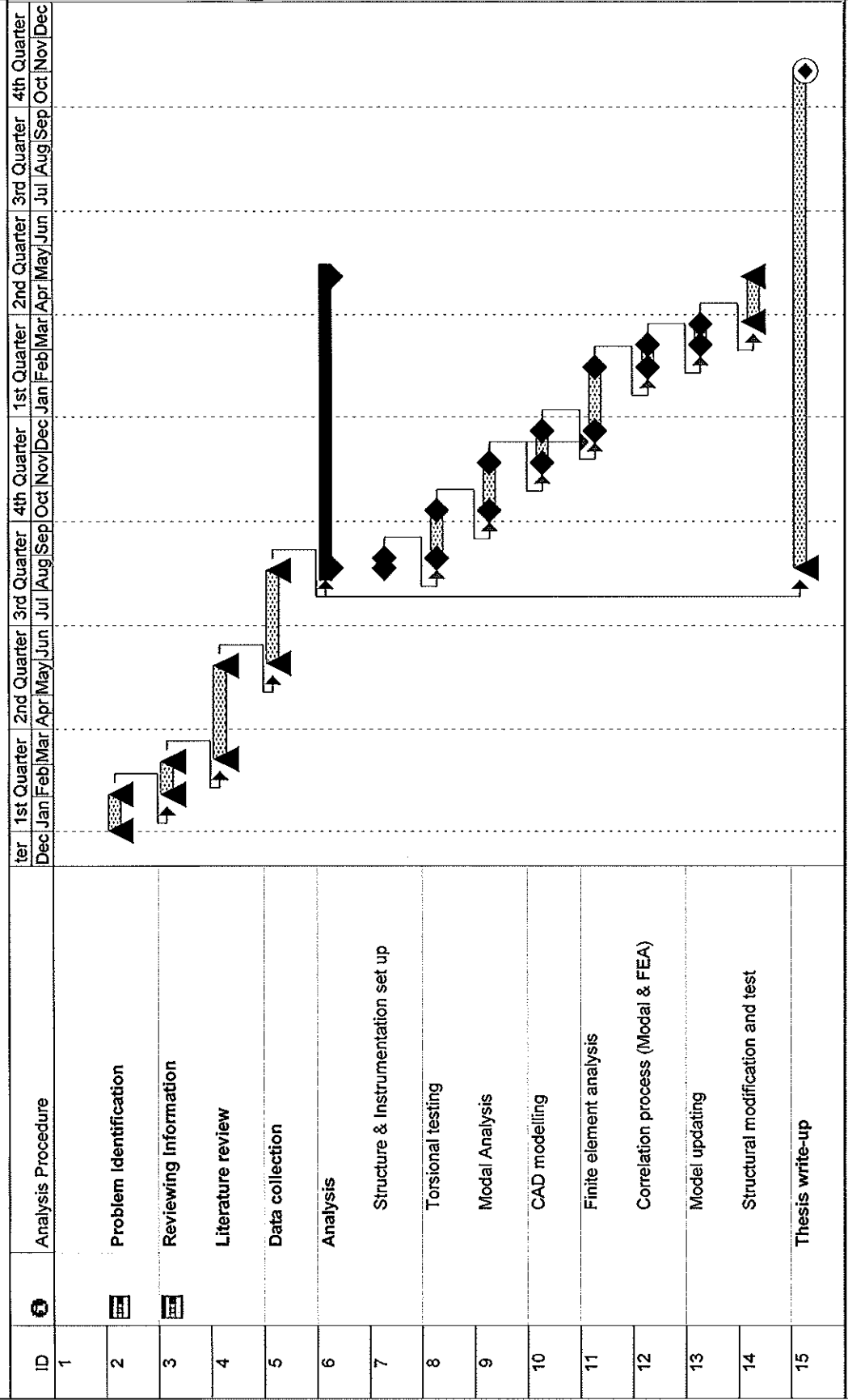
1. Dave Anderson and Grey Schede. *Development of a Multi- Body Dynamic Modal of a Tractor – Semi trailer for Ride Quality Prediction*. International Truck and Engine Corp. 2001.
2. I.M. Ibrahim, D.A.Crolla and D.C. Barton. *Effect Of Frame Flexibility On The Ride Vibration Of Trucks*. Department of Mechanical Engineering, University of Leeds LS2 9JT, U.K. August 1994.
3. Pomulo Rossi Pinto Filho. *Automotive Frame Optimization*. Universidade Federal de Uberlandia. November 2003.
4. Zaman @ Bujang, Izzudin and Abd. Rahman, Roslan (2006). *Application of Dynamic Correlation Technique and Model Updating on Truck Chassis*. 1st Regional Conference on Vehicle Engineering & Technology, July 2006.
5. Lonny L. Thomson, Jon K. Lampert and E. Harry Law. *Design of a Twist Fixture to measure the Torsional Stiffness of a Winston Cup Chassis*. Department of Mechanical Engineering, Clemson Univ.1998.
6. Murali M.R. Krisna. *Chassis Cross-Member Design Using Shape Optimization*. International Congress and Exposition Detroit, Michigan. February 23-26,1998.
7. Wesley Linton. *Analysis of Torsional Stiffness and Design Improvement Study of a Kit Car Prototype*. Cranfield University, September 2002.
8. Marco Antonio Alves Jr, Helio Kitagawa and Celso Nogueira. *Avoiding Structural Failure via Fault Tolerant Control – An Application on a Truck Frame*. Detroit, Michigan November 18-20, 2002.
9. <http://www-5.jeep/vensuite/vehiclecompare.jsp>
10. Jeroen Deweer and Tom Van Langenhove. *Identification of the Best Modal Parameters and Strategies for FE Model Updating*. Society of Automotive Engineers, 2001.
11. Wesley Linton. *Analysis of Torsion Stiffness and Design Improvement Study of A Kit Car Chassis Prototype*. Cranfield University 2001-2.
12. Lonny L. Thomson, Pipasu H. Soni, Srikanth Raju, E. Harry Law. *The Effects of Chassis Flexibility on Roll Stiffness of a Winston Cup Race car*. Departmental of Mechanical Engineering, Clemson University, 1998.

13. "ME'sope VES. *Demo Guide*. Vibrant Technology Inc., Central of America, 2003.
14. N. Moller, S.Gade. *Application of Operational Modal Analysis on Cars*. SAE Paper 2003-01-1599, Noise & Vibration Conference and Exhibition Traverse City, Michigan, 2003.
15. C.Cosme, A.Ghasemi, J.Gandevia. *Application of Computer Aided Engineering in the Design of Heavy-Duty Truck Frames*. SAE Paper 1999-01-3760, International Truck & Bus Meeting & Exposition, Detroit, Michigan, 1999.
16. "FEMtools Theoretical Manual. *Dynamic Design Solution NV*. Leuven, Belgium, 2002.
17. D.J.Ewins. *Modal Testing: Theory and Practice*. Research Studies Press Ltd., Hertfordshire, England, 1984.
18. Mohd Jailani Mohd Nor, Shahrur Abdullah, Nordin Jamaludin, Rozmi Ismail, Sallehuddin Mohamed Haris and Azli Arifin. *The regional conference on advances in noise, vibration and comfort*. Faculty of engineering, UKM, 2007.
19. Kenneth H.Huebner, Earl A.Thorton, Ted G.Byrom. *The Finite Element Method For Engineers*. Third Edition.
20. J.William Fitch. *Motor Truck Engineering Handbook-Fourth Edition*. SAE Inc., Warrendale, U.S.A, 1993.

APPENDIX A

Project Schedule

STATIC AND DYNAMIC TEST OF TRUCK CHASSIS



2005-2007

ter	1st Quarter	2nd Quarter	3rd Quarter	4th Quarter	1st Quarter	2nd Quarter	3rd Quarter	4th Quarter					
	Dec	Jan	Feb	Mar	Apr	May	Jun	Jul	Aug	Sep	Oct	Nov	Dec

ID	Analysis Procedure
1	
2	Problem Identification
3	Reviewing Information
4	Literature review
5	Data collection
6	Analysis
7	Structure & Instrumentation set up
8	Torsional testing
9	Modal Analysis
10	CAD modelling
11	Finite element analysis
12	Correlation process (Modal & FEA)
13	Model updating
14	Structural modification and test
15	Thesis write-up

APPENDIX B

Preparation of Truck Chassis

Original Chassis

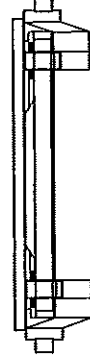
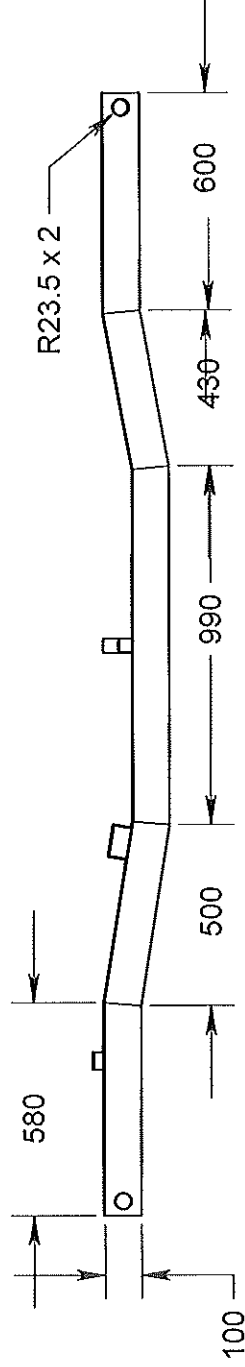
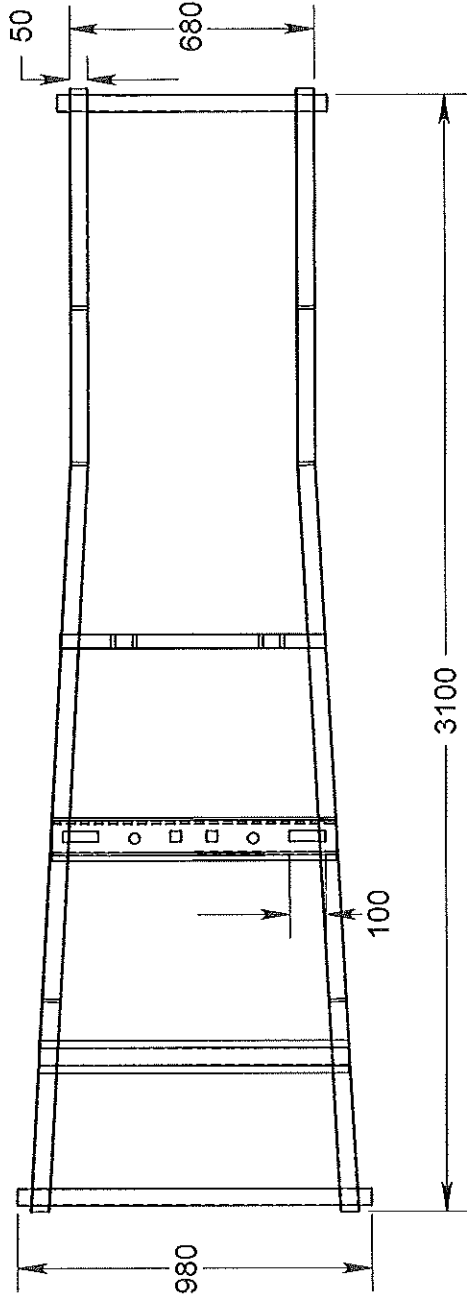


After Painting



APPENDIX C

Engineering Drawing



Thin Wall Thickness 2mm

THIRD ANGLE PROJECTION

REV: 0

UNIVERSITY TECHNOLOGY OF MALAYSIA

Drawn by

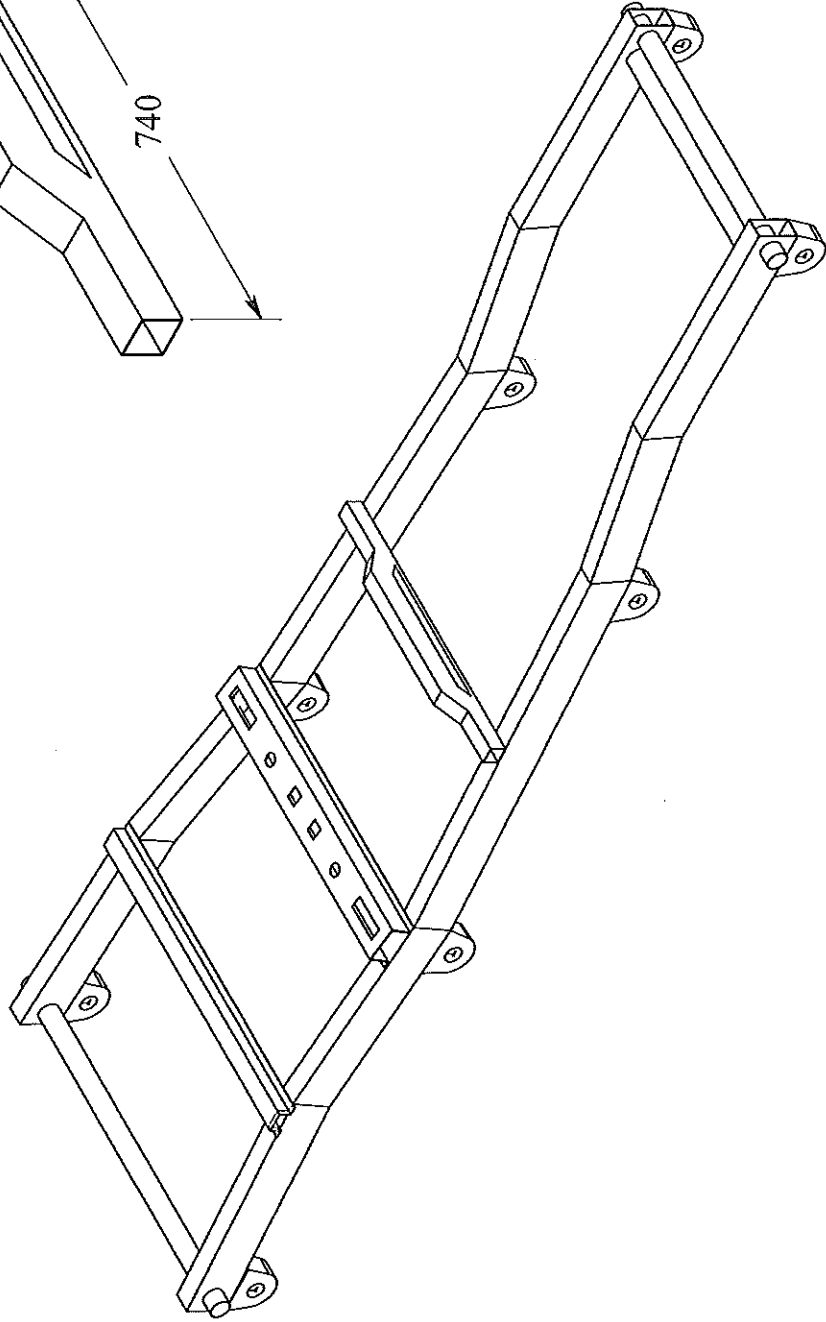
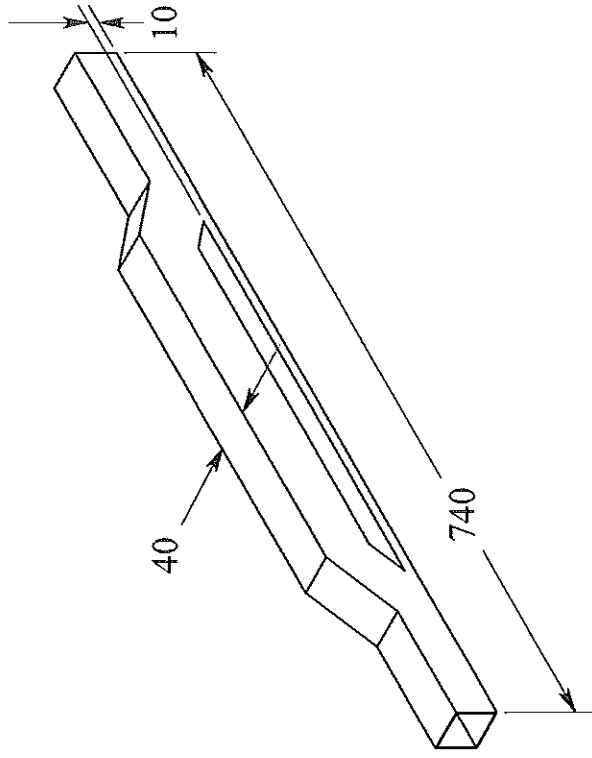
ISMAIL BIN MUSA

Project Title

Static & Dynamic Test of Truck Chassis

Date

14 October 2006



THIRD ANGLE PROJECTION

REV: 0

UNIVERSITY TECHNOLOGY OF MALAYSIA

Drawn by

ISMAIL BIN MUSA

Project Title

Static & Dynamic Analysis of Truck
Chassis-Final modification

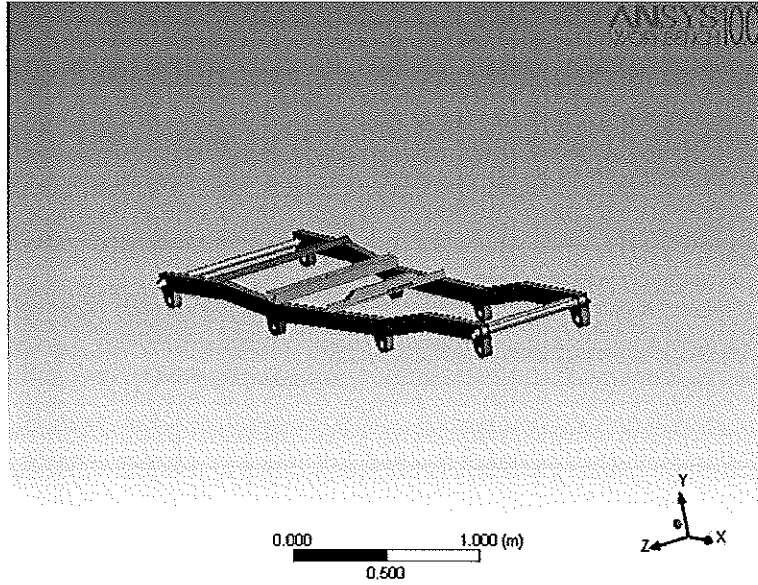
Date

14 October 2006

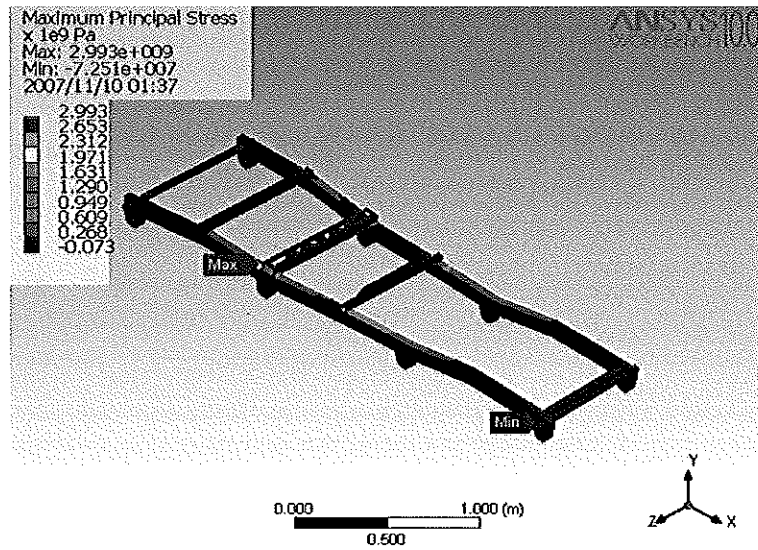
APPENDIX D

Test model, Stress test # 5 and Calibration result

FINITE ELEMENT MODEL

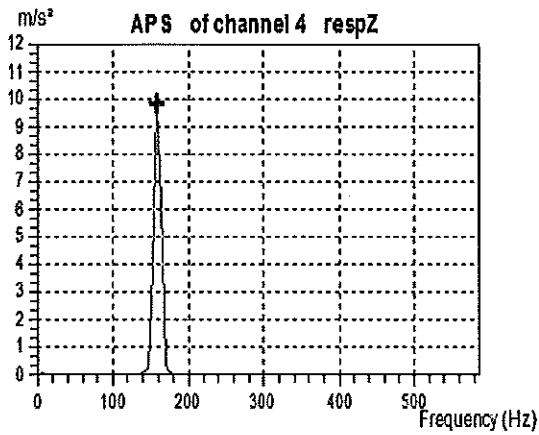
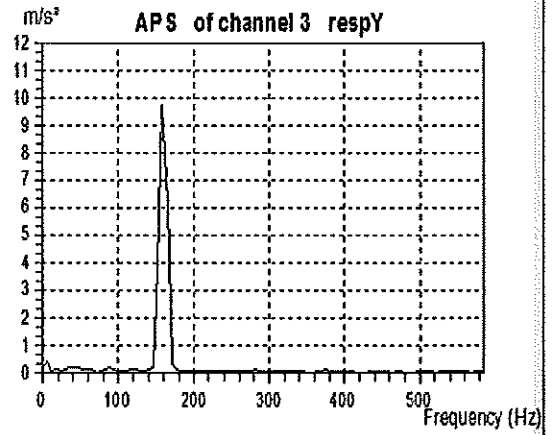
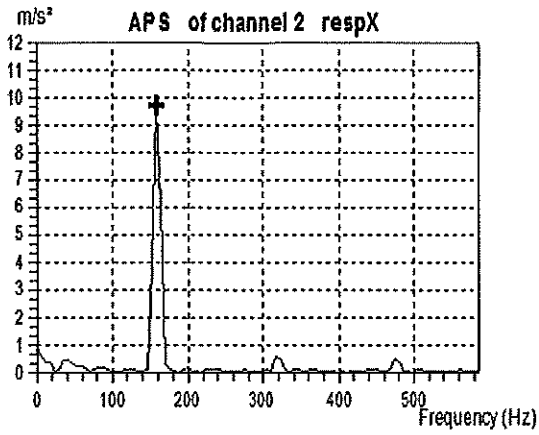


STRESS TEST # 5



Calibration result for Experimental Modal Analysis

Calibration of measurement channels



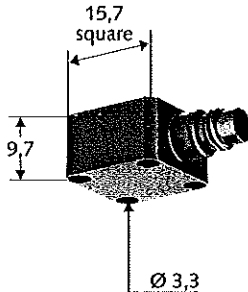
APPENDIX E

Instrumentation

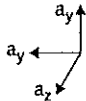
Triaxial

Voltage Output, Piezotron Accelerometer

K-Shear Triaxial Accelerometer Type 8793A...



Measuring direction Connection
4-pin pos.



Specifications		Type	Type	Type
		8793A500	8793A500M5	8793A500M8
Range	g	±500	±500	±500
Sensitivity	mV/g	10	10	10
Frequency Response, ±5%	Hz	2,5 ... 10 k	2,5 ... 10 k	2,5 ... 10 k
Threshold	g_{rms}	0,002	0,002	0,002
Transverse Sensitivity typ.	%	1,5	1,5	1,5
Non-Linearity	%FSO	±1	±1	±1
Shock (1 ms pulse) max.	g	5 000	5 000	5 000
Temp. Coeff. of Sensitivity	%/°C	-0,03	-0,03	-0,03
Operating Temperature	°C	-55 ... 120	-55 ... 165	-195 ... 120
Power Supply	mA	2 ... 18	2 ... 18	2 ... 18
	VDC	20 ... 30	20 ... 30	20 ... 30
Housing/Base	type	St. Stl.	St. Stl.	St. Stl.
Sealing	type	Hermetic	Hermetic	Hermetic
Mass	gram	11	11	11

Characteristics

Low impedance voltage mode, low profile design, quartz shear accuracy and stability, hermetically sealed, CE compliant
M3: low frequency 1 Hz option available
T: TEDS option available

Applications

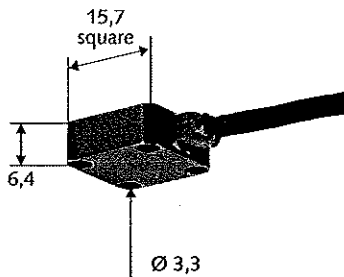
Useful for measuring small and lightweight structures, where mass loading must be kept at a minimum

Accessories

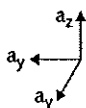
Cap screws 4-40 x 0,5" and M2,5 x 12 mm
Cable: Type 1756B..., 1578A...
Coupler: Type 5100 series

Datasheet 8793A_000-261

K-Shear Triaxial Accelerometer Type 8794A...



Measuring direction Connection
4-pin pos.



Specifications		Type	Type	Type
		8794A500	8794A500M5	8794A500M3
Range	g	±500	±500	±500
Sensitivity	mV/g	10	10	10
Frequency Response, ±5%	Hz	2,5 ... 10 k	2,5 ... 10 k	1 ... 10 k
Threshold	g_{rms}	0,002	0,002	0,002
Transverse Sensitivity typ.	%	1,5	1,5	1,5
Non-Linearity	%FSO	±1	±1	±1
Shock (1 ms pulse) max.	g	5 000	5 000	5 000
Temp. Coeff. of Sensitivity	%/°C	-0,02	-0,02	-0,02
Operating Temperature	°C	-55 ... 120	-55 ... 165	-55 ... 120
Power Supply	mA	2 ... 18	2 ... 18	2 ... 18
	VDC	20 ... 30	20 ... 30	20 ... 30
Housing/Base	type	St. Stl.	St. Stl.	St. Stl.
Sealing - Housing/Connector	type	Welded/Epoxy	Welded/Epoxy	Welded/Epoxy
Mass	gram	7,6	7,6	9

Characteristics

Low impedance voltage mode, low profile design, quartz shear accuracy and stability, CE compliant, ground isolation version available
M3: low frequency 1 Hz option available

Applications

Measurements in confined spaces. The low profile design provides an aerodynamic advantage for in-flight flutter testing

Accessories

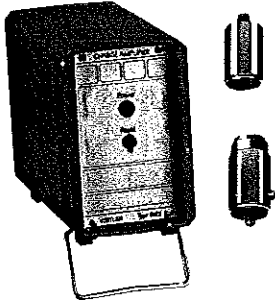
Mounting screw 4-40 x 0,375" and M2,5 x 10 mm
Cable: Type 1756B..., 1578A...
Coupler: Type 5100 series

Datasheet 8794A_000-263

Calibration

Charge Amplifier

Calibration Systems Types 8802, 8804



Connection
10-32 neg.

Specifications		Type	
		8802	8804
Acceleration Range	g	±250	±250
Acceleration Limit	g	±1000	±1000
Threshold	g_{rms}	0,02	0,01
Ref. Voltage Sensivity at 100 Hz, 10 g and 23,9 °C	mV/g	10 ±0,01	10 ±0,01
Frequency Response	Hz	10 ... 10 000	10 ... 10 000
Transverse Sensivity at 100 Hz	pC/s	≤2	≤2
Time Constant	s	1	1
Non-Linearity	%	±0,5	±0,5
Operating Temperature	°C	-21 ... 57	-21 ... 57
Temp. Coeff. of Sensivity	%/°C	-0,04	-0,04
Output Voltage FSO	V	±2,5	±2,5
Ground Isolation	Ω	--	>10 ⁷
Output Impedance	Ω	<15	<15
Power Supply	VAC	115/230	115/230
Mass	Gramm	20	80

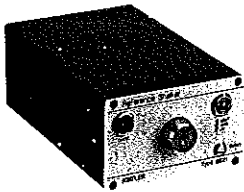
Characteristics
This system features unique stability, linearity and repeatability

Applications
System for calibration of sensors. Lab standard or back-to-back calibration transfer

System Components
8802 = 8002/5022
8804 = 8076/5022

Datasheet 8802_000-520
8804_000-521

Reference Shaker Type 8921



Specifications		Type
		8921Y26
Frequency	Hz (rads)	159,2 (1000)
Acceleration rms, ±3%	g	1
Velocity rms, ±3%	mm/sec	10
Displacement rms, ±3%	µm	10
Max. Load	gram	300
Operating Temp.	°C	10 ... 40
Power Supply	mA	300
	VDC	12
Battery	type	built-in rechargeable
Mass	kg	2
Dimensions	mm	76,2 H x 107 W x 178 D

Characteristics
Test measurement system integrity, convenient self-contained and portable, rechargeable battery, tests sensors up to 300 g of weight, CE compliant

Applications
The 8921 reference shaker can be used to confirm the sensitivity of acceleration, velocity, and displacement sensors

Accessories
10-32 to M5 stud: Type 8451
¼-28 to M5 stud: Type 8453

Specify Version
8921Y26: supplied with 115 VAC battery charger
8921: supplied with 230 VAC battery charger

Datasheet 8921_000-362

Coefficient Value For Transducer

No.	Type of Sensor	Serial No.	Coefficient Value	Decimel Point	Rated Output	Unit
1	Load Cell TCLP-500KA	GY9228	1.667	1	1.5mV/V	500Kgf
2	Load Cell CLP-50B	CQ 1309	2.5	3	1.0mV/V	5tf
3	CDP-50 Displacement transducer		0.5	2	5.0mV/V	50 mm
4	CDP-100 Displacement transducer		1	2	5.0mV/V	100mm
5	Load Cell CLP - 50B	CH1191	0.01667 (Com)			
6	Load cell TCLP-10B	CR 1253	0.005003 (Ten) 0.005008 (Com)			
7	Load Cell CLP-50B	CH 1191	0.01667 (Com)			
8	Load Cell TCLP-1B	CN 1211	0.0005000 (Ten) 0.0005030 (Com)			
9	Load Cell TCLP-1B	CN 1210	0.002503 (Ten) 0.002496 (Com)			
10	Load Cell TCLP-5B	CQ 1309	0.002503(Ten) 0.002496(Com)			
11	Load Cell TCLP-5B	CQ 1308	0.002500(Ten) 0.002500(Com)			
12	Load Cell TCLP - 10B	CR 1254	0.004988 (Ten) 0.004990 (Com)			
13	Load Cell CLP - 100B	CI 1144	0.03332 (Com)			

240908/8202/85 *

Calibration Chart for
Impact Hammer Type 8202

Brüel & Kjær



Nærum Denmark

Serial No.1123659.....

Type 8202 includes Force Transducer Type 8200

serial no.1149837.....
(see individual calibration chart)

Sensitivity at output of hammer4.0%..... pC/N
(includes the built-in attenuation of approx. 12 dB)

	Force Range (N)	Duration Range (ms)	Approx. Frequency Range (-10 dB) (Hz)
Rubber tip	100 - 700	5 - 1,5	0 - 500
Plastic tip	300 - 1000	1 - 0,5	0 - 2000
Steel tip	500 - 5000	0,25 - 0,2	0 - 7000

The additional mass decreases frequency range approx. 30%

Temperature dependence of pulse length using rubber tip

Temp. °C	-10	+5	+25	+40	+55
Duration ms	1,1	1,6	2,0	2,1	2,2

BC0157-12

Bailey - 92% (0-15)

Weight of the hammer: 280 g

Materials: anodized aluminium, stainless steel, titanium, neoprene rubber

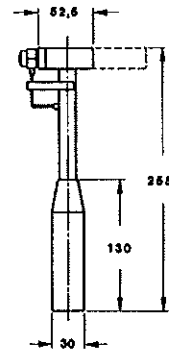
Weight of the additional mass: 122 g

Weight of the plastic tip: 3,0 g

Weight of the rubber tip: 4,1 g

Weight of the steel tip: 10,3 g

Dimensions (mm):



Date: 84.11.15 Signature: J.D.

荷重計 試験成績書

LOAD CELL TEST DATA

型名 Type	TCLP-5B	容量 Capacity	5 tf	製造番号 Serial No.	CQ1309
試験年月日 Date	1992.1.8	温度 Temperature	23 °C	湿度 Humidity	65 %

	Ten.	Comp.	
定格出力 Rated output	+999	-1002	μV / V
(ひずみ出力 K=2.00) Strain	+1998	-2003	× 10 ⁻⁶
校正係数 Calibration coefficient	0.002503	0.002496 tf	/ 1 × 10 ⁻⁶
非直線性 Non-linearity	0.07		% R O
ヒステリシス Hysteresis	0.07		% R O
零点の温度影響 Temperature effect on zero	0.1		% R O / 10°C
出力の温度影響 Temperature effect on span	0.05		% / 10°C
零バランス Zero balance	0		× 10 ⁻⁶
入出力端子間抵抗 Input & output resistance	350.8	Ω	出力 output 352.0 Ω
絶縁抵抗 Insulation resistance	1000	MΩ (DC 50V)	
入出力コード Connection cable	0.5	mm	10 m

仕 様
Specifications

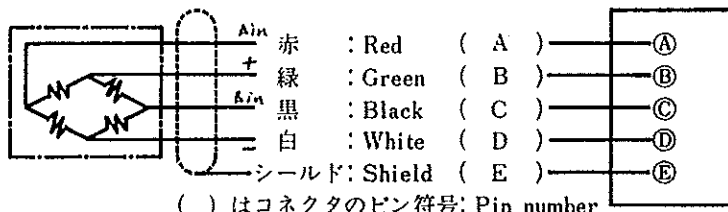
1. 許容過負荷 : Safe overload rating
2. 限界過負荷 : Ultimate overload rating
3. 補償温度範囲 : Compensated temperature range
4. 許容温度範囲 : Safe temperature range
5. 許容印加電圧 : Safe excitation

	200	%
	300	%
	0	°C ~ +40 °C
	-10	°C ~ +60 °C
	20	V

接 続 法
Connection

入力: 赤 黒
Input Red Black

出力: 緑 白
Output Green White



スイッチボックス
または測定器
Instrument

() はコネクタのピン符号; Pin number

計 算 法
Calculation

ひずみ測定器を使用して測定する場合 (K=2.00)
: When measured by strain meter

測定量 = 校正係数 × 指示値
Load = Calibration coefficient × Readout strain

注 意 事 項
Remarks

使用前に下記項目が試験成績表の記載値に近いことを確認して下さい。
: Before use, check the following items.

1. 零バランス : Zero balance
2. 入出力端子間抵抗 : Input & output resistance
3. 絶縁抵抗 (印加電圧50V以下でチェックして下さい。)
: Insulation resistance (at less than 50V DC)



株式会社 東京測器研究所

〒140 東京都品川区南大井 6-8-2 TEL (03)3763-5611

Tokyo Sokki Kenkyujo Co., Ltd.

8-BAN 2-GO, MINAMI-OHI 6-CHOME, SHINAGAWA-KU, TOKYO, JAPAN TEL

試験者
Tested by

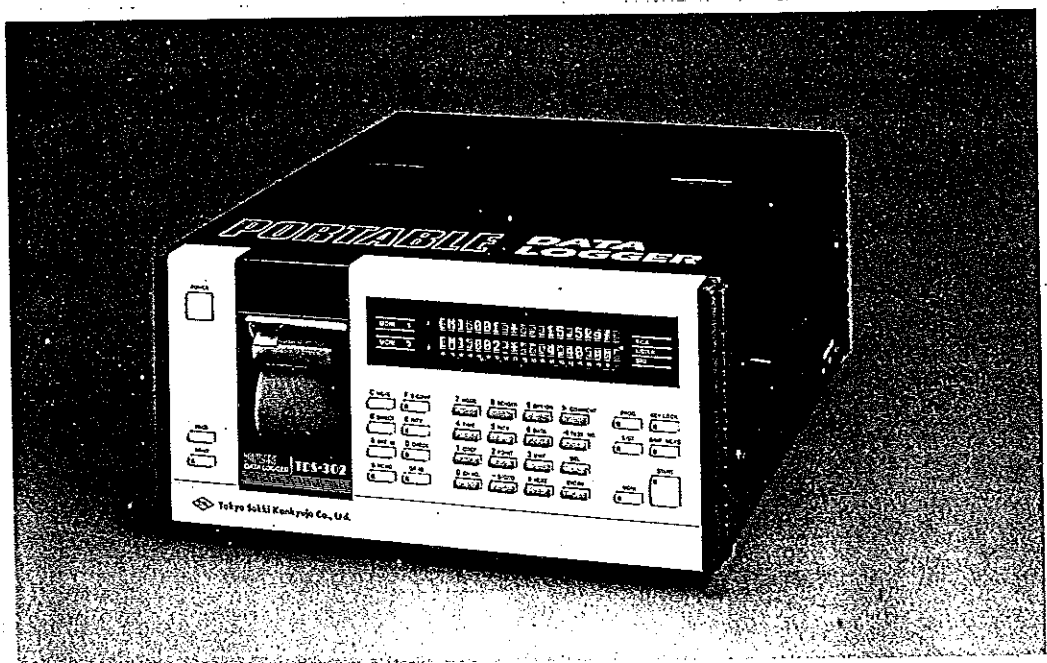
責任者
Supervised by



OPERATION MANUAL

TML Portable Data Logger

Model **TDS-302**



Tokyo Sokki Kenkyujo Co., Ltd.

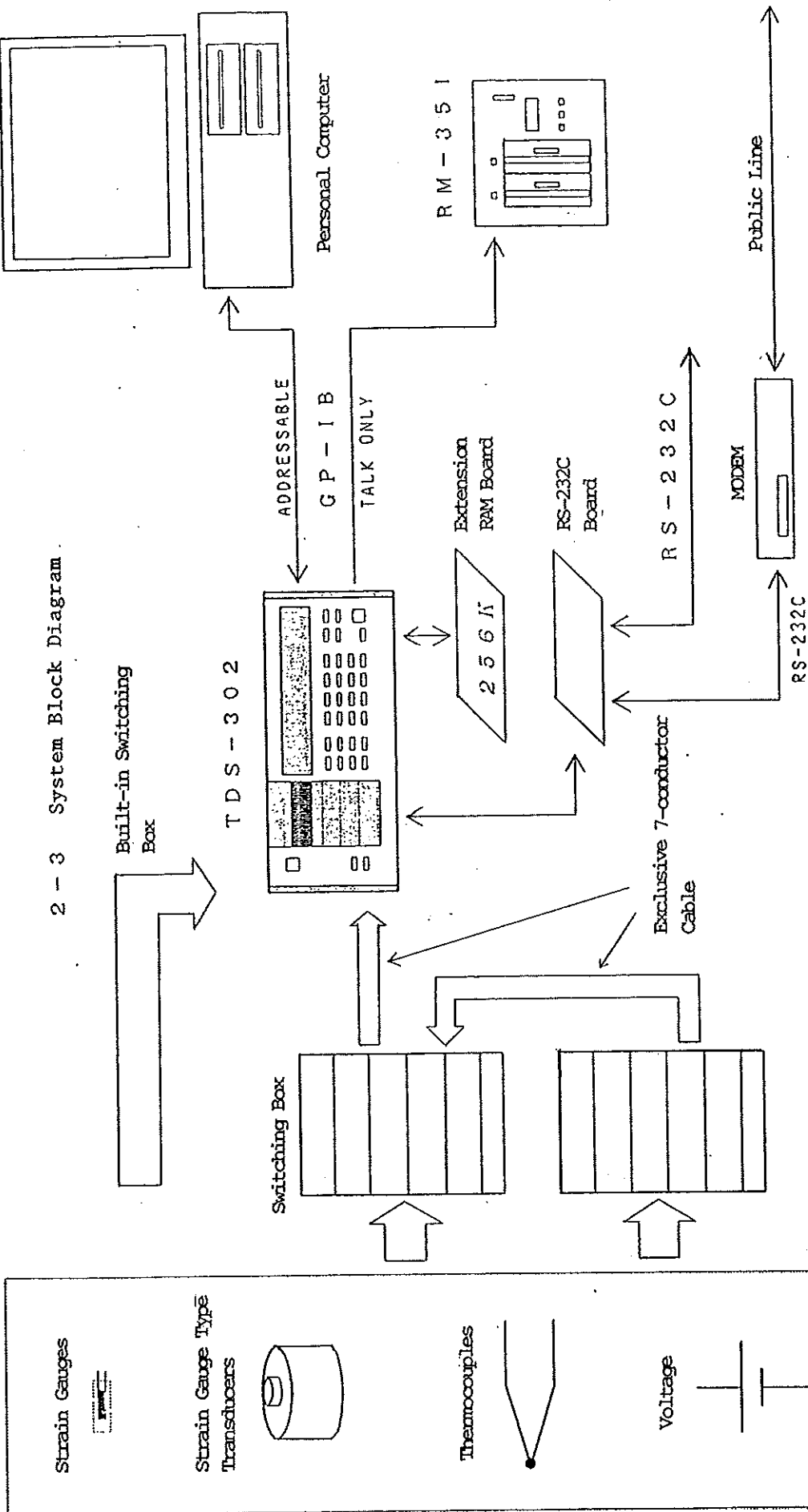
8-2, Minami-Ohi 6-Chome, Shinagawa-Ku, Tokyo, 140, JAPAN

Tel: Tokyo 03-763-5611

Fax: Tokyo 03-763-6128

Cable Address: STRAINGAUGE TOKYO

Telex: 0246-8083 STRAIN

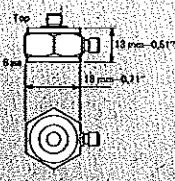
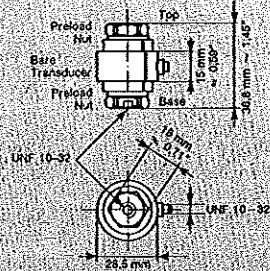


2 - 3 System Block Diagram

Connectable Switching Boxes (Representative)

- ASW-50B : On-board temperature unit & Constant current excitation available
- ASW-50AM : Small
- ASW-50C : Control Type & Compatible with temperature
- SSW-50C : Semiconductor-relay type of ASW-50C

Specifications 8200 and 8201

	8200	8201
Force Range	1000N tensile to 5000N compressive (-225 lbf to +1125 lbf)	4000N tensile to 16000N compressive (-900 lbf to +3600 lbf) with preloading nuts, 20000N compressive (+4500 lbf) without preloading nuts
Linearity*	< ± 1% of Max. Force	< ± 2% of Max. Force
Reproducibility of original sensitivity with remounting of preloading nuts	—	< ± 2% of Max. Force
Charge Sensitivity* (typical)	4 pC/N (17,8 pC/lbf)	4 pC/N (17,8 pC/lbf)
Capacitance (typical)	25 pF	70 pF
Leakage Resistance (at 25°C)	> 10 ⁹ MΩ	> 10 ⁹ MΩ
Stiffness	5 × 10 ⁸ N/m (2,9 × 10 ⁸ lbf/in)	7 × 10 ⁸ N/m (4 × 10 ⁸ lbf/in)
Deformation at Maximum Force	0,01 mm (0,0004 in)	0,03 mm (0,0012 in)
Resonant Frequency* with 5 grams load mounted on top (typical)	35 kHz	20 kHz
Effective Seismic Mass:		
Above Piezoelectric Element (Top)	3 grams	With preloading nuts 43 grams Without preloading nuts 16 grams
Below Piezoelectric Element (Base)	18 grams	With preloading nuts 69 grams Without preloading nuts 43 grams
Temperature Range	-196°C to + 200°C (-321°F to + 392°F)	-196°C to + 150°C (-321°F to + 302°F)
Temperature Transient Sensitivity (typical)	0,5 N/°C (0,06 lbf/°F)	0,4 N/°C (0,05 lbf/°F) (with preloading nuts)
Transverse Sensitivity+ (typical)	5%	4% (with preloading nuts mounted)
Maximum Transverse Force for Stated Transverse Sensitivity	100N (22,5 lbf)	500N (112 lbf)
Bending Moment Sensitivity++ (typical)	100 pC/Nm (136 pC/lbf ft)	25 pC/Nm (34 pC/lbf ft) (with preloading nuts mounted)
Maximum Bending Moment for Stated Bending Moment Sensitivity	1 Nm (0,74 lbf ft)	10 Nm (7,4 lbf ft)
Strain Sensitivity** (top and base)	< 0,04 N (0,009 lbf) per μStrain	< 0,004 N (0,0009 lbf) per μStrain (with preloading nuts mounted)
Magnetic Sensitivity** at 50Hz (typical)	0,2 N/T ^Δ (0,05 lbf/T)	0,9 N/T ^Δ (0,2 lbf/T)
Material	Stainless Steel AISI 316	Stainless Steel AISI 316
Weight	21 grams (0,046 lb)	With preloading nuts 112 grams (0,25 lb). Without preloading nuts 58 grams (0,13 lb)
Dimensions		
Accessories Supplied (Type 8200P packages contain accessories marked p for each transducer)	AO 0038 Cable (p), YQ 2962 Threaded Stud 0,31" long (p) YQ 2960 Threaded Stud 0,5" long, YP 0160 Insulated Stud 0,5" long YQ 0534 Mica Washer, QA 0029 Threadlap 10-32NF, QA 0013 Allen Key DB 1374 Beryllium nut (with 8200 only), DB 1375 and DB 1376 Spherical Nuts Calibration Chart and Instruction Manual (p)	

* Individual values given on the calibration chart

** Ref. ANSI S2.11-1969

+ For forces transverse to the main axis of the transducer

++ The total bending moment is the sum of the resultant bending moments due to axial and transverse forces taken about the mid-point of the transducer

Δ 1 Testa = 10k Gauss

Table 1: Different MKII system slot configurations

Main Frame	Slot Number	Card Name	Function
MF02 (2 slot)	1	PQ11/PQ11W	System controller and power supply (combined)
	2	SC41	Data acquisition
MF03 (3 slot)	1	PQ11/PQ11W	System controller and power supply (combined)
	2-3	SC41	Data acquisition
MF06 (6 slot)	1	EP1A/PPC4	System controller
	2-5	SC41	Data acquisition
	6	PM11	Power supply
MF10 (10 slot)	1	EP1A/PPC4	System controller
	2-9	SC41	Data acquisition
	10	PV11	Power supply

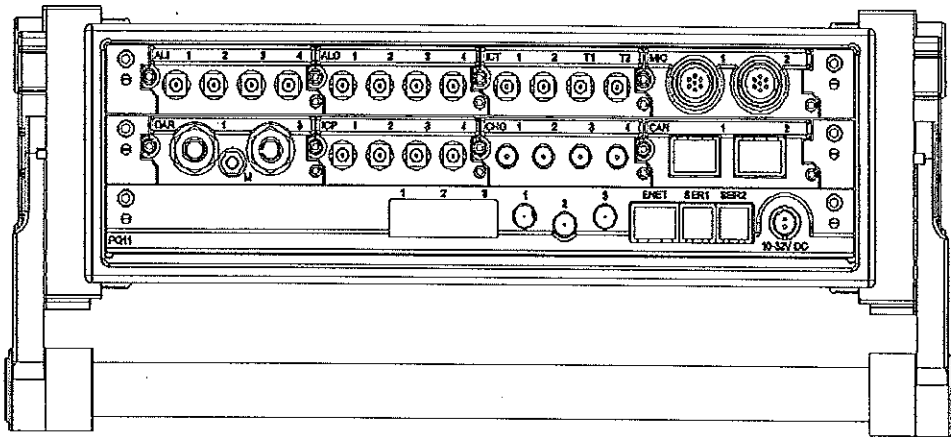


Figure 1: 3 slot MKII (front view)

1.3 System cards

1.3.1 SC41

The Signal Conditioning or SC41 data acquisition card provides the physical interfaces to external measurement sensors, devices and equipment through small modular signal conditioning units (referred to as SC41 Modules or just Modules). Each SC41 contains 4 Module slots into which various different Modules may be inserted.

A specific type of Module would normally handle a certain group of related measurement signals (for instance, analog input versus analog output). Therefore, the interfaces of an SC41 are determined by which Modules a user has inserted into its Module slots.

This high degree of modularity allows MKII to be optimally configured for a particular test. It can grow in capacity and capability through acquiring additional SC41 cards as well as different Module types from the currently available (and expanding) range of Modules.

More information on the Modules is given below (see section 4.3 'Connecting signals to SC41 Modules').

Metering and Monitoring

The RMS values of output current and voltage for sinusoidal and Gaussian waveforms are displayed on multirange front panel meters. An additional zero-center DC current scale is provided for Exciter Head centering purposes. The output voltage and current waveforms can be monitored at front panel BNC sockets.

Use in Multiple Exciter-Amplifier Systems

In multiple systems the Power Amplifiers are interconnected in such a way that a trigger signal in any amplifier will remove the input signal from all the other amplifiers as well.

The high impedance mode is particularly suitable when multiple

exciters are used for resonant mode determination of structures. The forces generated by the exciters are in phase or shifted 180° by a switch if desired, adjustable in magnitude and are insensitive to changes in impedance of the structure as frequency is swept. In this respect the operation is similar to that of multiple exciters connected in series and driven by a single amplifier, but it provides greater flexibility in adjusting the relative forces generated by the exciters.

Use in Single Exciter Systems

The low impedance mode keeps the voltage applied to the exciter independent of test object changes. This mode provides the best acceleration waveform and is therefore preferable for most single exciter applications. However, the

low impedance mode is also useful for multiple exciter systems in the lower frequency range when the same motion is desired from each exciter. An example is the use of one exciter to push and another to pull on a model of a bridge.

Power Requirements

The Power Amplifier Type 2707 is powered from a single phase AC power line. Type 2708 needs a three phase power supply. Power for the exciter is also controlled by the amplifier power switch. Transformer taps are provided to accommodate all common 50 or 60 Hz line voltages: 9 different single phase voltages and 13 different three phase line voltages.

Specifications 2707 and 2708

Power Amplifier	Type 2707		Type 2708	
Capacity	220 VA into 0,5Ω exciter or resistor load		1200 VA into 0,6Ω exciter or resistor load	
Voltage	10 V RMS DC to 10 kHz		27 V RMS DC to 5 kHz 13,5 V RMS at 10 kHz	
Current	10 A DC 11 A RMS at and below 5 Hz 22 A RMS 40 Hz to 10 kHz		20 A DC 25 A RMS at and below 0.1 Hz 45 A RMS 5 Hz to 10 kHz	
Frequency Range Full capacity Reduced capacity	40 Hz to 10 kHz DC to 100 kHz		5 Hz to 5 kHz DC to 100 kHz	
Frequency Response	Typical small signal response, low impedance mode			
DC input	DC to 10 kHz ± 0,5 dB DC to 100 kHz ± 3 dB		DC to 10 kHz ± 0,5 dB DC to 100 kHz ± 3 dB	
AC input	15 Hz to 100 kHz ± 3 dB		15 Hz to 100 kHz ± 3 dB	
Input Impedance	at least 10kΩ		at least 10 kΩ	
Gain at 1 kHz	Low Impedance	High Impedance	Low Impedance	High Impedance
	5 V/V ± 1 dB	14 A/V ± 2 dB	13,5 V/V ± 1 dB	24 A/V ± 2 dB
Output Impedance	< 0,02 Ω DC to 1 kHz < 0,05 Ω 1 kHz to 10 kHz	> 20 Ω 5 Hz to 1 kHz > 50 Ω 20 Hz to 300 Hz > 80 Ω 40 Hz to 100 Hz	< 0,01 Ω DC to 1 kHz < 0,05 Ω 1 kHz to 10 kHz	> 10 Ω 2.5 Hz to 1.5 kHz > 20 Ω 5 Hz to 700 Hz > 70 Ω 20 Hz to 200 Hz
Harmonic Distortion	0,5 Ω resistive load		0,6 Ω resistive load	
	Full capacity	< 0,1% DC to 5 kHz < 0,5% 5 kHz to 10 kHz	< 0,2% DC to 2 kHz < 0,7% 2 kHz to 10 kHz	< 0,2% DC to 5 kHz < 0,4% 5 kHz to 10 kHz
Noise and Hum below full output	at least 85 dB	at least 75 dB	at least 80 dB	at least 70 dB

APPENDIX F

ANSYS Report of Test # 5

Project

Author

Ismail Bin Musa

Subject

Test 1

Prepared For

Master's Degree of Mechanical Engineering

Project Created

Saturday, April 28, 2007 at 11:37:01 AM

Project Last Modified

Monday, March 24, 2008 at 6:16:04 PM

Report Created

Thursday, March 27, 2008 at 4:04:53 AM

Software Used

ANSYS 10.0

Database

C:\thesis\Finite Element_2nd Mac 2008\baru test\baru test 2\Dynamic test\Assem17 final_14 April 2007 rev_main structure_4mm_center_stress_strain_test 1_remote force..@58.91 Hz.dsdb

1. Scenario 1

1.1. "Model"

"Model" obtains geometry from the SolidWorks® assembly "F:\Thesis\DWG\Assem17 final_14 April 2007 rev_main structure_4mm_center.SLDASM".

- The bounding box for all positioned bodies in the model measures 3.1 by 0.31 by 0.98 m along the global x, y and z axes, respectively.
- The model has a total mass of 70.35 kg.
- The model has a total volume of $7.11 \times 10^{-3} \text{ m}^3$.

Name	Material	Nonlinear Material Effects	Bounding Box(m)	Mass (kg)	Volume (m ³)	Nodes	Elements
"Part_support 1-2"	"Structural Steel"	Yes	0.12, 0.1, 4.85×10^{-2}	3.96	4.0×10^{-4}	574	84
"CHASSIS 11M-1"	"Structural Steel"	Yes	3.1, 0.18, 0.98	29.46	2.98×10^{-3}	108470	55048
"part d 3-1"	"Structural Steel"	Yes	4.0×10^{-2} , 8.38×10^{-2} , 0.74	4.36	4.4×10^{-4}	680	110
"Part10-1"	"Structural Steel"	Yes	0.13, 7.32×10^{-2} , 0.79	2.41	2.44×10^{-4}	5364	2530
"Part_support 1-1"	"Structural Steel"	Yes	0.12, 0.1, 4.85×10^{-2}	3.96	4.0×10^{-4}	574	84
"Part_support 1-3"	"Structural Steel"	Yes	0.12, 0.1, 5.14×10^{-2}	3.96	4.0×10^{-4}	574	84
"Part_support 1-4"	"Structural Steel"	Yes	0.12, 0.1, 5.25×10^{-2}	3.96	4.0×10^{-4}	574	84
"Part_support 1-5"	"Structural Steel"	Yes	0.12, 0.1, 4.8×10^{-2}	3.96	4.0×10^{-4}	574	84
"Part_support 1-6"	"Structural Steel"	Yes	0.12, 0.1, 4.9×10^{-2}	3.96	4.0×10^{-4}	574	84
"Part_support 1-7"	"Structural Steel"	Yes	0.14, 0.12, 5.56×10^{-2}	3.96	4.0×10^{-4}	574	84
"Part_support 1-8"	"Structural Steel"	Yes	0.14, 0.12, 5.64×10^{-2}	3.96	4.0×10^{-4}	574	84
"Part9-5"	"Structural Steel"	Yes	9.07×10^{-2} , 0.03, 0.86	2.47	2.5×10^{-4}	878	110

1.1.1. Contact

- "Contact" uses a tolerance of 0.0 for automatic detection.

Table 1.1.1.1. Contact Conditions							

Name	Type	Associated Bodies	Scope	Normal Stiffness	Scope Mode	Behavior	Update Stiffness	Formulation	Thermal Conductance	Pinball Region
"Contact Region"	Bonded	"Part_support 1-2" and "CHASSIS 11M-1"	Face, Face	Program Controlled	Automatic	Symmetric	Never	Pure Penalty	Program Controlled	Program Controlled
"Contact Region 2"	Bonded	"CHASSIS 11M-1" and "part d 3-1"	Face, Face	Program Controlled	Automatic	Symmetric	Never	Pure Penalty	Program Controlled	Program Controlled
"Contact Region 3"	Bonded	"CHASSIS 11M-1" and "Part10-1"	Face, Face	Program Controlled	Automatic	Symmetric	Never	Pure Penalty	Program Controlled	Program Controlled
"Contact Region 4"	Bonded	"CHASSIS 11M-1" and "Part_support 1-1"	Face, Face	Program Controlled	Automatic	Symmetric	Never	Pure Penalty	Program Controlled	Program Controlled
"Contact Region 5"	Bonded	"CHASSIS 11M-1" and "Part_support 1-3"	Face, Face	Program Controlled	Automatic	Symmetric	Never	Pure Penalty	Program Controlled	Program Controlled
"Contact Region 6"	Bonded	"CHASSIS 11M-1" and "Part_support 1-4"	Face, Face	Program Controlled	Automatic	Symmetric	Never	Pure Penalty	Program Controlled	Program Controlled
"Contact Region 7"	Bonded	"CHASSIS 11M-1" and "Part_support 1-5"	Face, Face	Program Controlled	Automatic	Symmetric	Never	Pure Penalty	Program Controlled	Program Controlled
"Contact Region 8"	Bonded	"CHASSIS 11M-1" and "Part_support 1-6"	Face, Face	Program Controlled	Automatic	Symmetric	Never	Pure Penalty	Program Controlled	Program Controlled
"Contact Region 9"	Bonded	"CHASSIS 11M-1" and "Part_support 1-7"	Face, Face	Program Controlled	Automatic	Symmetric	Never	Pure Penalty	Program Controlled	Program Controlled
"Contact Region 10"	Bonded	"CHASSIS 11M-1" and "Part_support 1-8"	Face, Face	Program Controlled	Automatic	Symmetric	Never	Pure Penalty	Program Controlled	Program Controlled
"Contact Region 11"	Bonded	"CHASSIS 11M-1" and "Part9-5"	Face, Face	Program Controlled	Automatic	Symmetric	Never	Pure Penalty	Program Controlled	Program Controlled

1.1.2. Mesh

- "Mesh", associated with "Model" has an overall relevance of 0.
- "Mesh" contains 119984 nodes and 58470 elements.

No mesh controls specified.

1.2. "Environment"

Simulation Type is set to Harmonic

Analysis Type is set to Harmonic

"Environment" contains all loading conditions defined for "Model" in this scenario.

1.2.1. Harmonic Loading

Name	Type	Magnitude	Vector	Phase Angle	Location	Associated Bodies
"Remote Force"	Remote Force	9,810.0 N	[0.0 N x, -9,809.87 N y, -50.52 N z]	0.0 °	[2.84 m x, -0.27 m y, 0.09 m z]	"CHASSIS 11M-1"
"Remote Force 2"	Remote Force	9,810.0 N	[0.0 N x, 9,809.87 N y, 50.52 N z]	0.0 °	[2.84 m x, -0.27 m y, -0.54 m z]	"CHASSIS 11M-1"

1.2.2. Structural Supports

Name	Type	Associated Bodies
"Fixed Support"	Fixed Surface	"CHASSIS 11M-1"
"Fixed Support 2"	Fixed Surface	"CHASSIS 11M-1"

NOTE: If a body contains two or more supports that share an edge or vertex, use caution in evaluating the listed reaction forces at those supports. Calculation of reaction forces includes the forces acting along bounding edges and vertices. When supports share edges or vertices the global summation of forces may not appear to balance.

1.3. "Solution"

Solver Type is set to Program Controlled

Weak Springs is set to Program Controlled

Large Deflection is set to Off

"Solution" contains the calculated response for "Model" given loading conditions defined in "Environment".

- Thermal expansion calculations use a constant reference temperature of 22.0 °C for all bodies in "Model". Theoretically, at a uniform temperature of 22.0 °C no strain results from thermal expansion or contraction.

1.3.1. Harmonic Results

Table 1.3.1.1. Definition

Range Minimum	Range Maximum	Solution Method	Solution Intervals	Cluster Results	Damping Ratio	Beta Damping	Define By
0.0	180.0	Mode Superposition	10	No	0.0	0.0	Direct Input

Table 1.3.1.2. Values

Name	Scope	Orientation	Minimum	Maximum	Frequency	Phase Angle	Alert Criteria
<i>"Total Deformation"</i>	All Bodies In <i>"Model"</i>	Global	0.0 m	1.34×10^{-2} m	58.91Hz	0.0°	None

Appendices

A1. Scenario 1 Figures

No figures to display.

A2. Definition of "Structural Steel"

Name	Value
Compressive Ultimate Strength	0.0 Pa
Compressive Yield Strength	2.5×10^8 Pa
Density	9,900.0 kg/m ³
Poisson's Ratio	0.23
Tensile Yield Strength	2.5×10^8 Pa
Tensile Ultimate Strength	4.6×10^8 Pa
Young's Modulus	1.45×10^{11} Pa
Thermal Expansion	1.2×10^{-5} 1/°C
Specific Heat	434.0 J/kg·°C
Thermal Conductivity	60.5 W/m·°C
Relative Permeability	10,000.0
Resistivity	1.7×10^{-7} Ohm·m

Table A2.2. Alternating Stress

Mean Value 0.0

Cycles	Alternating Stress

10.0	4.0×10^9 Pa
20.0	2.83×10^9 Pa
50.0	1.9×10^9 Pa
100.0	1.41×10^9 Pa
200.0	1.07×10^9 Pa
2,000.0	4.41×10^8 Pa
10,000.0	2.62×10^8 Pa
20,000.0	2.14×10^8 Pa
100,000.0	1.38×10^8 Pa
200,000.0	1.14×10^8 Pa
1,000,000.0	8.62×10^7 Pa

Table A2.4. Strain-Life Parameters

Strength Coefficient	9.2×10^8 Pa
Strength Exponent	-0.11
Ductility Coefficient	0.21
Ductility Exponent	-0.47
Cyclic Strength Coefficient	1.0×10^9 Pa
Cyclic Strain Hardening Exponent	0.2

APPENDIX G

Theory of Chassis Design

Appendix G

THEORY OF CHASSIS DESIGN AND DEVELOPMENT

This chapter looks on the introduction and basic theory of the components that are used in research. Among the components that will be discussed are fundamentals of truck chassis, theory and mechanics of vibration, basic concept of finite elements method, modal analysis, correlation and model updating. The study will cover the development of truck chassis with appropriate dynamic, structural behavior and taking into account the effect on rolling, handling and stability of the vehicle.

4.1 Truck Chassis

The chassis frame forms the backbone of the truck and its chief function is to safely carry the maximum load wherever the operation demands. Basically it must absorb engine and axle torque and absorb shock loads over twisting, pounding and uneven roadbeds when the vehicle is moving along the road. In a modern vehicle, it is also expected to fulfill the vital function which is to provide mounting points for the suspension systems, the steering mechanism, the engine and gearbox, the final

drive, the fuel tank and the seating for the occupants. While fulfilling these functions, the chassis should be light enough to reduce inertia and offer satisfactory performance. It should also be tough enough to resist fatigue loads that are produced due to the interaction between the driver, the engine and power transmission and the road.

A typical chassis design is of ladder frame, shaped like a large ladder, is used in body-on-frame construction. It was designed with two long “rails” run along the side, with cross member connecting each other. This type of frame is used in most pickup trucks and sport utility vehicles. It has a difference in shape, structure and thickness of the various elements. Figure 4.1 shows the ladder frame that is currently being used in the market.



Figure 4.1: The main structures of ladder-type chassis

4.2 Mode of Ladder Frame Deflection

The ladder frame chassis is subjected to three load cases: bending, torsion and dynamic loads when the truck is moving along the road. The bending and torsion load is used by the weight of the component and in cases like the truck hit a bump. The dynamic load case comprises of longitudinal and lateral loads during acceleration, braking and cornering. All these loading cases will cause the chassis to

deflect. Figure 4.2 shows the mode of chassis deflection. Strengthening of the ladder frame chassis is needed to reduce the effect of these deflections.

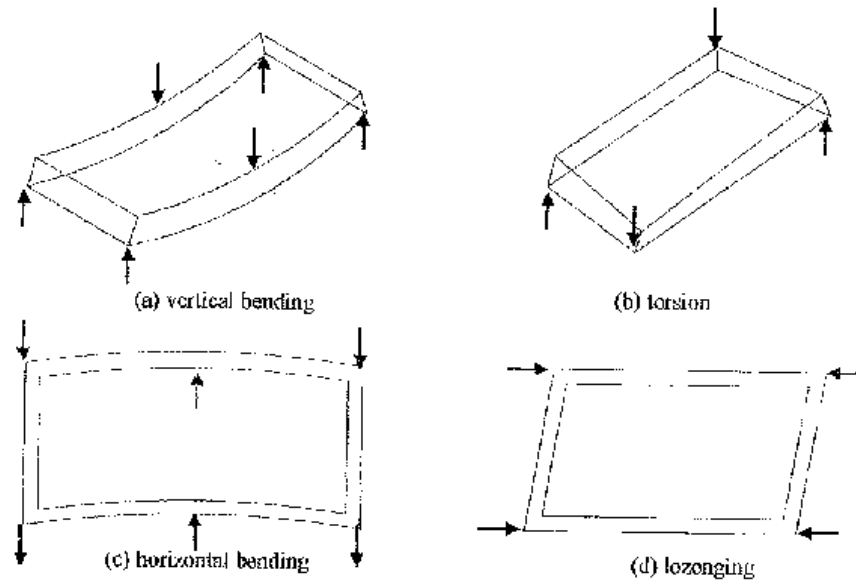


Figure 4.2: Mode of chassis frame deflection

4.3 Improvement study

Optimization is a group of numerical and programming techniques used to search for the optimum value of mathematical functions. In other words, the purpose of the optimization is to assist in finding the project that best fills out the needs.

Nowadays, the computational algorithms analyze a reduced project that the user considers to represent the real problem. Basic parameters can be modified and a solution is found. In other words, the physical experimentation is substituted by the numeric approach in a stage that precedes the construction of prototypes. Actually

the experimental is not eliminated, it is simply used as a final step for validation of the results suggested by the numeric experimentation or optimization. To optimize the structure, a finite element model based on beam elements was built in optimization software as can be seen in figure 4.3. The beam model was validated properly with the real structure according to the procedure. The comparison between the models and the real structure is shown in figure 4.4 below.

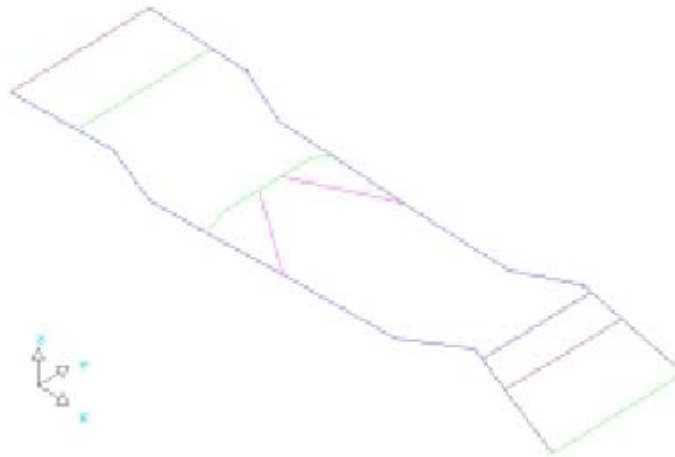


Figure 4.3: Finite Element model based on beam element [4]

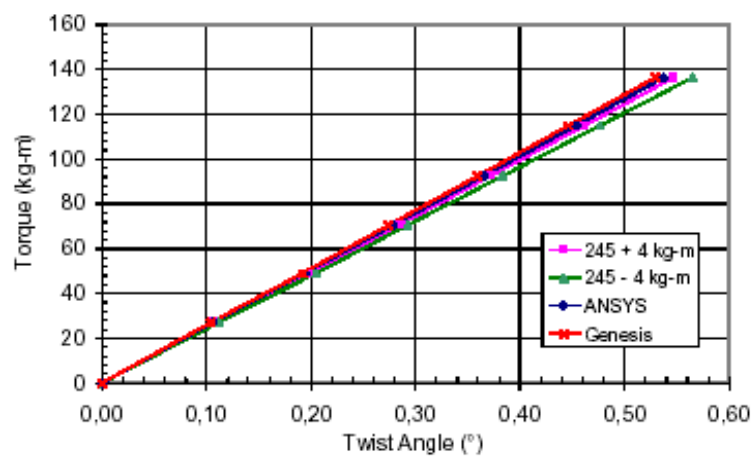


Figure 4.4: Comparison between model and real structure [4]

The structure after optimization procedure is shown in figure 4.5.

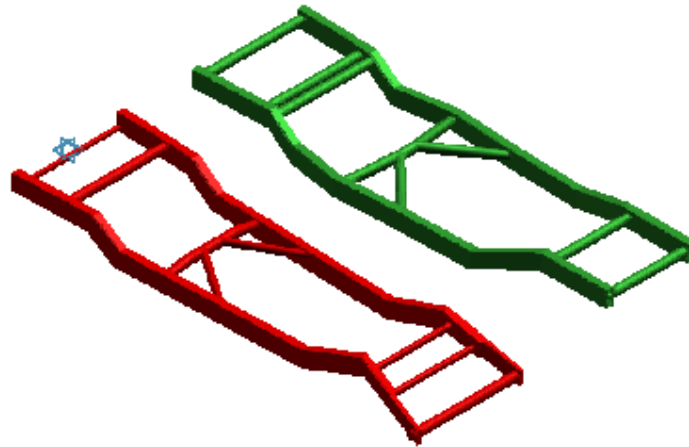


Figure 4.5: Optimized structure compared with the initial design [4]

Study by Izzuddin et al showed that the optimized structure can increase torsional stiffness by 75% as depicted in Figure 4.6. [3]. It also presented a 6% increase in its total weight. The center of gravity of the new structure was 30mm higher (position Z). The position in X and Y of center of gravity varied about 1% in the optimized structure.

The front of the optimized structure presents simpler geometry and will facilitate its construction and decrease the production costs. In other words, this study will be useful for future improvement of new truck chassis and other parameters such as plate thickness, mass density and Poisson's ratio will be incorporated into the analysis

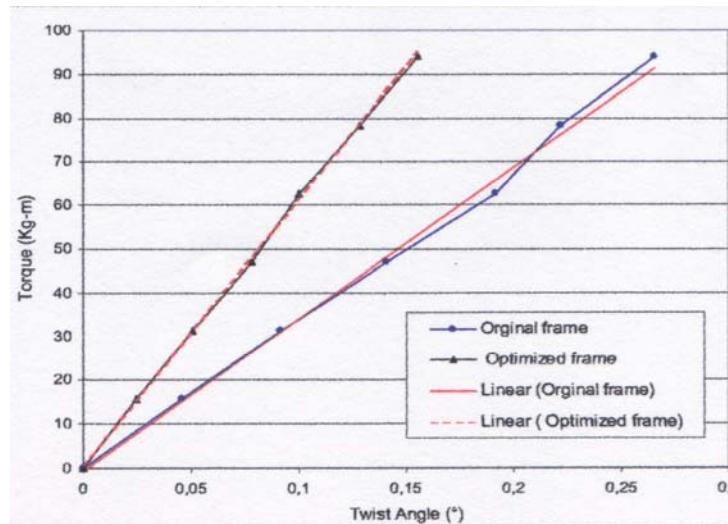


Figure 4.6: Comparison between the initial design structure and the optimized regarding torsion stiffness[3]

4.4 Natural Frequency

The natural frequency is one of the important criteria to determine the dynamic characteristics of structure. Basically natural frequency can be defined as the natural characteristic of a vibratory system. If the body or system is given an initial displacement from the equilibrium position and released, it will vibrate with a definite frequency known as the natural frequency. The vibration is said to be free since no external forces act upon it after the first displacement. For a simple spring mass system, the natural frequency is defined by:

$$f_n = \sqrt{k/m} , \text{ rad/s}$$

where k = spring stiffness, N/m

m =mass, kg

The formula shows that the natural frequency depends on the ratio of the spring stiffness to the mass. Stiffer spring or lighter mass will increase the natural frequency and vice versa.

Mode shape refers to the behaviors of the system when it vibrates freely. It can be expressed in the form of linear or translation, angular or torsion, flexural transverse or lateral. Each of the characteristic frequencies of a given body is associated with a different pattern or mode shape and it is described as any point that is stationary or has zero displacement amplitude at all time during the vibration of the system.

4.5 Resonance

Under some conditions, as in the case of an unbalanced machine, the body or system may be subjected to a periodic external force. In such cases a forced vibration occurs. If the periodic of this external force is the same as or close to the natural frequency, resonance will take place. In other words, resonance is a phenomenon that occurs whenever the natural frequency of vibration of a machine or structure coincides with the natural frequency of the external excitation. When resonance occurs, the system undergoes dangerously large oscillation and amplitudes, which leads to excessive deflection, high stresses and failure. Failures of such structure as buildings, bridges, turbines and airplane wing have been associated with the occurrence of resonance. Figure 4.7 below shows the example of the resonance occurred on the Tacoma Bridge in year 1940.



Figure 4.7: Failure of the Tacoma Bridge

4.6 Amount of Modal Damping

Damping does not play an important role in the region away from the natural frequencies. In fact, in this situation, the system can be treated as un-damped. However, closer to the natural frequency, a small change in damping would cause a large change in the response. Hence, obtaining accurate modal damping value may be crucial.

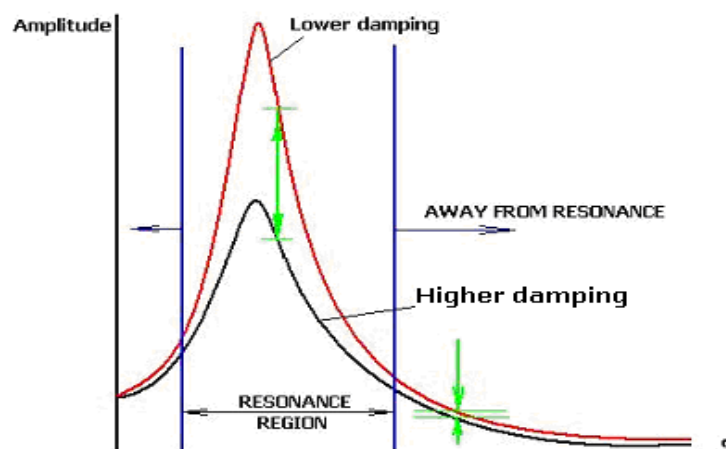


Figure 4.8: Effect of damping close to and away from resonance

Figure 4.8 implies that for region close to resonance, the amplitude is very much dependable on the damping of the system. Away from resonance, difference in damping does not cause much change in the response and depends mainly on the following:

$$\beta_r = \frac{1}{\left[1 - \frac{\omega^2}{P_r^2}\right]}$$

Where, β_r = magnification factor

P_r = un-damped frequency

ω^2 = Frequency response

At resonance, the structure's internal resistances, namely the stiffness and inertia cancel each other out. In a totally un-damped structure, all the excitation energy that enters the structure accumulates within, resulting in escalation of vibration amplitude eventually leading to structural destruction. The presence of damping in the structure causes it to act as an energy dissipater. The higher the damping the more of this energy is dissipated, implying lower vibration amplitude. From the equation below, it can be seen that damping is related to amount of mass and stiffness in the structure. Hence, for a given amount of excitation energy at resonance, the amplitude of vibration is reduced for a structure of higher mass or stiffness.

$$C = aM + bS$$

where C = damping value

M = amount of mass

S = amount of stiffness

4.7 Theory of Finite Element Analysis

Finite Element Method (FEM) is a computational method used in solving engineering problem involving stress analysis, heat transfer, electromagnetism, fluid flow, dynamics and others. It is a numerical method and coupled with a common algorithm, it forms a powerful unifying approach to obtain solution to a large class of engineering problems. Figure 4.9 (a) below shows the discretised domain

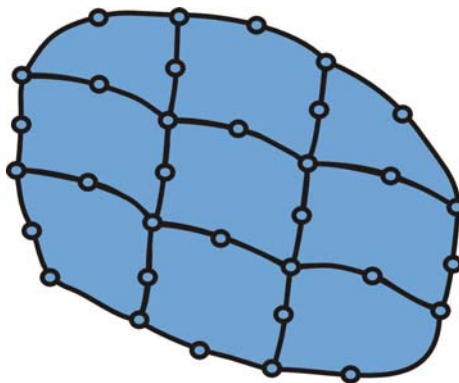


Figure 4.9(a) Discretised domain

In trying to determine the field governing equation describing the exact behavior of an engineering quantity in a domain, one faces with the following complex problems:

- 1) Geometry and boundary condition
- 2) Initial condition

To overcome this, FEA approximates the solution by breaking up the domain into small finite elements of simple geometry as shown in Figure 4.9(b). The behavior of the field primary variable for each element is then defined as functions of nodal values. The governing differential equations are integrated for each element. The elements are then assembled together to re-form the total structure by equating the values of common nodes.

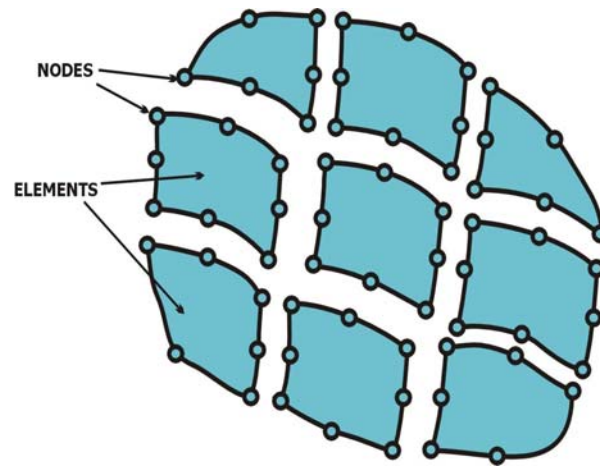


Figure 4.9(b) Domain broken up into finite elements

4.7.1 Basic Steps in the Finite Element Method

Pre-Processing Phase

- 1) Create and discretize the solution domain into finite elements

This is performed by subdividing the problem into nodes and elements. Fundamentally, FEM breaks up a complex domain into a number of simple finite elements, as shown in Figure 4.9, and treating each element one at a time. Figure 4.10 shows an example of how it is performed on a real model.

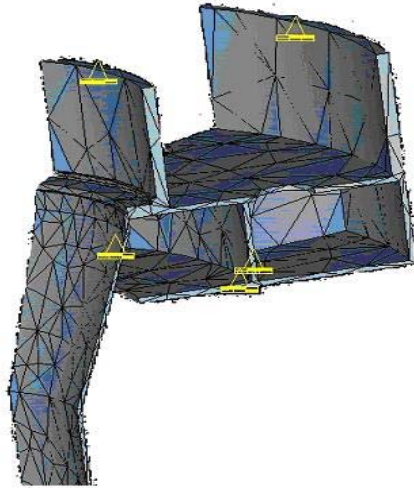


Figure 4.10: Real Model of FEM

2) Assume a shape function to represent the physical behavior of an element
 An approximate continuous function is assumed to represent the solution of an element. For each element, the field variable is described by shape functions relating to the nodes along the boundary of the element.

3) Develop matrix equation for an element

In elasto-static problem, each element forms a stiffness matrix, $[K]$, relating forces $[F]$ and displacements $[u]$ at nodes. The size of the stiffness matrix is equal to the number of nodes per element multiplies by the number of freedom per nodes, as in the following

$$[F] = [K][u]$$

In eigenvalue problem, the characteristic matrix is formed as

$$\{[K] - \omega^2 [M]\}[u] = 0$$

Where M is the mass matrix ω^2 are eigenvalues and u the eigenvectors. In structural dynamics, the values are the natural frequencies and the vectors are mode shapes.

4) Assemble the element to represent the entire problem.

Construct the global stiffness matrix. Each element matrix is assembled together to form a global matrix by equating the displacements at common nodes between adjacent elements. The size of the global matrix is equal to the total number of nodes multiplied by the number of freedom per nodes.

5) Apply boundary conditions, initial conditions and loading.

Boundary conditions are then applied to the nodes on the structural boundary, as shown in Figure 4.1

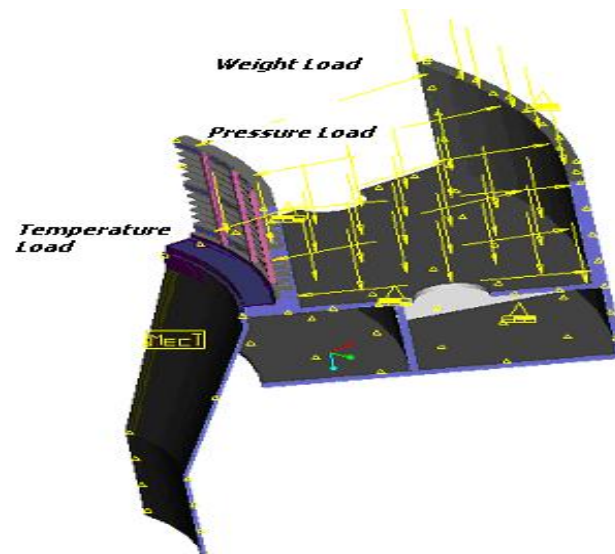


Figure 4.11 Real Model of FEM

Solution Phase

6) Sent the global matrix to the solver to solve for all unknowns.

The solver solves a set of linear or non-linear algebraic equations simultaneously to obtain nodal results, such as displacement values at different nodes or temperature

values at different nodes in a heat transfer problem. In eigenvalue problem, the eigenvalues and vectors are evaluated.

Post-Processing Phase

- 7) Obtain important information.

At this point, you may be interested in values of principal stresses, heat fluxes, etc. Displacement or temperature contours can be generated by interpolation of the nodal values and plotting, as shown in figure 4.12.

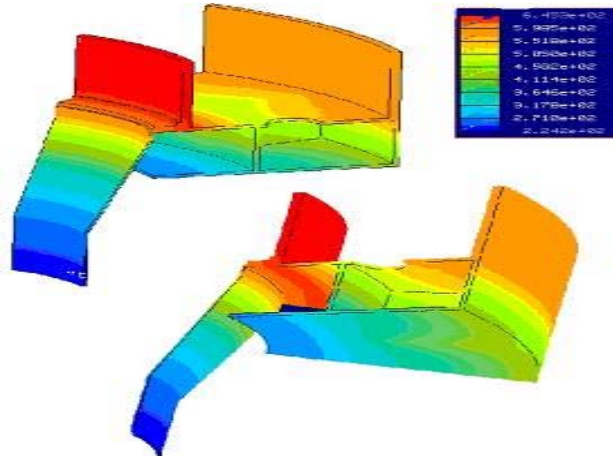


Figure 4.12 Interpolation of the nodal value and plotting

Today, there are quite a number of powerful computer aided design (CAD) software that can be used to perform 3 dimensional solid modeling of the structure, and then proceed to automatically mesh the model and export it to FEA software for subsequent processing. This has reduced substantially the pre-processing time. Similarly, on the other end, the post processing has become quite powerful with 3

dimensional view of various contours such as stress contour, temperature contour and animation of mode shape and kinematics. While before, when FEA could only run on supercomputers and workstations, another important development today is that most of the leading software houses have developed their modules that run on personal computers and in Windows environment. This has made initial set up of FEA laboratory well within reach for many. The ever-increasing power of personal computers has allowed even the most comprehensive of FEA software, including pre- and post- processing, to run on it. This is good news for application engineers.

4.8 Modal Analysis

Modal analysis, using Frequency Response Function (FRF) measurement techniques based on Fast Fourier Transformation (FFT), has been widely used in industries in determining the dynamic characteristics (natural frequencies, mode shapes and damping) of continuous linear systems. In this application, the measured input is force and the measured output is motion (displacement, velocity or acceleration). The equipment generally consists of multi-channel FFT analyzer, accelerometers, force transducers and modal analysis application software.

Modal analysis is a process of determining the dynamic characteristics (modal parameters) of a given structure, namely the mode shapes, modal frequencies and modal damping by measurement or computational techniques, and to develop a mathematical model simulating the dynamics of the structure. The inputs (excitations) and the outputs (responses) of the system are now related by only the system modal parameters contained in Frequency Response Function (FRF). Each FRF is a numerical curve (Fig.4.13), which relates one excitation point to one response point. By reciprocal theorem, an excitation point can be fixed while the response point is moved for all discrete points under consideration or the response can be fixed while the excitation points are moved. This is normally termed as single-input-multiple-output (SIMO) analysis. By curve fitting the FRF obtained from Fast

Fourier Transform (FFT) analysis for all measurement points, the modal parameters of a continuous system can be evaluated (Fig.4.14).

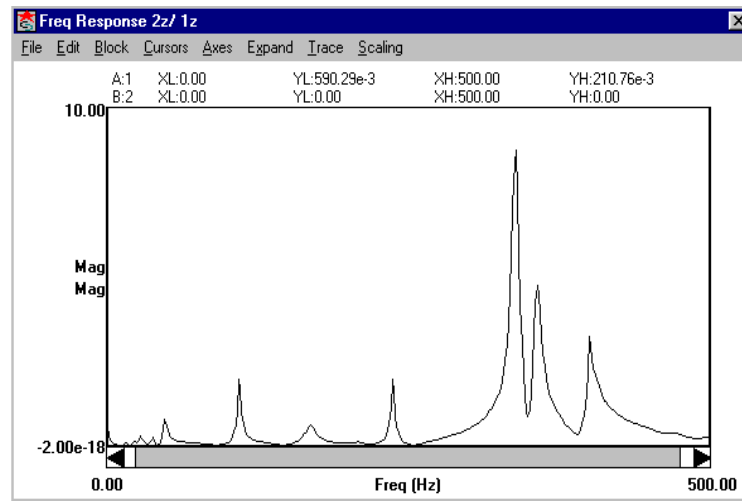


Figure: 4.13 Typical numerical FRF curve obtained using FFT analysis

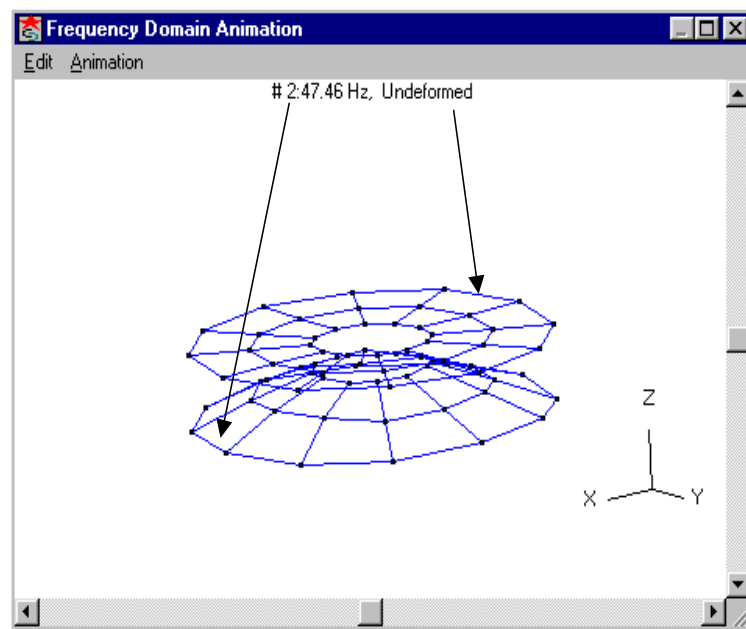


Figure 4.14: Typical mode shape and natural frequency obtained using FRF modal analysis

Multiple inputs and multiple outputs (MIMO) can also be used, depending on the number of channels on the FFT analyzer and the number of sensors available. The nature of the input forces maybe impulse, using impact hammer or random, using a vibration shaker. Both generate broadband spectrum that would excite the natural frequencies of a given system.

4.9 Correlation Process

The results from the experimental analysis and the finite element analysis will be correlated in order to generate accurate structural dynamic models of the truck chassis and support for immediate modification or future use. The correlation process will be done by FEM tools and base on the input parameters. After that, the updating process will be done in order to formulate an optimization problem in NASTRAN that minimizes the observed differences between measured and predicted dynamic responses. The objective function to be minimized is defined with an equation that expresses the norm of the response residues (reflecting the difference between the actual responses and the target responses). The results of the sensitivity analysis yield important information to limit the design variable set to parameters with significant modification impact. Discrepancies will always exist between the finite element and the experimental modal analysis model and there are at least three sources of discrepancies:

- (i) Errors in experimental data-noise exist in the experimental data; the measurement is carried out at an imperfect set-up. The origin experimental data (FRF) are processed as approximately to obtain the modal data (natural frequency and modes shapes) that will be used in the updating.
- (ii) Model parameter errors – some parameters in the finite element model have values specified that are different from the actual structure such as thickness, material properties and damping.

- (iii) Model structure errors – some features that are important to the dynamic properties of the structure in the specified frequency range are replaced by different features in the finite element model such as joints, etc.

Furthermore there is also the need to present this information in a logical and structured way. The correlation platform therefore is able to manage several Modal Analysis and Finite Element Analysis models at the same time and correlate any possible combination. Figure 4.15 below shows a few of the correlation platform of the system.

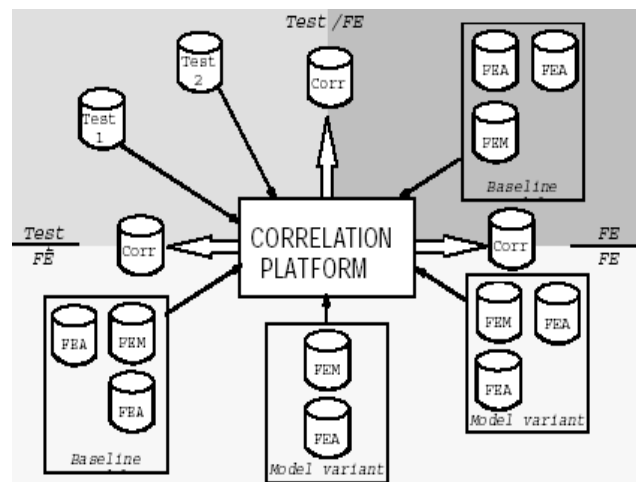


Figure 4.15: The correlation platform

Consistent post-processing means that the definition systems in which the Modal Analysis and Finite Element data are expressed are rendered compatible. This process involves geometrical mapping of Modal Analysis model on the FE model, the identification of (non) compatible nodal output coordinate systems and a unit management system.

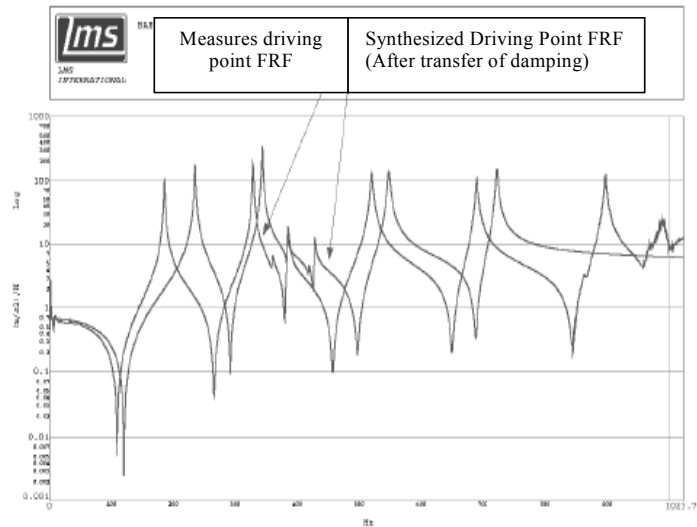


Figure 4.16: Modal Analysis versus Finite Element driving point FRF

An example of the visual comparison of a Modal Analysis – Finite Element driving point FRF's in a single window is shown in figure 4.16. Whilst the experimental FRF's are directly measured during the modal test, the FEA modal results files usually do not contain FRF's. A modal based FRF synthesis module is therefore an essential correlation tool. Realistic modal damping values for the FEA modes can be taken over from test modes that were correlated with the FEA modes in the modal correlation module.

4.10 Model Updating Process

Modal updating is a step in model validation process that modifies the values of parameters in FE model in order to bring the FE model prediction into a better agreement with the experimental data. The test data is used as the target and the FE parameters are updated. The parameters used to updated for the chassis model are listed below:

- a. Mass Density, ρ
- b. Poisson Ratio, ν

Parameter such as ρ , and ν were selected as global and local updating variables. A tremendous improvement in the finite element mode frequencies were then observed for overall changed parameters and finally the chassis was ready for better refinement.

The approach to FE model updating taken in the project is to formulate an optimization problem in NASTRAN that minimizes the observed differences between measured and predicted dynamic responses. The objective function to be minimized is defined with an equation that expresses the norm of the response residues that is reflecting the difference between the actual responses and the target responses.

The result of the sensitivity analysis yield important information to limit the design variable set to parameters with significant modification impact. After the optimization process within NASTRAN context, the iterative evolution of the parameters can be inspected with a 3D bar chart display and an updated FEA model file can be generated. The update design responses (mode for instance) can be read again in the correlation module to verify the updating process.

The implementation of this FE model updating approach will be finalized and validated with a number of test cases. These test cases show the validity of the model updating approach with small FEA models and high quality measurements. Figure 4.17 and 4.18 presents the modal correlation improvements for one of these test cases. Almost all of the initial mode switches are resolved and natural frequency differences are reduced within 5%. Figure 4.19 shows the improved FRF correlation.

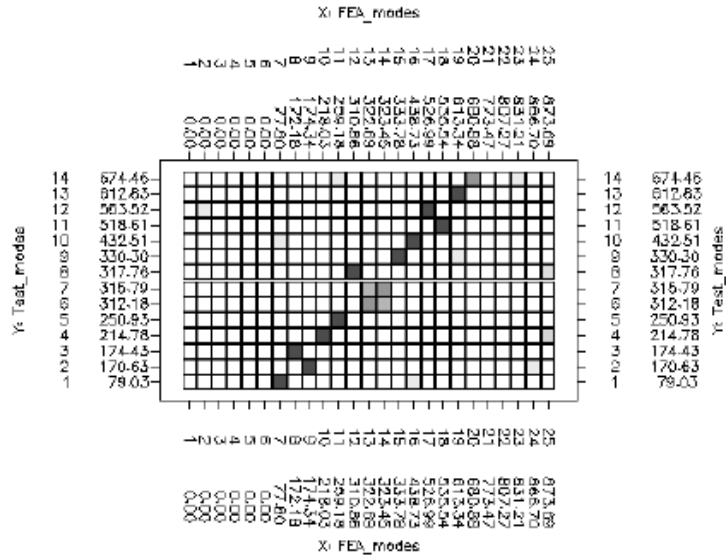


Figure 4.17 MAC matrix before updating (small size benchmark)

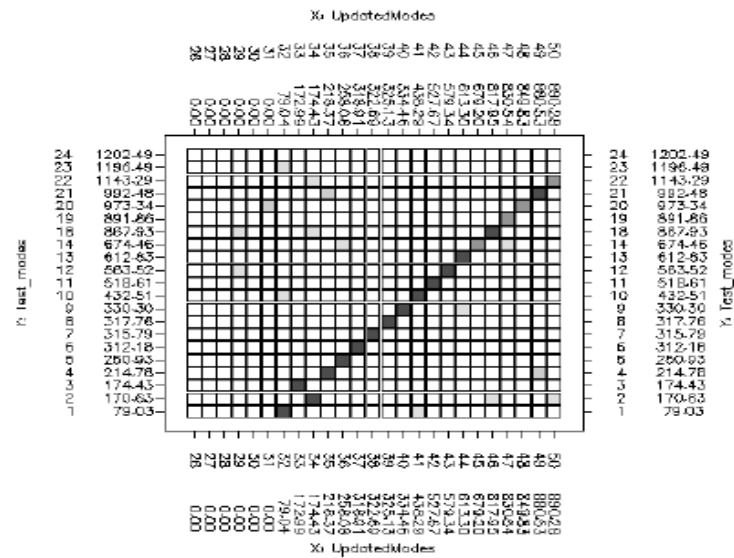


Figure 4.18 MAC matrix after updating (small size benchmark)

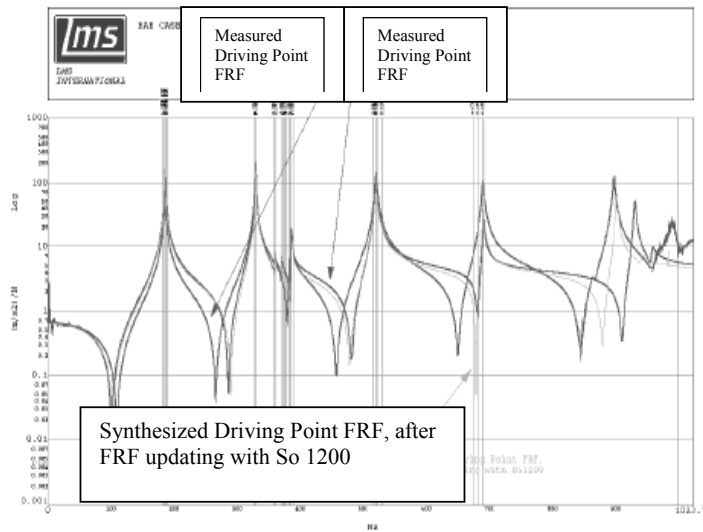


Figure 4.19 Driving point FRF correlations after updating (small size benchmark)

Close correlation between the two results implied that the CAD model is good. As the CAD model is accepted as good, then any design modification, such as changing the properties of the structure to shift the natural frequencies away from the operating range can be conducted ‘virtually’ using the model. Avoiding the unnecessary physical cycles of ‘modify-and-test’ would save time and money. Ideally, it is intended to ‘get-first-time-right’.

4.11 Structural Modification

Structural modification is important to improve the dynamic behavior of the truck chassis. In this study, after the model updating analysis is completed, the FE model is transferred to the ANSYS software for further analysis in the structural modification. At this stage, the FE truck chassis model would be assumed and believed this could represent the real chassis structure. Thus, any modification on the FE model will give an approximately the same result as to real structure. Normally the torsion mode is always defined as the critical mode and occurred near the working frequency. Some times, the torsion mode can cause fatigue failure due to

the bumps or road irregularities. Therefore, structure modification is required in order to strengthen the truck chassis structure and at the same time reduce the torsion effect. In order to optimize the structure, the designs of the truck chassis has been modified by adding stiffener to the chassis structure and also tested on the different material properties.